Exploring the Activation Landscape of Pro-Apoptotic BAK Through the Discovery of Human BH3-Only and Non-Native Peptide Binders

by

Fiona Aguilar

B.S. Biology
Brandeis University, 2014

SUBMITTED TO THE DEPARTMENT OF BIOLOGY IN PARTIAL FULFILLMENT OF THE REQUIREMENTS OF THE DEGREE OF

DOCTOR OF PHILOSOPHY IN BIOLOGY
AT THE
MASSACHUSETTS INSTITUTE OF TECHNOLOGY

MAY 2022

Signature of Author: _____
Department of Biology
May 18, 2022

Certified by: _____
Amy E. Keating
Professor of Biology and Biological Engineering
Co-Director, Biology Graduate Committee
Thesis Supervisor

Accepted by: _____
Mary Gehring
Associate Professor of Biology
Member, Whitehead Institute
Co-Director, Biology Graduate Committee

Exploring the Activation Landscape of Pro-Apoptotic BAK Through the Discovery of Human BH3-Only and Non-Native Peptide Binders

by

Fiona Aguilar

Submitted to the Department of Biology on May 18, 2022
in Partial Fulfillment of the Requirements
of the degree of Doctor of Philosophy in Biology

Abstract

BAK is one of the two pro-apoptotic members that form part of the BCL-2 protein family. Previous work has shown that binding of certain BH3-only proteins such as truncated BID (tBID), BIM, and PUMA to pro-apoptotic BAK leads to mitochondrial outer membrane permeabilization (MOMP), release of cytochrome c, and ultimately cell death. The BH3 binding event leads to a series of conformational changes that promote the conversion of BAK from monomer to dimer and subsequently to oligomers that disrupt membranes in a process referred to as *activation*. Putative intermediate crystal structures, crosslinking data, and *in vitro* functional tests have provided insights into the activation event, yet the sequence-function relationships that make some, but not all, BH3-only proteins function as activators remain largely unexamined.

In this thesis, I address the question using three methods: 1) computational design, 2) yeast surface-display screening of candidate BH3-like peptides, and 3) structure-based energy scoring. I identify ten new binders of BAK that span a large sequence space. Among the new binders are two peptides from human proteins BNIP5 and PXT1 that promote BAK activation in liposome assays and induce cytochrome-c release from mitochondria in HeLa cells. These new activators expand current views of how BAK-mediated cell death can be triggered. I show binding and kinetics measurements and solved crystal structures of BAK-peptide complexes, including complexes for two inhibitors and one activator. Results reveal a high degree of similarity in binding geometry, affinity, and association kinetics between peptide activators and inhibitors, including peptides described previously and those identified in this work. Here, I propose a free energy model for BAK activation that is based on the differential engagement of BAK monomers and the BAK activation transition state that integrates observations described in this thesis and previous reports of BAK binders, activators, and inhibitors.

Thesis Supervisor: Amy E. Keating
Title: Professor of Biology and Biological Engineering

Acknowledgements

Throughout my PhD, I crossed paths with so many people to whom I owe thanks to for their help, support, and kindness. I am extremely grateful to have been part of the MIT building 68 community. Whether it was to ask for help, discuss science, brainstorm ideas to troubleshoot assays, or chat near the elevators or in the kitchen area, there was always someone there to offer a hand or an ear.

I want to thank my PhD advisor Amy Keating for letting me be part of her research group and offering her scientific guidance and mentorship throughout the years. She provided an enormous amount of written feedback on any document I sent her including fellowship applications, paper outlines, and thesis. She also gave lots of feedback when presenting during group meetings as well as preparing for external presentations. I appreciate the incredible amount of work and time that she has put into discussing my research and shaping my scientific thinking. I'd also like to thank her for being reliable, supportive of her students' best interest, and her commitment to student training.

I want to thank my thesis committee members Bob Sauer and Matthew Vander Heiden for our meetings throughout the years. I always left those meetings feeling a lot more optimistic about the direction my project could take and what next steps to consider. Thank you for your scientific input and for reading my thesis. I also want to thank Joshua Kritzer for agreeing to be my external committee member and for reading my thesis.

I also want to thank the people who directly contributed to my project and made it possible. Thank you to our wonderful collaborators Stacey Yu and Kristopher Sarosiek for conducting the cell-based assays and providing data that have made the project all the more exciting. A huge thank you to Bob Grant for all his help and patience with the crystallography aspect of the project. This work also wouldn't have been possible without the computational expertise of Sebastian Swanson and the many hours of cloning and protein purification that Bonnie Su contributed. I also want to thank my rotation students Dia Ghose and Avi Singer and summer students Molly Carney and Hana Flores for their help with the project. Other colleagues I'd like to thank are Keating lab members Jackson Halpin and Israel Desta for their computational support and guidance, members of the Drennan lab for their help with crystallography, and members of the Bell lab, Walker lab, Baker lab, Sauer lab, and Imperiali lab for always letting me borrow their lab equipment when in need.

Certainly, my experience in the Keating lab wouldn't have been the same without my awesome lab mates and colleagues. I want to thank Theresa Hwang, who joined the lab at a similar time as I did, for being such a fun, compassionate, helpful, resourceful, and knowledgeable classmate and friend. This also brings me to the people who welcomed me to the lab when I first joined including Vincent Frappier, Vincent Xue, Lindsey Stretz, and Raheleh Rezaei Araghi. I enjoyed spending time with all of them both in and out of lab. I also want to thank the second wave of graduate students who have taken charge of ensuring lab socialness and fun including Sebastian Swanson, Dia Ghose, Avi Singer, and Jennifer Kosmatka.

During my time at MIT, I was lucky to find a support network of friends that pushed me through and helped me regain my confidence when graduate school felt like a huge whirlpool. Thank you to my MIT Biology friends and classmates, especially Emily Jackson, Theresa Hwang, Alexandra Navarro, Elaine Kuo, Andrew Cangelosi, and Luis Millan Barrea for their help during our first year of graduate school. I am proud of everything they have accomplished thus far. Also, thank you to the friends I have made through the MIT Mexican community and beyond for their camaraderie. I think fondly of the fun times we had during this chapter of our lives.

I also want to thank the people outside of my graduate school bubble for being there for me. Special thanks to my college and lifelong friends for spending time with me, responding to all my late night texts, proofreading emails and documents, and offering advice in all aspects of life.

Thank you to my partner, Daniel Young, for the past eight years of companionship. His partnership has been invaluable during my graduate school experience and beyond. In addition to being my travel buddy and everyday rock, he has also helped me with my graduate school work. I want to acknowledge the time and work that he put into the computational side projects that I pursued, despite them ultimately did not ending up in this thesis.

Lastly, I want to thank my family. Thank you to my aunts, uncles, cousins, and grandmother for being by my side throughout all stages of life. Certainly, life wouldn't be as beautiful or meaningful without my sister, Edna, and my parents. I wouldn't be here today if not for their hard work, support of my career decisions, and unconditional love. Thank you.

Table of Contents

CHAPTER 1 7

List of Figures 8

PART I. BCL-2 DISCOVERY AND CLASSIFICATION 9

SECTION 1.1 HISTORY OF APOPTOSIS 9

SECTION 1.2 DISCOVERY OF BCL-2 PROTEINS 9

SECTION 1.3 APOPTOSIS AND BCL-2 FAMILY CLASSIFICATION 10

SECTION 1.4 REGULATORY INTERACTIONS AMONG BCL-2 PROTEIN FAMILY MEMBERS 13

PART II. BAK ACTIVATION AND MOMP 15

SECTION 2.1 PUTATIVE INTERMEDIATE STRUCTURES OF BAK AND BAX 15

SECTION 2.2 MECHANISMS OF BAK AND BAX ACTIVATION AND PORE FORMATION 20

SECTION 2.3 METHODS TO STUDY BAK ACTIVATION 21

PART III. TARGETING BAK AND BAX 23

SECTION 3.1 BCL-2 MISREGULATION IN CANCER AND DISEASE 23

SECTION 3.2 BAK AND BAX BINDING BY SMALL MOLECULES, ANTIBODIES, AND PEPTIDES 24

REFERENCES 27

CHAPTER 2 38

Author Contribution 39

List of Tables 42

INTRODUCTION 43

RESULTS 47

SECTION 1.1 STRUCTURE-BASED DESIGN AND LIBRARY SCREENING IDENTIFY NOVEL PEPTIDE BINDERS OF BAK 47

SECTION 1.2 DISCOVERY OF NEW HUMAN BH3-ONLY BINDERS OF BAK 50

SECTION 1.3 NOVEL BH3 BINDERS OF BAK FUNCTION AS ACTIVATORS OR INHIBITORS 55

SECTION 1.4 HUMAN PROTEOME BNIP5 AND PXT1 BH3 PEPTIDES AND NON-NATIVE PEPTIDES ACTIVATE BAK IN CELLS 65

SECTION 1.5 ACTIVATORS AND INHIBITORS BIND BAK WITH SIMILAR BINDING MODES 69

SECTION 1.6 BINDING AFFINITIES AND KINETICS DO NOT DISTINGUISH ACTIVATORS AND INHIBITORS OF BAK 79

DISCUSSION 83

METHODS 90

Peptide synthesis, purification, and concentration determination 90

Fluorescence anisotropy binding assays 90

Yeast surface-display 90

Liposome assay 91

Protein expression and purification 93

Bio-layer Interferometry 94

Crystallography 95

CD measurements 95

Structure-based design of BH3-only binders of BAK 96

dTERMen scoring of human proteome sequences 97

Cavity detection 97

siRNA transfection 97

BH3 profiling 97
Immunoblotting 98
Acknowledgements and Funding 98
Author Contribution 98
Competing Interests 99
REFERENCES 102
CHAPTER 3 109
FUTURE DIRECTIONS 110
SECTION 1.1 BAK VS. BAX ACTIVATION SPECIFICITY 110
SECTION 1.2 BAK INHIBITOR SPECIFICITY 111
SECTION 1.3 USING PEPTIDES TO STUDY MOMP 112
SECTION 1.4 BIOLOGICAL FUNCTION OF BNIP5 AND PXT1 113
SECTION 1.5 SEARCHING FOR ADDITIONAL HUMAN BH3-ONLY BAK BINDERS 114
REFERENCES 115

CHAPTER 1

List of Figures

Figure 1. Diagram of the intrinsic and extrinsic pathways leading to apoptosis 11
Figure 2. Diagram of BCL-2 protein family classification 12
Figure 3. Structures of BCL-X_L and MCL-1 including apo and BH3-peptide complexes……..… 15
Figure 4. Superposition of apo BAK and BAK-peptide complex structures 16
Figure 5. Crystal structure of BAK domain-swapped dimer bound to BIM-RT BH3 peptide 17
Figure 6. Cavity detection in BAK:peptide complex 19
Figure 7. Crystal structure of BH3:groove symmetric homodimer 19

INTRODUCTION

PART I. BCL-2 DISCOVERY AND CLASSIFICATION

SECTION 1.1 HISTORY OF APOPTOSIS

The molecular biology term 'apoptosis' derived from the Greek "apo" (separation) and "ptosis" (falling off) was first used in 1972 to describe a physiological type of cell death observed in human and animal tissues (Duque-Parra, 2005; Kerr et al., 1972). The term referred to the formation of small spherical bodies (denoted 'apoptotic bodies') resulting from nuclear fragmentation and both nuclear and cytoplasmic condensation (Kerr et al., 1972). Apoptosis describes the elimination or 'suicide' of unwanted cells and depends on signals which determine the time of cell death commitment (Mazarakis et al., 1997). This 'intrinsic clock' that directs specific cell types to undergo death makes apoptosis a 'programmed' cell death (Duque-Parra, 2005; Kerr et al., 1972). Apoptosis is an evolutionarily conserved process important for normal development and maintenance of tissue homeostasis, which also serves as a defense mechanism to cope with cell infection and damage (Kerr et al., 1972). Its mis-regulation can lead to diseases including cancer, autoimmunity, and degenerative diseases (Kelly & Strasser, 2011).

SECTION 1.2 DISCOVERY OF BCL-2 PROTEINS

The relationship between apoptosis and cancer became apparent with the identification of the B-cell-lymphoma-2 (BCL-2) gene and its involvement in the t(14;18) chromosomal translocation (Youle & Strasser, 2008). Briefly, in this translocation, the *bcl-2* gene normally located on chromosome 18 is rearranged into the heavy chain locus on chromosome 14 and placed under the control of the IgH promoter and downstream IgH Eμ enhancer, leading to altered *bcl-2* regulation in acute leukemia and B-cell lymphomas (Cleary et al., 1986; Kelly & Strasser, 2011; Tsujimoto et al., 1984).

Further studies showed that overexpression of BCL-2 prevented death of cytokine-dependent lymphoma cell lines, yet did not promote cell proliferation (Bakhshi et al., 1985; Cleary et al., 1986, 1986; Tsujimoto et al., 1984, 1985) Over the years, different approaches were used to discover members of the BCL-2 regulation network. For example, degenerate oligonucleotides were used to PCR amplify conserved BCL-2 domains of homologs, leading to the discovery of Bcl-2 homologous antagonist/killer (BAK) (Chittenden et al., 1995). Like BCL-2, BAK contains a series of hydrophobic residues in its C-terminus, suggesting membrane localization; however,

functional studies showed an opposite effect on cell survival when overexpressed (Chittenden et al., 1995). Interestingly, BAK overexpression counteracted the anti-apoptotic function of BCL-2 during cytokine deprivation or oncogene expression (Chittenden et al., 1995). Another example is the identification of Bcl-2 Associated X protein (BAX) through a co-immunoprecipitation assay using a BCL-2 specific antibody and subsequent washes with detergent-containing buffer (Oltvai et al., 1993). Similar to BAK, high levels of BAX expression resulted in accelerated cell death. Importantly, this study also showed heterodimerization of BAX with BCL-2 in cells, which sheds light on the biochemical mechanistic regulation of the Bcl-2 network.

Subsequent studies in mice reported functional redundancy of BAK and BAX. BAK knockout mice appeared like wild-type, whereas BAX knockout mice appeared normal expect for having a bigger spleen compared to wild-type. Also, males were sterile, and it was later discovered that BAX is required during spermatogenesis (Knudson et al., 1995; Lindsten et al., 2000). BAK/BAX double knockout mice, on the other hand, showed severe developmental defects and cells were resistant to apoptotic stimuli, highlighting the functional significance of these proteins in the apoptotic pathway.

SECTION 1.3 APOPTOSIS AND BCL-2 FAMILY CLASSIFICATION

Caspases are the main effectors of cell death and can be subdivided into initiator caspases (caspase-2, -8, -9, and-10) and effector caspases (caspase-3, -6, -7) (Jin & El-Deiry, 2005). Both classes are initially expressed in an inactive zymogen form, but become active upon proteolytic cleavage (Shi, 2004). There are two major signaling pathways that lead to apoptosis: the extrinsic pathway and the intrinsic pathway (Shi, 2004) (**Figure 1**). Both pathways converge on caspase-3, leading to protein degradation and cell death (Shi, 2004). BCL-2 protein regulation of cell death occurs upstream of caspase activation in intrinsic cell death, and provides a positive feedback loop in extrinsic cell death (Jin & El-Deiry, 2005).

The extrinsic pathway or death receptor pathway is regulated by ligand stimulation of cell surface death receptors including TRAIL receptors, tumor necrosis factor receptors, or Fas (Elmore, 2007). Ligand binding induces conformational changes or formation of higher order receptor complexes that recruit adaptor proteins, including caspase-8, to form a death-inducing signaling complex (DISC) (J. W. Kim et al., 2000). Activation of caspase-8 leads to downstream activation of effector caspases (Shi, 2004). On the other hand, the intrinsic pathway or mitochondrial pathway is triggered by diverse internal stimuli such as growth factor withdrawal or genotoxic damage and culminates in mitochondrial outer membrane permeabilization (MOMP),

which results in the release of DIABLO (also known as SMAC) and cytochrome c, formation of the apoptosome, and activation of downstream caspases. MOMP is tightly controlled by the BCL-2 protein family. Crosstalk between the extrinsic pathway and the intrinsic pathway may occur through activation of caspase-8 and cleavage of its target BID, forming truncated BID or tBID, which acts at the mitochondria.

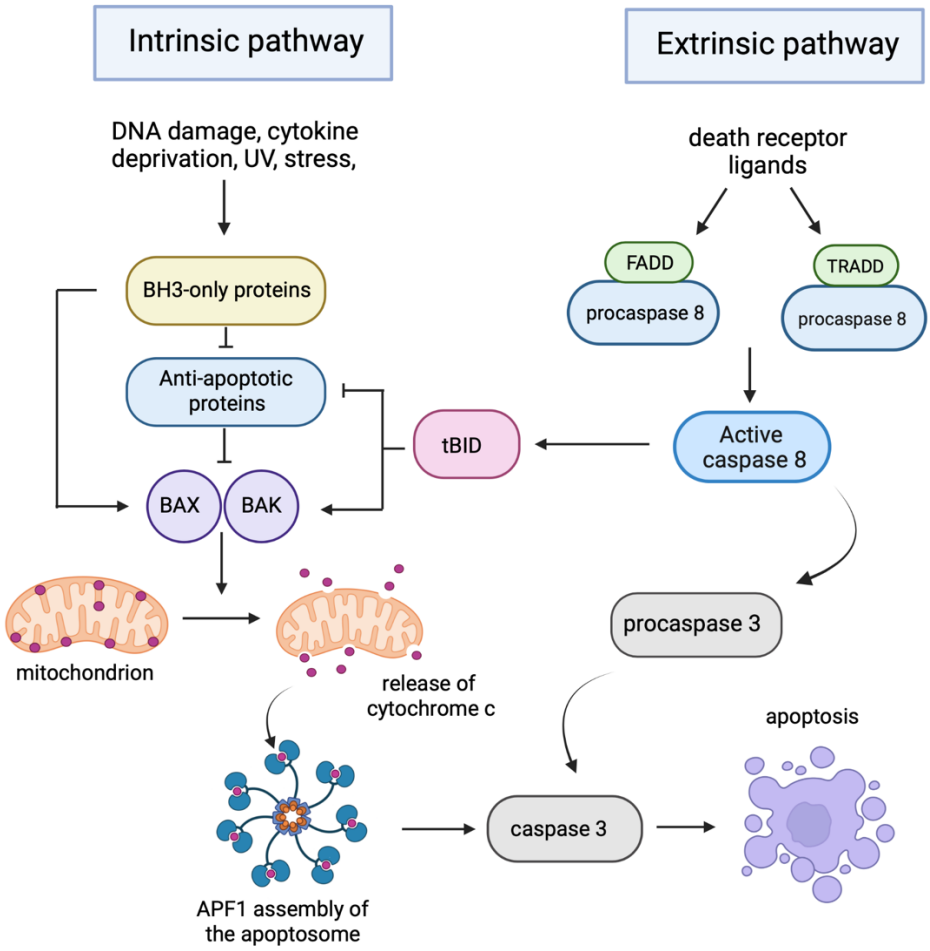

Figure 1. Diagram of the intrinsic and extrinsic pathways leading to apoptosis. Figure was adapted from (Czabotar et al., 2014) and (Youle & Strasser, 2008).

The BCL-2 family can be subdivided into three different groups: anti-apoptotic proteins, pro-apoptotic proteins, and BH3-only proteins; all of which contain at least one of four BCL-2 homology (BH) motifs. The anti-apoptotic proteins and pro-apoptotic proteins are structurally very similar; they are globular proteins containing eight or nine alpha-helices and a hydrophobic surface groove that can accommodate an additional helix from a binding partner. BH3-only

proteins solely contain the BH3 motif and, with the exception of BID prior to cleavage, are predominantly unstructured.

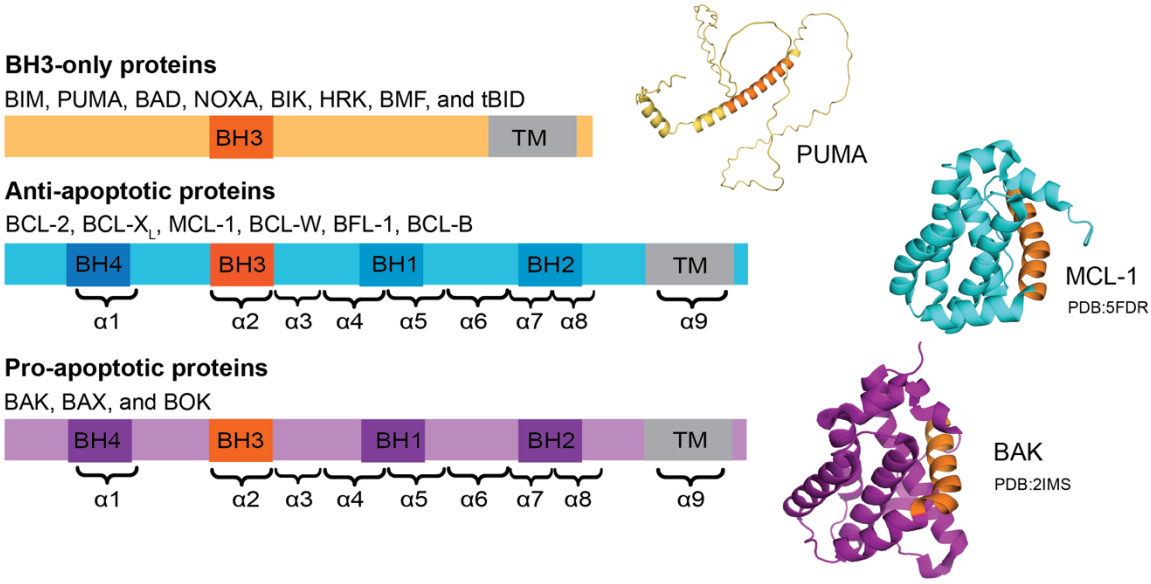

Figure 2. Diagram of BCL-2 protein family classification. All three BCL-2 subgroups contain a BH3 motif highlighted in bright orange. Structures on the right are representative of each subclass. PUMA was generated using AlphaFold (Jumper et al., 2021). Figure was adapted from (Czabotar et al., 2014).

Mammalian **pro-survival proteins** or **anti-apoptotic proteins** include BCL-2, BCL-X_L, MCL-1, BCL-W, A1/BFL-1, and BCL-B and contain eight α-helices, with the exception of BCL-W having 9 α-helices, plus a carboxy terminal transmembrane region. The BH1, BH2, and BH3 motifs are found in the globular core of the folded proteins (Youle & Strasser, 2008). Over-expression of these proteins prevents cell death from occurring despite the presence of apoptotic stimuli. Loss of anti-apoptotic proteins can have detrimental effects on tissue homeostasis. For example, BCL-X_L is required for survival of neuronal cells during embryogenesis and human erythropoiesis (Kelly & Strasser, 2011; Afreen et al., 2020). Studies in mice have shown BCL-W to be essential for spermatogenesis (Print et al., 1998). Homologs of anti-apoptotic proteins have also been found in viruses. For example, all gamma-herpesviruses contain at least one BCL-2 homolog. KS-BCL-2 is a Kaposi's sarcoma-associated herpesvirus (KSHV) (Bcl-2 homolog) and has anti-apoptotic function (Gallo et al., 2017).

Pro-apoptotic proteins or **BCL-2 effector proteins** include BAK, BAX, and the less-studied BOK. BAX and BAK are the key death effector proteins that homodimerize or heterodimerize to induce MOMP. These proteins can remain inactive as monomers or can be

held inactive by direct interaction with anti-apoptotic proteins. The critical step for triggering membrane permeabilization is controversial, but it is broadly accepted that dimerization of BAK and BAX leads to further oligomerization that results in formation of membrane disruption through which cytochrome c and SMAC/DIABLO can be released. Mechanisms that have been proposed for induction of MOMP will be discussed below (Uren et al., 2017; Youle & Strasser, 2008).

Because of the difficulty associated with expression and solubilization of membrane proteins with hydrophobic regions, biochemical and biophysical characterization of anti-apoptotic proteins and BAK has been performed on mutants with truncated C-termini (Pedersen et al., 2011). Hence, sequence-function studies have been focused on the core globular part of the protein rather than full-length proteins (Pedersen et al., 2011).

BH3-only proteins are intrinsically disordered proteins (with the exception of BID) that form helices upon binding globular BCL-2 family proteins and function as the initiators of mitochondrial apoptosis (Kelly & Strasser, 2011). BH3-only proteins within the BCL-2 family include BID, BIM, PUMA, NOXA, BAD, BMF, HRK, and BIK (Youle & Strasser, 2008). Other BH3-only proteins may remain unidentified as reported in the literature (Aouacheria et al., 2015). Some BH3-only proteins contain a C-terminal transmembrane (TM) region for membrane localization that can be transcriptionally regulated (Aouacheria et al., 2013; Kelly & Strasser, 2011). Interestingly, BH3-only proteins (with the exception of BID) likely arose through convergent evolution, as opposed to anti- and pro-apoptotic proteins that are clearly descended from a common ancestral gene (Aouacheria et al., 2013). For example, p53 transcriptionally upregulates PUMA and NOXA during γ-irradiation-induced DNA damage. BH3-only proteins can also be post-translationally regulated; as is the case of BAD dephosphorylation leading to its association with p53 and translocation to the mitochondria to activate apoptosis (Jiang et al., 2007).

SECTION 1.4 REGULATORY INTERACTIONS AMONG BCL-2 PROTEIN FAMILY MEMBERS

BCL-2 proteins form a finely tuned, multilayered, and complex regulatory network. Protein-protein interactions among the BCL-2 members are mediated through the BH3 motif contained by all members. The BH3 motif is an amphipathic α-helix with the initially proposed sequence: L-x(3)-G/A-D/E, where 'x' represents any amino acid (Aouacheria et al., 2015; DeBartolo et al., 2014). However, not all sequences that match the BH3 motif pattern function as BH3-only proteins. When seeking to identify new candidate regulators, additional information regarding secondary structure, function, or evolutionary relatedness is necessary to filter out false positives (Aouacheria et al., 2015). Studies conducted by Lee et al., for example, indicate residue

requirements at key positions surrounding the BH3 motif that are necessary for binding to anti-apoptotic or pro-apoptotic proteins (Lee et al., 2014).

Much of the biochemical and structural work on BCL-2 protein interactions has been done using chemically synthesized BH3 motif peptides (Kelly & Strasser, 2011). Functional assays in cells and cell extracts have also been done using tBID variants with altered BH3 motifs. Full-length BID is a globular α-helical bundle that, upon caspase-8 cleavage, forms two fragments (p7 and p15) (McDonnell et al., 1999). The p15 fragment contains the transmembrane segment and the BH3 motif, which becomes exposed upon cleavage and able to interact with its binding partners (McDonnell et al., 1999). To probe the function of different BH3 motifs, researchers have made protein chimeras consisting of tBID backbones with the native BID BH3 substituted with exogenous BH3 sequences. Such chimeras are mitochondrially localized by the native tBID transmembrane region (Llambi et al., 2011). Protein chimeras have also been made in the context of full-length BIM and tested in mice (Mérino et al., 2009).

All known BH3-only proteins can bind to at least a subset of anti-apoptotic proteins with tight affinities ($K_d \leq 10$ nM) to inhibit their function (Dutta et al., 2015); this interaction occurs in a structurally conserved hydrophobic groove present in anti-apoptotic proteins (**Figure 3**). Pro-apoptotic proteins BAK and BAX can be held in check by binding of their BH3 to the same groove in the anti-apoptotic proteins, such that there is competition for binding between pro-apoptotic and BH3-only proteins. When BAK or BAX BH3 are displaced by a BH3-only protein, they are no longer restrained and can undergo activation leading to MOMP.

Crystal structures of anti-apoptotic proteins bound to α-helical peptides of BH3-only proteins as well as BAK and BAX BH3 peptides show evidence of the interplay between all three BCL-2 protein subgroups. Conserved polar contacts involve a salt bridge formed between the aspartate residue in the L-x(3)-A/G-D/E motif of the peptide and an arginine on the receptor as shown in **Figure 3**.

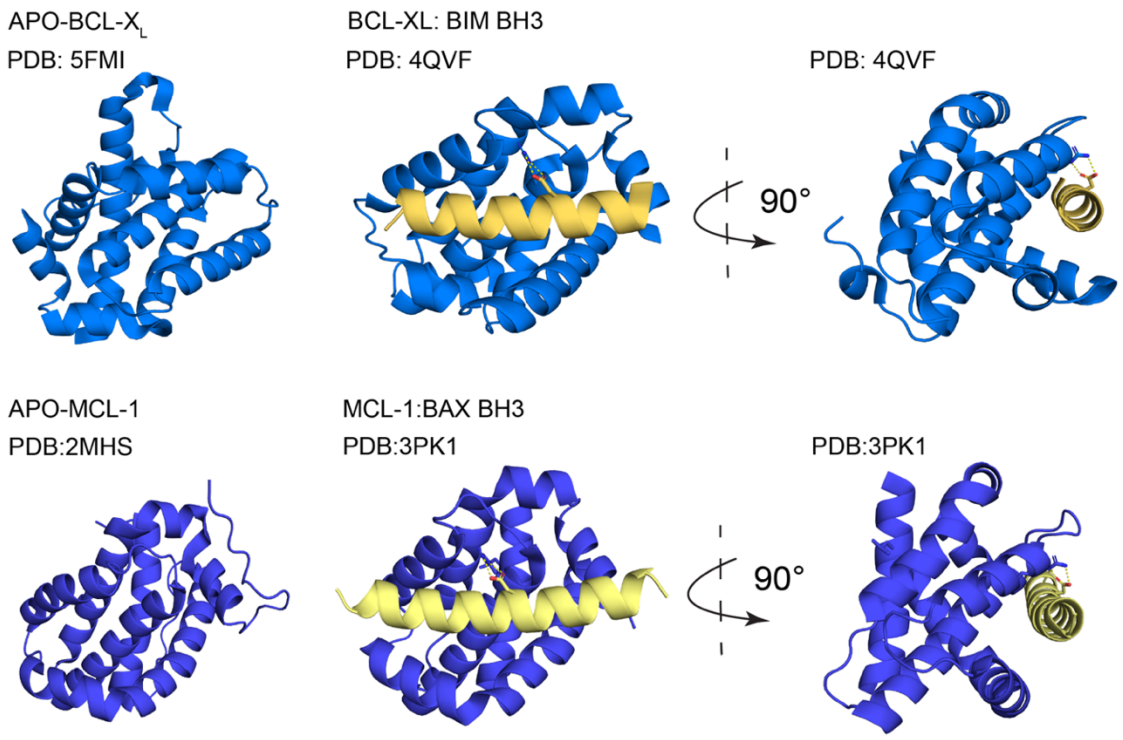

Figure 3. Structures of BCL-X$_L$ and MCL-1 including apo and BH3-peptide complexes. Top panel shows apo (PDB:5FMI) and BIM BH3 (light orange) bound anti-apoptotic BCL-X$_L$ (PDB:4QVF). Bottom panel shows apo (PDB:2MHS) and BAX BH3 bound (light yellow) anti-apoptotic MCL-1 (PDB:3PK1). Conserved aspartate in the canonical L-x(3)-A/G-D/E motif with interacting arginine are shown in sticks.

PART II. BAK ACTIVATION AND MOMP

In a process that is not yet fully understood, certain BCL-2 proteins can transiently interact with BAK and BAX, resulting in protein conformational rearrangements that lead to mitochondrial outer membrane permeabilization (MOMP), an irreversible step towards cell death. In this process termed *activation*, BAX or BAK undergo homodimer or heterodimer formation via BH3 helix exchange and subsequently assemble into higher-order oligomers that give rise to membrane disruption and release of cytochrome c. Various cell and biochemical assays combined with crystal structures have given insight into the intermediate steps of BAK and BAX activation.

SECTION 2.1 PUTATIVE INTERMEDIATE STRUCTURES OF BAK AND BAX

Truncated forms of human BAK have been crystallized, providing structures that may correspond to intermediates en route to MOMP. Given the low affinity of known activators (BIM,

BID, and PUMA) for BAK, no crystal structure of monomeric BAK bound to native activator have been obtained; however, point mutations of native sequences, detergents, and biochemical modifications such as non-natural amino acids or hydrocarbon staples have given proxy structures.

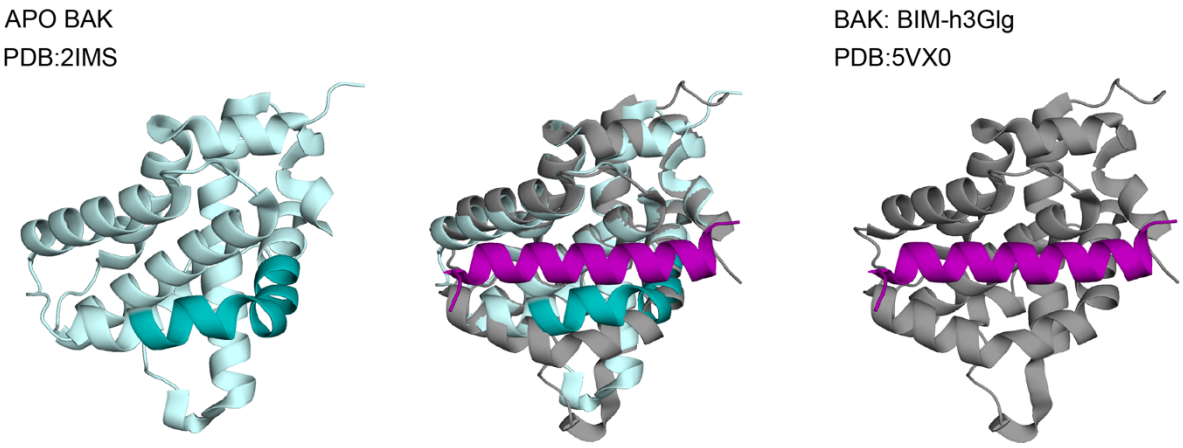

Figure 4. Superposition of apo BAK and BAK-peptide complex structures. Apo BAK (PDB:2IMS) is shown in pale cyan with the BH3 region in teal. BH3-peptide bound BAK **(PDB:5VX0)** is shown in grey. BIM-h3Glg is an BH3 BIM peptide (purple) containing a non-natural amino acid that functions as an inhibitor.

In addition to the apo structure, several crystal structure of BAK:BH3-peptide complexes have been obtained and given insight into similarities between anti-apoptotic and pro-apoptotic BCL-2 members. For example, similarly to anti-apoptotic proteins, BH3-only proteins bind the canonical hydrophobic groove of pro-apoptotic BAK as shown in **Figure 4**. Direct comparison of apo vs. BH3-peptide bound monomeric BAK structure shows that the BAK BH3 domain (teal) shifts downwards to accommodate BH3 binding (**Figure 4**). This slight opening of the canonical groove is also observed in anti-apoptotic BCL-2 members upon BH3 binding (Lee & Fairlie, 2019).

Four structures of BAK:activator complexes have been obtained. This includes one NMR structure of human BAK bound to a stapled BID peptide (PDB:2M5B), 2 crystal structures of BAK:BID complexes with peptide mutants (PDB:7M5A and PDB:7M5B) and one crystal structure of BAK:BAK BH3 peptide complex (PDB:7M5C) (G. Singh et al., 2022). Furthermore, two BAK:inhibitor complexes involving peptides containing non-natural amino acids (NAAs) (PDB: 5VWZ and PDB: 5VX0) have demonstrated that tight binders (nM to low μM affinities) are able to stabilize the monomeric BAK conformation, preventing it from undergoing activation (Brouwer et al., 2017). Specifically, native leucine at the hydrophobic pocket 3 (h3) position was substituted

for a NNAA consisting of a variation of a pentyl-carboxylate (Brouwer et al., 2017). This extended NNAA is able to form polar contacts with BAK R42 and R137 in the core of the protein and prevent BAK activation from occurring (Brouwer et al., 2017). Addition of a methyl group to this NAA increased its hydrophobicity and resulted in a tight 14.9 nM peptide binder (Brouwer et al., 2017).

Incubating BAK with BID BH3 peptide and CHAPS resulted in a dimeric protein according to size-exclusion chromatography (Brouwer et al., 2014). Crystallization of the dimer with excess BIM BH3 peptide resulted in a BAK domain-swapped structure with α2-α5 helices forming an undisturbed 'core' and α6-α8 forming a flexible 'latch' (PDB: 5VWV and PDB: 5VWW) as indicated in **Figure 5A** (Brouwer et al., 2014). In this structure, the latch region of one BAK molecule binds to the core region of the second BAK molecule and vice versa resulting in a stable dimer.

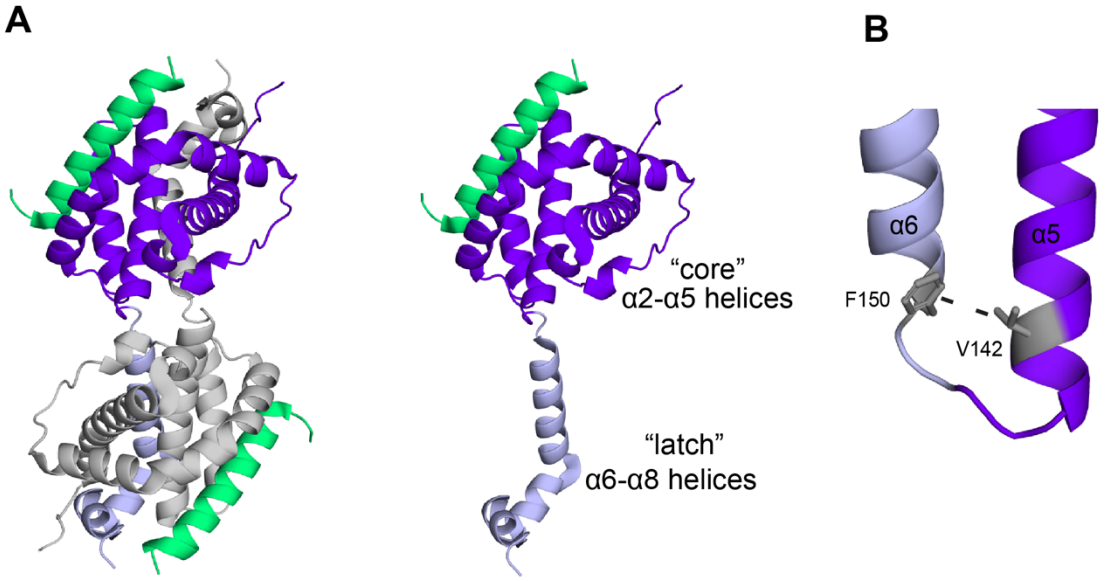

Figure 5. Crystal structure of BAK domain-swapped dimer bound to BIM-RT BH3 peptide. A) One BAK molecule is colored in grey and the second one is colored in dark purple (core region) and light purple (latch region) (PDB:5VWV). B) Residues F150 and V142 were mutated to cysteine to crosslink the latch and core. Figure was adapted from (Brouwer et al., 2014).

Previous groups have reported similar domain-swapped dimers of BAX in the presence of a BID BH3 peptide (PDB IDs: 4BD2, 4ZIG, and 4ZII) or BIM BH3 peptide (PDB IDs: 4ZIE, 4ZIF, and 4ZIH) bound at the canonical hydrophobic groove, primarily through hydrophobic moieties (h0-h4) (Czabotar et al., 2013; Robin et al., 2015). All BAX:peptide structures show the presence of the conserved salt bridge between aspartate and BAX R127.

Given that BAK is constitutively localized to the mitochondrial outer membrane, it is hypothesized that this domain-swapped dimer does not occur in the cell, since the latch would have restricted mobility due to its attachment to transmembrane α-9 helix (Brouwer et al., 2014). Despite this limitation, the so-called "core-latch dimer" structure is informative because it demonstrates a propensity for the α5-α8 helices to dissociate from the rest of the BAK domain. *In vivo* crosslinking studies support a model where upon activator BH3 binding, the BAK latch dissociates from the core. More specifically, a disulfide crosslink on the α5-α6 helices (V142C/F150C) was engineered into cysteine-less full-length BAK and expressed in BAK-/-BAX-/- MEF cells (Brouwer et al., 2014) (**Figure 5B**). Oxidation with CuPhe induced formation of a disulfide bond and prevented cytochrome c release. As a control, reduced V142C/F150C BAK treated with tBID gave release of cytochrome c, indicating the biological relevance of this dissociation (Brouwer et al., 2014).

Both monomeric and dimeric BAK/BAX-peptide complexes indicate the presence of a cavity at the interface between the peptide and BAK or BAX (**Figure 6**). This cavity is not observable in BH3 bound anti-apoptotic structures despite the structural similarities of BAK and BAX to these proteins. The exact location and size of the cavities observed in different structures varies, though the literature reports them to be approximately 435 Å for BAK and 140 Å for BAX (Brouwer et al., 2017; Czabotar et al., 2013). In structures of inhibitor peptides containing non-natural amino acids (NNAAs) bound to BAK, the NNAA occupies the cavity (Brouwer et al., 2017), suggesting a functional role in the BAK activation mechanism.

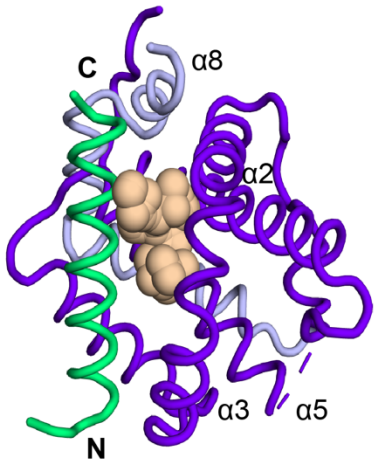

Figure 6. Cavity detection in BAK:peptide complex. Crystal structure of BAK core (dark purple) and latch (light purple) bound to BIM-RT peptide (green) (PDB:5VWV) contains a cavity shown in wheat color. Cavity was detected using F-pocket (Guilloux et al., 2009).

In contrast to the domain-swapped dimer, a BAK crystal structure referred to as the "BH3:groove symmetric dimer" was obtained when BAK core helices α2-α5 were fused to a GFP molecule (PDB IDs: 4U2V and 4BDU) (Brouwer et al., 2014). In this structure (**Figure 7**), the BH3 α2 helix of one BAK molecule binds to the α3-α5 hydrophobic groove of a second BAK molecule and vice versa, forming a symmetric homodimer (Brouwer et al., 2014). Similar BH3 in-groove homodimers have been obtained for BAX (PDB: 4BDU), suggesting that both BAK and BAX undergo similar intermediate steps during activation (Czabotar et al., 2013).

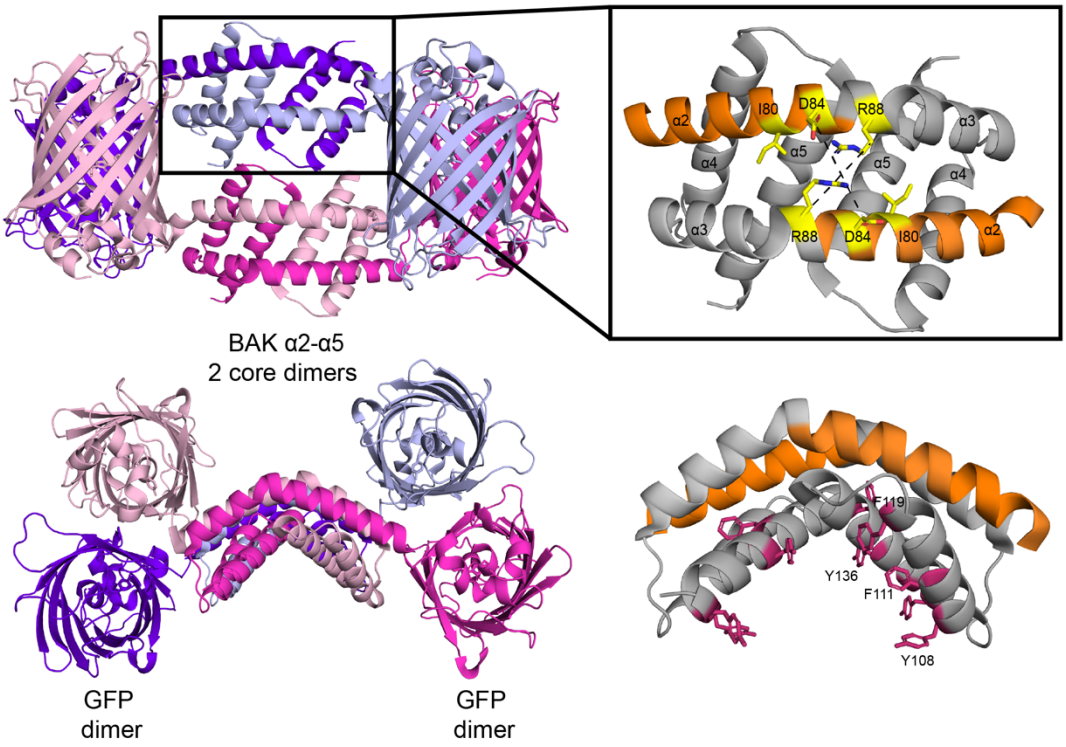

Figure 7. Crystal structure of BH3:groove symmetric homodimer. A GFP-BAK α2-α5 structure (PDB: 4U2V) includes two BAK core dimers. Top panel shows top view. BAK molecules swap α2 helices (BH3 domain) shown in orange and bind the α3, α4, and α5 groove of the partner molecule. Residues tested for crosslinking are shown in yellow. Bottom panel shows side view. Hydrophobic residues shown in red are thought to interact with the mitochondrial outer membrane. Figure was adapted from (Brouwer et al., 2014).

Although the BH3:groove symmetric homodimer structure was solved using a severely truncated construct, it is thought to represent an "on-pathway" structure, based on several sources of evidence. First, the dimer displays a slightly curved amphipathic structure with a hydrophilic

surface on one side and a lipophilic surface with exposed tyrosines and phenylalanines on the opposite side, similar to monotropic membrane proteins (Cowan et al., 2020). Presumably, these hydrophobic residues face the mitochondrial outer-membrane and form hydrophobic interactions with membrane lipids, leading to membrane disruption and pore formation (Brouwer et al., 2014). Supporting this, cysteine-crosslinking experiments involving residues in close proximity on the dyad axis have been performed after treatment of BAK with tBID. As expected, dimers were observed through reducing SDS-PAGE Western blot analysis upon addition of a bismaleimidoethane (BMOE) covalent crosslinker for D84C and R84C BAK, but not for I80C (a residue located further away) **Figure 7**. Finally, a 3D model of BAX in the membrane using double electron-electron resonance (DEER) spectroscopy distances supports the formation of a stable dimeric core consistent with the BH3-in-groove dimer structure (Bleicken et al., 2014).

SECTION 2.2 MECHANISMS OF BAK AND BAX ACTIVATION AND PORE FORMATION

Two different models have been proposed to explain the mechanism of BAK or BAX activation. The 'indirect activation model' assumes that apoptosis is triggered by a BH3-only protein functioning as a 'sensitizer' or 'de-repressor', via the mechanism of competitive binding. That is, binding of BH3 proteins to anti-apoptotic proteins localized at the mitochondria is sufficient to allow unimpeded, spontaneous activation of BAK or BAX, perhaps triggered by the mitochondrial membrane itself (K. Huang et al., 2019). The strongest evidence for this model comes from experiments involving inducible expression of sensitizer BAD (a BH3-only binder of anti-apoptotics BCL-2, BCL-X_L, and BCL-W, but not BAK or BAX) in cells lacking all other BH3-only proteins and anti-apoptotic MCL-1 (K. Huang et al., 2019). In this setting, expression of BAD alone is sufficient to displace anti-apoptotic proteins and induce BAX-mediated MOMP (K. Huang et al., 2019)

An alternative mechanism for inducing MOMP is that of 'direct activation' in which a BH3-only protein directly interacts with BAK or BAX to trigger a conformational change and subsequence oligomerization leading to MOMP. Of the many BH3-only proteins, only three are consistently reported to directly activate BAK and BAX: truncated BID (tBID), BIM, and less so PUMA in addition to the BAK and BAX BH3 domains (Kuwana et al., 2002; H. Kim et al., 2009; Llambi et al., 2011; Moldoveanu et al., 2013; Dai et al., 2014). A study using human BID chimeras in which the BH3 region was swapped for the BH3 region of other BH3-only members (NOXA, HRK, BIK, and BMF) showed that localization of all eight BH3-only members to the mitochondrial outer membrane can give different amounts of cytochrome c release (Hockings et al., 2015).

Activation potency was significantly higher for activators vs. non-activators and when tested in a liposome assay with purified proteins, the BID^{BIK} chimera showed minimal activation of BAK and BAX (Hockings et al., 2015).

BAX is primarily localized in the cytosol while BAK is constitutively localized on the mitochondrial outer membrane. Retrotranslocation rates between the cytosol and the mitochondrial outer membrane differ between BAK and BAX (Große et al., 2016). It has been suggested by several groups that BAX undergoes a two-step activation mechanism as opposed to BAK which simply involves one step (H. Kim et al., 2009). The first step in the two-step BAX activation mechanism is binding of a BH3-only protein to a site opposite to the canonical hydrophobic binding groove, termed the "trigger site". This event induces displacement of the $\alpha 9$ helix, which can then be inserted into the mitochondrial outer membrane (Gavathiotis et al., 2008; Subburaj et al., 2015). Second, an activator BH3-only protein binds the canonical groove and induces similar conformational changes as occur for BAK (Czabotar et al., 2013; Brouwer et al., 2014).

How BAK and BAX dimeric structures lead to oligomerization and membrane disruption is also not fully understood. However, crystal structures of BAK BH3:groove homodimers bound to lipids and detergents have helped explain a model. Specifically, it has been noted that different BAK:groove homodimer structures contain recurring pockets on the lipophilic α4α5α5′α4′ surfaces bound by different lipids (Cowan et al., 2020). It is thought that these lipid-protein interactions lead to thinning of the membrane bilayer and clustering of homodimers (Cowan et al., 2020). Mutational analysis of lipid binding regions led to a decrease in pore formation, indicating the direct role of membrane lipids in oligomerization (Cowan et al., 2020).

Although the exact model for how dimers cluster together is not known, lines, arcs, and ring-like structures of BAK and BAX have been visualized using single-molecule microscopy techniques (Uren et al., 2017; Große et al., 2016; Cosentino et al., 2022). Data shows that these hollow pore-like structures are delineated by pro-apoptotic proteins (Große et al., 2016). Super-resolution microscopy studies have also detected ring structures with diameters ranging from 200 to 800 nm (Große et al., 2016). Other studies have shown more homogeneous assemblies of BAK or BAX in apoptotic cells, with an average ring radius of 18 nm (Cosentino et al., 2022) and 34 nm (Salvador-Gallego et al., 2016), respectively.

SECTION 2.3 METHODS TO STUDY BAK ACTIVATION

Liposomes

Cell-based assays are critical to understanding BCL-2 protein family regulation in its native biological context, but pose difficulties when studying biochemical interactions. Cell contents can lead to uncertain or incorrect interpretation of results, due to all the elements that are unaccounted for, hence the field has established the use of cell-free systems consisting of artificially reconstituted vesicles with protein components to study biochemical events occurring on the mitochondrial outer membrane. The first liposomal system was developed in 2002 and has subsequently been adopted by various groups to study BAK/BAX activation (Brouwer et al., 2017; Gavathiotis et al., 2008; Hockings et al., 2015).

The idea that liposomes could be used as substitute for mitochondria came from the discovery that the mitochondrial outer membrane alone is involved in BCL-2 regulated apoptosis (Kuwana et al., 2002). Kuwana et al. showed that treatment of mitochondrial membranes with hypotonic solution led to the isolation of outer membrane vesicles (OMVs) with 80 nm in diameter (Kuwana et al., 2002). OMVs were loaded with fluorescein-dextran and incubated with tBID and BAX. Similar concentrations of BAX and tBID were required for dye release compared to cytochrome c release in mitochondrial membranes (Kuwana et al., 2002). Furthermore, addition of anti-apoptotic protein BCL-X_L was able to prevent dye release (Kuwana et al., 2002). Comparisons between ER membrane and mitochondrial membrane isolates showed that membrane composition is important, as ER liposomes were significantly less responsive. Kuwana et al. recapitulated BAX activation by making artificial liposomes with lipid composition matching that of mitochondria and noted that addition of cardiolipin to ER liposomes restored similar release response to that of mitochondria, indicating the importance of cardiolipin for membrane localization and protein function (Kuwana et al., 2002).

This cell-free system has both advantages and limitations. One advantage is that liposomes with varying lipid mixtures can be made within hours, which compares favorably to the amount of time required to grow cells and isolate heavy membrane fractions. Also, the obtained liposome yield is much greater compared to that of heavy membrane fractions extracted from cells or animal tissue. The limitations, however, are that homogeneous liposomes are not fully representative of the biological reality. Despite being able to regulate the diameter size of the liposome, the number of membranes within may vary despite freeze-thaw cycles aimed at creating unilamellar vesicles. Membrane curvature and tension is another factor that is not accounted for and could influence membrane pre-disposition to undergo disruption. Lastly, membrane channel VDAC2 is known to interact and restrain BAK activation, though it is typically not included in these *in vitro* assays.

Detergents

Detergents are used in biochemistry for membrane proteins and membrane-associated cell extraction and purification because of their amphiphilic nature which helps solubilize hydrophobic regions. Different detergents have different physical-chemical properties that can help stabilize specific proteins in their native conformation or alternatively in an altered conformation. How a detergent will perturb protein structure or function, and how similar this is to effects of native cell lipid membranes, must be determined empirically.

The apoptosis field has made use of detergents to study protein conformational changes and interactions. Numerous detergents have been shown to induce heteroligomerization and homoligomerization of BCL-2 members as indicated through size-exclusion chromatography (SEC) and co-immunoprecipitation assays. For example, the use of NP-40 detergent was essential for immunoprecipitation experiments of cell lysates and the discovery of BAX/BCL-2 interaction (Oltvai et al., 1993) and BAX/BCL-X_L (Hsu & Youle, 1997). Triton X-100 and NP-40 detergents both heterodimerize and homodimerize human and murine BAX. This process is dependent on detergents since these processes do not occur in the its absence (Hsu & Youle, 1997). Non-ionic detergents IGEPAL and 2% CHAPS have no effects on the structure of anti-apoptotic protein MCL-1, as shown through NMR, but allow for BAK binding the MCL-1 canonical groove. This interaction was characterized through SEC, *in vitro* pull-downs, NMR, and isothermal titration calorimetry (ITC) (Liu et al., 2010). Similarly, BAK was shown to interact with BCL-X_L in the presence of CHAPS (Willis et al., 2005). In all these cases, detergent in necessary to allow for BAK or BAX BH3 exposure and for heterodimerization or homodimerization to occur.

PART III. TARGETING BAK AND BAX

SECTION 3.1 BCL-2 MISREGULATION IN CANCER AND DISEASE

Failure of cells to undergo apoptosis is one of the hallmarks of cancer. Elevated anti-apoptotic BCL-2 protein expression levels, due to genetic or epigenetic mechanisms, can give rise to apoptotic blockades and different BCL-2 family dependencies (Delbridge et al., 2016). These blockades can be linked to chemotherapeutic resistance and depending on their position in the apoptotic pathway they can be classified as: A) suppression of BH3-only proteins, B) loss of BAK or BAX (refractory cells), and C) up-regulation of anti-apoptotic proteins (Deng et al., 2007).

Researchers have been interested in understanding a cell's cancer-specific apoptotic state to better predict its response to specific therapeutic treatments. To identify mechanisms leading to chemotherapeutic resistance, the Letai lab has developed a method called 'BH3 profiling'. The goal of BH3 profiling is to identify and measure the amount and type of pro-apoptotic signal that is required for a cell to undergo apoptosis (Fraser et al., 2019).

Misregulation in cancerous cells can lead to BH3-only protein up-regulation and dependency on anti-apoptotic proteins to restrain cell death. When anti-apoptotic proteins in a cell are largely occupied by BH3-only proteins, this occupancy titrates out the protective function and the cell is referred to as "primed for death" (Deng et al., 2007). On the other hand, a cell that expresses a surplus of anti-apoptotic proteins to the point where it can buffer any pro-apoptotic signal, is considered to be "unprimed" (Fraser et al., 2019). The BH3 profiling assay makes use of a dye localized to the mitochondrial intermembrane space, release of which reports on MOMP. To measure a BH3 profile, cells are permeabilized to allow entry of BH3 peptides (without disrupting the mitochondrial membrane), treated with different amounts of peptide, and monitored over time for MOMP. The amount of peptide required to induce MOMP is indicative of the 'priming' status of the cell; that is, small amounts of peptide are sufficient to induce MOMP in highly primed cells, while larger amounts of peptide are required in less primed cells (Fraser et al., 2019). Information about which peptides can vs. cannot induce MOMP also provide information about the specific dependency of a particular tumor or blood cancer.

In addition, protein engineering efforts have resulted in BH3 mimetics that can be easily made and used to characterize the priming' status of cancerous cells. Novel and selective peptides have been created through a combination of computational design and directed evolution methods. Sub-nanomolar binders of anti-apoptotic BCL-X_L (Dutta et al., 2015), BFL-1 (Jenson et al., 2017), and MCL-1 (Araghi et al., 2018) have been developed and used as BH3 diagnostic probes in the laboratory. Electrophilic entities have been added to peptides to create cysteine-reactive covalent peptide inhibitors (Jenson et al., 2017; Huhn et al., 2016; Araujo et al., 2017). Modifying peptides with crosslinking hydrocarbon staples has also resulted in cell-penetrating peptides (Araghi et al., 2018).

SECTION 3.2 BAK AND BAX BINDING BY SMALL MOLECULES, ANTIBODIES, AND PEPTIDES

Given their therapeutic potential to treat cancer or neurodegenerative diseases, researchers have been interested in developing tools including small molecules, antibodies, and

peptides to both probe BAK and BAX function and understand their complex activation mechanism.

Small molecules have shed light on ways of targeting BAX activation. For example, Gavathiotis et al. discovered small molecule BAM7 through *in silico* docking of small molecules to the BAX trigger site (Gavathiotis et al., 2012). A pharmacophore model was then used to optimize BAM7 interactions, resulting in the identification of BAX trigger site activator 1 (BTSA1). BTSA1 has been shown to be effective at inducing BAX-mediated apoptosis in acute myeloid leukemia (AML) cells and patient samples, demonstrating its therapeutic potential (Reyna et al., 2017). Other groups have developed small molecules that promote BAX activation (Pritz et al., 2017) as well as inhibit BAX oligomerization (Niu et al., 2017).

Another strategy for activating BAX using small molecules is to target the S184 site (Xin et al., 2014). Previous research has shown that nicotine-induced phosphorylation at the serine 184 site plays a role in inhibiting BAX pro-apoptotic activity (Xin et al., 2014). BAX-binding small molecules SMBA1, SMBA2 and SMBA3 interact with a pocket located near the S184 site, and have been shown to induce apoptosis of human lung cancer cells (Xin et al., 2014).

Efforts to target BAK have led to the discovery of small molecule WEHI-9625 (Delft et al., 2019). Although its exact mechanism of action remains unclear, WEHI-9625 stabilizes the BAK-VDAC2 interaction and selectively inhibit murine BAK, but not human BAK, mediated MOMP (Delft et al., 2019; Yuan et al., 2021). This illustrates an alternative strategy for indirectly inhibiting BAK and raises the possibility of the opposite scenario, where activation could potentially be enhanced by preventing formation of the BAK-VDAC2 complex.

Antibodies with specificity for BAK or BAX have provided mechanistic insights into auto-activation events. Available reagents include: 1) antibody 3C10 that activates constitutively membrane localized BAX S184L by binding its trigger site, and 2) antibody 7D10 that binds the BAK α1-α2 loop, inducing dissociation of the α1 helix and resulting in activation (Iyer et al., 2016). This second antibody suggests the presence of a “hidden” trigger site on BAK that can be exploited for therapeutic purposes (Iyer et al., 2016). By using both of these antibodies, Iyer et al. discovered that BAK is a more potent auto-activator compared to BAX, as antibody-activated BAK could activate BAK and cytosolic and mitochondrial BAX, whereas antibody-activated BAX appeared to be a weak activator in all three cases (Iyer et al., 2020).

Peptides containing hydrocarbon staples or non-natural amino acids have also been used to modulate BAK function. A series of crosslinked BID peptides, referred to as BID SAHBs, bind with low nanomolar affinities to murine full-length BAK and activate it in liposome assays (Leshchiner et al., 2013). On the other hand, the introduction of non-natural amino acids (NNAAs)

into a BIM BH3 peptide has shown that is it possible for a BH3 peptide to bind BAK and inhibit rather than activate it. The presence of NNAAs in the BAK:peptide cavity region resulted in additional interactions that stabilized the monomeric BAK complex (Brouwer et al., 2017).

Despite all these examples of ways researchers have targeted BAK and BAX function, the underlying fundamental mechanism by which binding to BAK leads to activation or inhibition remains unclear. Why do only a subset of BH3-only proteins activate BAK? What structural requirements allow some BH3-peptides to inhibit vs activate BAK? Are there any additional undiscovered BH3-only proteins that regulate function? In this thesis, I will attempt to answer this question by exploring a greater sequence space of BAK peptide binders and characterizing their function through structural and biophysical studies.

REFERENCES

Afreen, S., Bohler, S., Müller, A., Demmerath, E.-M., Weiss, J. M., Jutzi, J. S., Schachtrup, K., Kunze, M., & Erlacher, M. (2020). BCL-XL expression is essential for human erythropoiesis and engraftment of hematopoietic stem cells. *Cell Death & Disease*, *11*(1), 8. https://doi.org/10.1038/s41419-019-2203-z

Aouacheria, A., Combet, C., Tompa, P., & Hardwick, J. M. (2015). Redefining the BH3 Death Domain as a 'Short Linear Motif.' *Trends in Biochemical Sciences*, *40*(12), 736–748. https://doi.org/10.1016/j.tibs.2015.09.007

Aouacheria, A., Laval, V. R. de, Combet, C., & Hardwick, J. M. (2013). Evolution of Bcl-2 homology motifs: homology versus homoplasy. *Trends in Cell Biology*, *23*(3), 103–111. https://doi.org/10.1016/j.tcb.2012.10.010

Araghi, R. R., Bird, G. H., Ryan, J. A., Jenson, J. M., Godes, M., Pritz, J. R., Grant, R. A., Letai, A., Walensky, L. D., & Keating, A. E. (2018). Iterative optimization yields Mcl-1–targeting stapled peptides with selective cytotoxicity to Mcl-1–dependent cancer cells. *Proceedings of the National Academy of Sciences*, *115*(5), E886–E895. https://doi.org/10.1073/pnas.1712952115

Araghi, R. R., Ryan, J. A., Letai, A., & Keating, A. E. (2016). Rapid Optimization of Mcl-1 Inhibitors using Stapled Peptide Libraries Including Non-Natural Side Chains. *ACS Chemical Biology*, *11*(5), 1238–1244. https://doi.org/10.1021/acschembio.5b01002

Araujo, A. D. de, Lim, J., Good, A. C., Skerlj, R. T., & Fairlie, D. P. (2017). Electrophilic Helical Peptides That Bond Covalently, Irreversibly, and Selectively in a Protein–Protein Interaction Site. *ACS Medicinal Chemistry Letters*, *8*(1), 22–26. https://doi.org/10.1021/acsmedchemlett.6b00395

Assafa, T. E., Nandi, S., Śmiłowicz, D., Galazzo, L., Teucher, M., Elsner, C., Pütz, S., Bleicken, S., Robin, A. Y., Westphal, D., Uson, I., Stoll, R., Czabotar, P. E., Metzler-Nolte, N., & Bordignon, E. (2021). Biophysical Characterization of Pro-apoptotic BimBH3 Peptides Reveals an Unexpected Capacity for Self-Association. *Structure*, *29*(2), 114-124.e3. https://doi.org/10.1016/j.str.2020.09.002

Bakhshi, A., Jensen, J. P., Goldman, P., Wright, J. J., McBride, O. W., Epstein, A. L., & Korsmeyer, S. J. (1985). Cloning the chromosomal breakpoint of t(14;18) human lymphomas: clustering around Jh on chromosome 14 and near a transcriptional unit on 18. *Cell*, *41*(3), 899–906. https://doi.org/10.1016/s0092-8674(85)80070-2

Birkinshaw, R. W., Iyer, S., Lio, D., Luo, C. S., Brouwer, J. M., Miller, M. S., Robin, A. Y., Uren, R. T., Dewson, G., Kluck, R. M., Colman, P. M., & Czabotar, P. E. (2021). Structure of detergent-activated BAK dimers derived from the inert monomer. *Molecular Cell*, *81*(10), 2123-2134.e5. https://doi.org/10.1016/j.molcel.2021.03.014

Bleicken, S., Jeschke, G., Stegmueller, C., Salvador-Gallego, R., García-Sáez, A. J., & Bordignon, E. (2014). Structural Model of Active Bax at the Membrane. *Molecular Cell*, *56*(4), 496–505. https://doi.org/10.1016/j.molcel.2014.09.022

Brouwer, J. M., Lan, P., Cowan, A. D., Bernardini, J. P., Birkinshaw, R. W., Delft, M. F. van, Sleebs, B. E., Robin, A. Y., Wardak, A., Tan, I. K., Reljic, B., Lee, E. F., Fairlie, W. D., Call, M. J., Smith, B. J., Dewson, G., Lessene, G., Colman, P. M., & Czabotar, P. E. (2017). Conversion of Bim-BH3 from Activator to Inhibitor of Bak through Structure-Based Design. *Molecular Cell*, *68*(4), 659-672.e9. https://doi.org/10.1016/j.molcel.2017.11.001

Brouwer, J. M., Westphal, D., Dewson, G., Robin, A. Y., Uren, R. T., Bartolo, R., Thompson, G. V., Colman, P. M., Kluck, R. M., & Czabotar, P. E. (2014). Bak Core and Latch Domains Separate during Activation, and Freed Core Domains Form Symmetric Homodimers. *Molecular Cell*, *55*(6), 938–946. https://doi.org/10.1016/j.molcel.2014.07.016

Chao, G., Lau, W. L., Hackel, B. J., Sazinsky, S. L., Lippow, S. M., & Wittrup, K. D. (2006). Isolating and engineering human antibodies using yeast surface display. *Nature Protocols*, *1*(2), 755–768. https://doi.org/10.1038/nprot.2006.94

Chen, L., Willis, S. N., Wei, A., Smith, B. J., Fletcher, J. I., Hinds, M. G., Colman, P. M., Day, C. L., Adams, J. M., & Huang, D. C. S. (2005). Differential Targeting of Prosurvival Bcl-2 Proteins by Their BH3-Only Ligands Allows Complementary Apoptotic Function. *Molecular Cell*, *17*(3), 393–403. https://doi.org/10.1016/j.molcel.2004.12.030

Chittenden, T., Harrington, E. A., O'Connor, R., Remington, C., Lutz, R. J., Evan, G. I., & Guild, B. C. (1995). Induction of apoptosis by the Bcl-2 homologue Bak. *Nature*, *374*(6524), 733–736. https://doi.org/10.1038/374733a0

Cho, K. F., Branon, T. C., Udeshi, N. D., Myers, S. A., Carr, S. A., & Ting, A. Y. (2020). Proximity labeling in mammalian cells with TurboID and split-TurboID. *Nature Protocols*, *15*(12), 3971–3999. https://doi.org/10.1038/s41596-020-0399-0

Cleary, M. L., Smith, S. D., & Sklar, J. (1986). Cloning and Structural Analysis of cDNAs for bcl-2 and a Hybrid bcl-2/Immunoglobulin Transcript Resulting from the t(14;18) Translocation. *Cell*, *47*, 19–28.

Cosentino, K., Hertlein, V., Jenner, A., Dellmann, T., Gojkovic, M., Peña-Blanco, A., Dadsena, S., Wajngarten, N., Danial, J. S. H., Thevathasan, J. V., Mund, M., Ries, J., & Garcia-Saez, A. J. (2022). The interplay between BAX and BAK tunes apoptotic pore growth to control mitochondrial-DNA-mediated inflammation. *Molecular Cell*. https://doi.org/10.1016/j.molcel.2022.01.008

Cowan, A. D., Smith, N. A., Sandow, J. J., Kapp, E. A., Rustam, Y. H., Murphy, J. M., Brouwer, J. M., Bernardini, J. P., Roy, M. J., Wardak, A. Z., Tan, I. K., Webb, A. I., Gulbis, J. M., Smith, B. J., Reid, G. E., Dewson, G., Colman, P. M., & Czabotar, P. E. (2020). BAK core dimers bind lipids and can be bridged by them. *Nature Structural & Molecular Biology*, *27*(11), 1024–1031. https://doi.org/10.1038/s41594-020-0494-5

Czabotar, P. E., Lessene, G., Strasser, A., & Adams, J. M. (2014). Control of apoptosis by the BCL-2 protein family: implications for physiology and therapy. *Nature Reviews Molecular Cell Biology*, *15*(1), 49–63. https://doi.org/10.1038/nrm3722

Czabotar, P. E., Westphal, D., Dewson, G., Ma, S., Hockings, C., Fairlie, W. D., Lee, E. F., Yao, S., Robin, A. Y., Smith, B. J., Huang, D. C. S., Kluck, R. M., Adams, J. M., & Colman, P. M. (2013). Bax Crystal Structures Reveal How BH3 Domains Activate Bax and Nucleate Its Oligomerization to Induce Apoptosis. *Cell*, *152*(3), 519–531. https://doi.org/10.1016/j.cell.2012.12.031

Dai, H., Pang, Y.-P., Ramirez-Alvarado, M., & Kaufmann, S. H. (2014). Evaluation of the BH3-only Protein Puma as a Direct Bak Activator*. *Journal of Biological Chemistry*, *289*(1), 89–99. https://doi.org/10.1074/jbc.m113.505701

DeBartolo, J., Taipale, M., & Keating, A. E. (2014). Genome-Wide Prediction and Validation of Peptides That Bind Human Prosurvival Bcl-2 Proteins. *PLoS Computational Biology*, *10*(6), e1003693. https://doi.org/10.1371/journal.pcbi.1003693

Delbridge, A. R. D., Grabow, S., Strasser, A., & Vaux, D. L. (2016). Thirty years of BCL-2: translating cell death discoveries into novel cancer therapies. *Nature Reviews Cancer*, *16*(2), 99–109. https://doi.org/10.1038/nrc.2015.17

Delft, M. F. van, Chappaz, S., Khakham, Y., Bui, C. T., Debrincat, M. A., Lowes, K. N., Brouwer, J. M., Grohmann, C., Sharp, P. P., Dagley, L. F., Li, L., McArthur, K., Luo, M.-X., Chin, H. S., Fairlie, W. D., Lee, E. F., Segal, D., Duflocq, S., Lessene, R., … Kile, B. T. (2019). A small molecule interacts with VDAC2 to block mouse BAK-driven apoptosis. *Nature Chemical Biology*, *15*(11), 1057–1066. https://doi.org/10.1038/s41589-019-0365-8

Deng, J., Carlson, N., Takeyama, K., Cin, P. D., Shipp, M., & Letai, A. (2007). BH3 Profiling Identifies Three Distinct Classes of Apoptotic Blocks to Predict Response to ABT-737 and Conventional Chemotherapeutic Agents. *Cancer Cell*, *12*(2), 171–185. https://doi.org/10.1016/j.ccr.2007.07.001

Duque-Parra, J. E. (2005). Note on the origin and history of the term “apoptosis.” *The Anatomical Record Part B: The New Anatomist*, *283B*(1), 2–4. https://doi.org/10.1002/ar.b.20047

Dutta, S., Ryan, J., Chen, T. S., Kougentakis, C., Letai, A., & Keating, A. E. (2015). Potent and Specific Peptide Inhibitors of Human Pro-Survival Protein Bcl-xL. *Journal of Molecular Biology*, *427*(6), 1241–1253. https://doi.org/10.1016/j.jmb.2014.09.030

Elmore, S. (2007). Apoptosis: A Review of Programmed Cell Death. *Toxicologic Pathology*, *4*(35), 495–516. https://doi.org/10.1080/01926230701320337

Frappier, V., Jenson, J. M., Zhou, J., Grigoryan, G., & Keating, A. E. (2019). Tertiary Structural Motif Sequence Statistics Enable Facile Prediction and Design of Peptides that Bind Anti-apoptotic Bfl-1 and Mcl-1. *Structure*, *27*(4), 606-617.e5. https://doi.org/10.1016/j.str.2019.01.008

Fraser, C., Ryan, J., & Sarosiek, K. (2019). BCL-2 Family Proteins, Methods and Protocols. *Methods in Molecular Biology*, *1877*, 61–76. https://doi.org/10.1007/978-1-4939-8861-7_4

Gallo, A., Lampe, M., Günther, T., & Brune, W. (2017). The Viral Bcl-2 Homologs of Kaposi's Sarcoma-Associated Herpesvirus and Rhesus Rhadinovirus Share an Essential Role for Viral Replication. *Journal of Virology*, *91*(6), e01875-16. https://doi.org/10.1128/jvi.01875-16

Garner, T. P., Reyna, D. E., Priyadarshi, A., Chen, H.-C., Li, S., Wu, Y., Ganesan, Y. T., Malashkevich, V. N., Almo, S. S., Cheng, E. H., & Gavathiotis, E. (2016). An Autoinhibited Dimeric Form of BAX Regulates the BAX Activation Pathway. *Molecular Cell*, *63*(3), 485–497. https://doi.org/10.1016/j.molcel.2016.06.010

Gavathiotis, E., Reyna, D. E., Bellairs, J. A., Leshchiner, E. S., & Walensky, L. D. (2012). Direct and selective small-molecule activation of proapoptotic BAX. *Nature Chemical Biology*, *8*(7), 639–645. https://doi.org/10.1038/nchembio.995

Gavathiotis, E., Suzuki, M., Davis, M. L., Pitter, K., Bird, G. H., Katz, S. G., Tu, H.-C., Kim, H., Cheng, E. H.-Y., Tjandra, N., & Walensky, L. D. (2008). BAX Activation is Initiated at a Novel Interaction Site. *Nature*, *455*(7216), 1076–1081. https://doi.org/10.1038/nature07396

Grigoryan, G., Reinke, A. W., & Keating, A. E. (2009). Design of protein-interaction specificity affords selective bZIP-binding peptides. *Nature*, *458*(7240), 859–864. https://doi.org/10.1038/nature07885

Große, L., Wurm, C. A., Brüser, C., Neumann, D., Jans, D. C., & Jakobs, S. (2016). Bax assembles into large ring-like structures remodeling the mitochondrial outer membrane in apoptosis. *The EMBO Journal*, *35*(4), 402–413. https://doi.org/10.15252/embj.201592789

Grzmil, P., Burfeind, C., Preuss, T., Dixkens, C., Wolf, S., Engel, W., & Burfeind, P. (2007). The putative peroxisomal gene Pxt1 is exclusively expressed in the testis. *Cytogenetic and Genome Research*, *119*(1–2), 74–82. https://doi.org/10.1159/000109622

Guilloux, V. L., Schmidtke, P., & Tuffery, P. (2009). Fpocket: An open source platform for ligand pocket detection. *BMC Bioinformatics*, *10*(1), 168–168. https://doi.org/10.1186/1471-2105-10-168

Hockings, C., Anwari, K., Ninnis, R. L., Brouwer, J., O'Hely, M., Evangelista, M., Hinds, M. G., Czabotar, P. E., Lee, E. F., Fairlie, W. D., Dewson, G., & Kluck, R. M. (2015). Bid chimeras indicate that most BH3-only proteins can directly activate Bak and Bax, and show no preference for Bak versus Bax. *Cell Death & Disease*, *6*(4), e1735. https://doi.org/10.1038/cddis.2015.105

Holland, J., Pan, Q., & Grigoryan, G. (2018). Contact prediction is hardest for the most informative contacts, but improves with the incorporation of contact potentials. *PLoS ONE*, *13*(6), e0199585. https://doi.org/10.1371/journal.pone.0199585

Hsu, Y.-T., & Youle, R. J. (1997). Nonionic Detergents Induce Dimerization among Members of the Bcl-2 Family*. *Journal of Biological Chemistry*, *272*(21), 13829–13834. https://doi.org/10.1074/jbc.272.21.13829

Huang, D. C. S., & Strasser, A. (2000). BH3-Only Proteins—Essential Initiators of Apoptotic Cell Death. *Cell*, *103*(6), 839–842. https://doi.org/10.1016/s0092-8674(00)00187-2

Huang, K., O'Neill, K. L., Li, J., Zhou, W., Han, N., Pang, X., Wu, W., Struble, L., Borgstahl, G., Liu, Z., Zhang, L., & Luo, X. (2019). BH3-only proteins target BCL-xL/MCL-1, not BAX/BAK, to initiate apoptosis. *Cell Research*, *29*(11), 942–952. https://doi.org/10.1038/s41422-019-0231-y

Huhn, A. J., Guerra, R. M., Harvey, E. P., Bird, G. H., & Walensky, L. D. (2016). Selective Covalent Targeting of Anti-Apoptotic BFL-1 by Cysteine-Reactive Stapled Peptide Inhibitors. *Cell Chemical Biology*, *23*(9), 1123–1134. https://doi.org/10.1016/j.chembiol.2016.07.022

Hwang, T., Parker, S. S., Hill, S. M., Grant, R. A., Ilunga, M. W., Sivaraman, V., Mouneimne, G., & Keating, A. E. (2022). Native proline-rich motifs exploit sequence context to target actin-remodeling Ena/VASP protein ENAH. *ELife*, *11*, e70680. https://doi.org/10.7554/elife.70680

Iyer, S., Anwari, K., Alsop, A. E., Yuen, W. S., Huang, D. C. S., Carroll, J., Smith, N. A., Smith, B. J., Dewson, G., & Kluck, R. M. (2016). Identification of an activation site in Bak and mitochondrial Bax triggered by antibodies. *Nature Communications*, *7*(1), 11734. https://doi.org/10.1038/ncomms11734

Iyer, S., Uren, R. T., Dengler, M. A., Shi, M. X., Uno, E., Adams, J. M., Dewson, G., & Kluck, R. M. (2020). Robust autoactivation for apoptosis by BAK but not BAX highlights BAK as an important therapeutic target. *Cell Death & Disease*, *11*(4), 268. https://doi.org/10.1038/s41419-020-2463-7

Jenson, J. M., Ryan, J. A., Grant, R. A., Letai, A., & Keating, A. E. (2017). Epistatic mutations in PUMA BH3 drive an alternate binding mode to potently and selectively inhibit anti-apoptotic Bfl-1. *ELife*, *6*, e25541. https://doi.org/10.7554/elife.25541

Jenson, J. M., Xue, V., Stretz, L., Mandal, T., Reich, L. "Luther," & Keating, A. E. (2018). Peptide design by optimization on a data-parameterized protein interaction landscape. *Proceedings of the National Academy of Sciences*, *115*(44), 201812939. https://doi.org/10.1073/pnas.1812939115

Jiang, P., Du, W., & Wu, M. (2007). p53 and Bad: remote strangers become close friends. *Cell Research*, *17*(4), 283–285. https://doi.org/10.1038/cr.2007.19

Jin, Z., & El-Deiry, W. S. (2005). Overview of cell death signaling pathways. *Cancer Biology & Therapy*, *4*(2), 147–171. https://doi.org/10.4161/cbt.4.2.1508

Jumper, J., Evans, R., Pritzel, A., Green, T., Figurnov, M., Ronneberger, O., Tunyasuvunakool, K., Bates, R., Žídek, A., Potapenko, A., Bridgland, A., Meyer, C., Kohl, S. A. A., Ballard, A. J., Cowie, A., Romera-Paredes, B., Nikolov, S., Jain, R., Adler, J., … Hassabis, D. (2021). Highly accurate protein structure prediction with AlphaFold. *Nature*, *596*(7873), 583–589. https://doi.org/10.1038/s41586-021-03819-2

Kaczmarek, K., Studencka, M., Meinhardt, A., Wieczerzak, K., Thoms, S., Engel, W., & Grzmil, P. (2011). Overexpression of peroxisomal testis-specific 1 protein induces germ cell

apoptosis and leads to infertility in male mice. *Molecular Biology of the Cell*, *22*(10), 1766–1779. https://doi.org/10.1091/mbc.e09-12-0993

Kelly, P. N., & Strasser, A. (2011). The role of Bcl-2 and its pro-survival relatives in tumourigenesis and cancer therapy. *Cell Death & Differentiation*, *18*(9), 1414–1424. https://doi.org/10.1038/cdd.2011.17

Kerr, J. F. R., Wyllie, A. H., & Currie, A. R. (1972). Apoptosis: A Basic Biological Phenomenon with Wideranging Implications in Tissue Kinetics. *British Journal of Cancer*, *26*(4), 239–257. https://doi.org/10.1038/bjc.1972.33

Kim, H., Tu, H.-C., Ren, D., Takeuchi, O., Jeffers, J. R., Zambetti, G. P., Hsieh, J. J.-D., & Cheng, E. H.-Y. (2009). Stepwise Activation of BAX and BAK by tBID, BIM, and PUMA Initiates Mitochondrial Apoptosis. *Molecular Cell*, *36*(3), 487–499. https://doi.org/10.1016/j.molcel.2009.09.030

Kim, J. W., Choi, E.-J., & Joe, C. O. (2000). Activation of death-inducing signaling complex (DISC) by pro-apoptotic C-terminal fragment of RIP. *Oncogene*, *19*(39), 4491–4499. https://doi.org/10.1038/sj.onc.1203796

Kitamura, Y., Shimohama, S., Kamoshima, W., Ota, T., Matsuoka, Y., Nomura, Y., Smith, M. A., Perry, G., Whitehouse, P. J., & Taniguchi, T. (1998). Alteration of proteins regulating apoptosis, Bcl-2, Bcl-x, Bax, Bak, Bad, ICH-1 and CPP32, in Alzheimer's disease. *Brain Research*, *780*(2), 260–269. https://doi.org/10.1016/s0006-8993(97)01202-x

Knudson, C. M., Tung, K. S. K., Tourtellotte, W. G., Brown, G. A. J., & Korsmeyer, S. J. (1995). Bax-Deficient Mice with Lymphoid Hyperplasia and Male Germ Cell Death. *Science*, *270*(5233), 96–99. https://www.jstor.org/stable/2888222

Kuwana, T., Mackey, M. R., Perkins, G., Ellisman, M. H., Latterich, M., Schneiter, R., Green, D. R., & Newmeyer, D. D. (2002). Bid, Bax, and Lipids Cooperate to Form Supramolecular Openings in the Outer Mitochondrial Membrane. *Cell*, *111*(3), 331–342. https://doi.org/10.1016/s0092-8674(02)01036-x

Lee, E. F., Dewson, G., Evangelista, M., Pettikiriarachchi, A., Gold, G. J., Zhu, H., Colman, P. M., & Fairlie, W. D. (2014). The Functional Differences between Pro-survival and Pro-apoptotic B Cell Lymphoma 2 (Bcl-2) Proteins Depend on Structural Differences in Their Bcl-2 Homology 3 (BH3) Domains*. *Journal of Biological Chemistry*, *289*(52), 36001–36017. https://doi.org/10.1074/jbc.m114.610758

Lee, E. F., & Fairlie, W. D. (2019). The Structural Biology of Bcl-xL. *International Journal of Molecular Sciences*, *20*(9), 2234. https://doi.org/10.3390/ijms20092234

Leshchiner, E. S., Braun, C. R., Bird, G. H., & Walensky, L. D. (2013). Direct activation of full-length proapoptotic BAK. *Proceedings of the National Academy of Sciences*, *110*(11), E986–E995. https://doi.org/10.1073/pnas.1214313110

Lindsten, T., Ross, A. J., King, A., Zong, W.-X., Rathmell, J. C., Shiels, H. A., Ulrich, E., Waymire, K. G., Mahar, P., Frauwirth, K., Chen, Y., Wei, M., Eng, V. M., Adelman, D. M., Simon, M. C., Ma, A., Golden, J. A., Evan, G., Korsmeyer, S. J., … Thompson, C. B. (2000).

The Combined Functions of Proapoptotic Bcl-2 Family Members Bak and Bax Are Essential for Normal Development of Multiple Tissues. *Molecular Cell*, *6*(6), 1389–1399. https://doi.org/10.1016/s1097-2765(00)00136-2

Liu, Q., Moldoveanu, T., Sprules, T., Matta-Camacho, E., Mansur-Azzam, N., & Gehring, K. (2010). Apoptotic Regulation by MCL-1 through Heterodimerization*. *Journal of Biological Chemistry*, *285*(25), 19615–19624. https://doi.org/10.1074/jbc.m110.105452

Llambi, F., Moldoveanu, T., Tait, S. W. G., Bouchier-Hayes, L., Temirov, J., McCormick, L. L., Dillon, C. P., & Green, D. R. (2011). A Unified Model of Mammalian BCL-2 Protein Family Interactions at the Mitochondria. *Molecular Cell*, *44*(4), 517–531. https://doi.org/10.1016/j.molcel.2011.10.001

Luck, K., Kim, D.-K., Lambourne, L., Spirohn, K., Begg, B. E., Bian, W., Brignall, R., Cafarelli, T., Campos-Laborie, F. J., Charloteaux, B., Choi, D., Coté, A. G., Daley, M., Deimling, S., Desbuleux, A., Dricot, A., Gebbia, M., Hardy, M. F., Kishore, N., … Calderwood, M. A. (2020). A reference map of the human binary protein interactome. *Nature*, *580*(7803), 402–408. https://doi.org/10.1038/s41586-020-2188-x

Mazarakis, N. D., Edwards, A. D., & Mehmet, H. (1997). Apoptosis in neural development and disease. *Archives of Disease in Childhood*, *77*(3), F165–F170. https://doi.org/10.1136/fn.77.3.f165

McDonnell, J. M., Fushman, D., Milliman, C. L., Korsmeyer, S. J., & Cowburn, D. (1999). Solution Structure of the Proapoptotic Molecule BID A Structural Basis for Apoptotic Agonists and Antagonists. *Cell*, *96*(5), 625–634. https://doi.org/10.1016/s0092-8674(00)80573-5

Mérino, D., Giam, M., Hughes, P. D., Siggs, O. M., Heger, K., O'Reilly, L. A., Adams, J. M., Strasser, A., Lee, E. F., Fairlie, W. D., & Bouillet, P. (2009). The role of BH3-only protein Bim extends beyond inhibiting Bcl-2–like prosurvival proteins. *The Journal of Cell Biology*, *186*(3), 355–362. https://doi.org/10.1083/jcb.200905153

Moldoveanu, T., & Czabotar, P. E. (2019). BAX, BAK, and BOK: A Coming of Age for the BCL-2 Family Effector Proteins. *Cold Spring Harbor Perspectives in Biology*, *12*(4), a036319. https://doi.org/10.1101/cshperspect.a036319

Moldoveanu, T., Grace, C. R., Llambi, F., Nourse, A., Fitzgerald, P., Gehring, K., Kriwacki, R. W., & Green, D. R. (2013). BID-induced structural changes in BAK promote apoptosis. *Nature Structural & Molecular Biology*, *20*(5), 589–597. https://doi.org/10.1038/nsmb.2563

Moldoveanu, T., Liu, Q., Tocilj, A., Watson, M., Shore, G., & Gehring, K. (2006). The X-Ray Structure of a BAK Homodimer Reveals an Inhibitory Zinc Binding Site. *Molecular Cell*, *24*(5), 677–688. https://doi.org/10.1016/j.molcel.2006.10.014

Niu, X., Brahmbhatt, H., Mergenthaler, P., Zhang, Z., Sang, J., Daude, M., Ehlert, F. G. R., Diederich, W. E., Wong, E., Zhu, W., Pogmore, J., Nandy, J. P., Satyanarayana, M., Jimmidi, R. K., Arya, P., Leber, B., Lin, J., Culmsee, C., Yi, J., & Andrews, D. W. (2017). A Small-Molecule Inhibitor of Bax and Bak Oligomerization Prevents Genotoxic Cell Death and Promotes Neuroprotection. *Cell Chemical Biology*, *24*(4), 493-506.e5. https://doi.org/10.1016/j.chembiol.2017.03.011

Oltvai, Z. N., Milliman, C. L., & Korsmeyer, S. J. (1993). Bcl-2 heterodimerizes in vivo with a conserved homolog, Bax, that accelerates programed cell death. *Cell*, *74*(4), 609–619. https://doi.org/10.1016/0092-8674(93)90509-o

Pedersen, A., Wallgren, M., Karlsson, B. G., & Gröbner, G. (2011). Expression and purification of full-length anti-apoptotic Bcl-2 using cell-free protein synthesis. *Protein Expression and Purification*, *77*(2), 220–223. https://doi.org/10.1016/j.pep.2011.02.003

Placzek, W. J., Wei, J., Kitada, S., Zhai, D., Reed, J. C., & Pellecchia, M. (2010). A survey of the anti-apoptotic Bcl-2 subfamily expression in cancer types provides a platform to predict the efficacy of Bcl-2 antagonists in cancer therapy. *Cell Death & Disease*, *1*(5), e40. https://doi.org/10.1038/cddis.2010.18

Print, C. G., Loveland, K. L., Gibson, L., Meehan, T., Stylianou, A., Wreford, N., Kretser, D. D., Metcalf, D., ̈ntgen, F. K., Adams, J. M., & Cory, S. (1998). Apoptosis regulator Bcl-w is essential for spermatogenesis but appears otherwise redundant. *Proceedings of the National Academy of Sciences of the United States of America*, *95*, 12424–12431.

Pritz, J. R., Wachter, F., Lee, S., Luccarelli, J., Wales, T. E., Cohen, D. T., Coote, P. W., Heffron, G. J., Engen, J. R., Massefski, W., & Walensky, L. D. (2017). Allosteric Sensitization of Pro-Apoptotic BAX. *Nature Chemical Biology*, *13*(9), 961–967. https://doi.org/10.1038/nchembio.2433

Rathmell, J. C., Lindsten, T., Zong, W.-X., Cinalli, R. M., & Thompson, C. B. (2002). Deficiency in Bak and Bax perturbs thymic selection and lymphoid homeostasis. *Nature Immunology*, *3*(10), 932–939. https://doi.org/10.1038/ni834

Reich, L. “Luther,” Dutta, S., & Keating, A. E. (2016). Generating High-Accuracy Peptide-Binding Data in High Throughput with Yeast Surface Display and SORTCERY. In *Stoddard B. (eds) Computational Design of Ligand Binding Proteins* (Vol. 1414, pp. 233–247). Humana Press, New York, NY. https://doi.org/https://doi-org.libproxy.mit.edu/10.1007/978-1-4939-3569-7_14

Reyna, D. E., Garner, T. P., Lopez, A., Kopp, F., Choudhary, G. S., Sridharan, A., Narayanagari, S.-R., Mitchell, K., Dong, B., Bartholdy, B. A., Walensky, L. D., Verma, A., Steidl, U., & Gavathiotis, E. (2017). Direct Activation of BAX by BTSA1 Overcomes Apoptosis Resistance in Acute Myeloid Leukemia. *Cancer Cell*, *32*(4), 490-505.e10. https://doi.org/10.1016/j.ccell.2017.09.001

Robin, A. Y., Kumar, K. K., Westphal, D., Wardak, A. Z., Thompson, G. V., Dewson, G., Colman, P. M., & Czabotar, P. E. (2015). Crystal structure of Bax bound to the BH3 peptide of Bim identifies important contacts for interaction. *Cell Death & Disease*, *6*(7), e1809–e1809. https://doi.org/10.1038/cddis.2015.141

Roehrl, M. H. A., Wang, J. Y., & Wagner, G. (2004). A General Framework for Development and Data Analysis of Competitive High-Throughput Screens for Small-Molecule Inhibitors of Protein-Protein Interactions by Fluorescence Polarization. *Biochemistry*, *43*(51), 16056–16066. https://doi.org/10.1021/bi048233g

Salvador-Gallego, R., Mund, M., Cosentino, K., Schneider, J., Unsay, J., Schraermeyer, U., Engelhardt, J., Ries, J., & García-Sáez, A. J. (2016). Bax assembly into rings and arcs in apoptotic mitochondria is linked to membrane pores. *The EMBO Journal*, *35*(4), 389–401. https://doi.org/10.15252/embj.201593384

Sandow, J. J., Tan, I. K., Huang, A. S., Masaldan, S., Bernardini, J. P., Wardak, A. Z., Birkinshaw, R. W., Ninnis, R. L., Liu, Z., Dalseno, D., Lio, D., Infusini, G., Czabotar, P. E., Webb, A. I., & Dewson, G. (2021). Dynamic reconfiguration of pro-apoptotic BAK on membranes. *The EMBO Journal*, *40*(20), e107237. https://doi.org/10.15252/embj.2020107237

Sarosiek, K. A., Chi, X., Bachman, J. A., Sims, J. J., Montero, J., Patel, L., Flanagan, A., Andrews, D. W., Sorger, P., & Letai, A. (2013). BID Preferentially Activates BAK while BIM Preferentially Activates BAX, Affecting Chemotherapy Response. *Molecular Cell*, *51*(6), 751–765. https://doi.org/10.1016/j.molcel.2013.08.048

Sarosiek, K. A., Fraser, C., Muthalagu, N., Bhola, P. D., Chang, W., McBrayer, S. K., Cantlon, A., Fisch, S., Golomb-Mello, G., Ryan, J. A., Deng, J., Jian, B., Corbett, C., Goldenberg, M., Madsen, J. R., Liao, R., Walsh, D., Sedivy, J., Murphy, D. J., … Letai, A. (2017). Developmental Regulation of Mitochondrial Apoptosis by c-Myc Governs Age- and Tissue-Specific Sensitivity to Cancer Therapeutics. *Cancer Cell*, *31*(1), 142–156. https://doi.org/10.1016/j.ccell.2016.11.011

Sattler, M., Liang, H., Nettesheim, D., Meadows, R. P., Harlan, J. E., Eberstadt, M., Yoon, H. S., Shuker, S. B., Chang, B. S., Minn, A. J., Thompson, C. B., & Fesik, S. W. (1997). Structure of Bcl-XL_-Bak Peptide Complex: Recognition between Regulators of Apoptosis. *Science*, *275*(5302), 983–986.

Shepherd, N. E., Hoang, H. N., Abbenante, G., & Fairlie, D. P. (2005). Single Turn Peptide Alpha Helices with Exceptional Stability in Water. *Journal of the American Chemical Society*, *127*(9), 2974–2983. https://doi.org/10.1021/ja0456003

Shi, Y. (2004). Caspase activation, inhibition, and reactivation: A mechanistic view. *Protein Science*, *13*(8), 1979–1987. https://doi.org/10.1110/ps.04789804

Singh, G., Guibao, C. D., Seetharaman, J., Aggarwal, A., Grace, C. R., McNamara, D. E., Vaithiyalingam, S., Waddell, M. B., & Moldoveanu, T. (2022). Structural basis of BAK activation in mitochondrial apoptosis initiation. *Nature Communications*, *13*(1), 250. https://doi.org/10.1038/s41467-021-27851-y

Singh, R., Letai, A., & Sarosiek, K. (2019). Regulation of apoptosis in health and disease: the balancing act of BCL-2 family proteins. *Nature Reviews Molecular Cell Biology*, *20*(3), 175–193. https://doi.org/10.1038/s41580-018-0089-8

Subburaj, Y., Cosentino, K., Axmann, M., Pedrueza-Villalmanzo, E., Hermann, E., Bleicken, S., Spatz, J., & García-Sáez, A. J. (2015). Bax monomers form dimer units in the membrane that further self-assemble into multiple oligomeric species. *Nature Communications*, *6*(1), 8042. https://doi.org/10.1038/ncomms9042

Swanson, S., Sivaraman, V., Grigoryan, G., & Keating, A. E. (2022). Tertiary motifs as building blocks for the design of protein-binding peptides. *Protein Science, Submitted*.

Tait, S. W. G., & Green, D. R. (2010). Mitochondria and cell death: outer membrane permeabilization and beyond. *Nature Reviews Molecular Cell Biology*, *11*(9), 621–632. https://doi.org/10.1038/nrm2952

Takeuchi, O., Fisher, J., Suh, H., Harada, H., Malynn, B. A., & Korsmeyer, S. J. (2005). Essential role of BAX,BAK in B cell homeostasis and prevention of autoimmune disease. *Proceedings of the National Academy of Sciences*, *102*(32), 11272–11277. https://doi.org/10.1073/pnas.0504783102

Truebestein, L., & Leonard, T. A. (2016). Coiled-coils: The long and short of it. *BioEssays*, *38*(9), 903–916. https://doi.org/10.1002/bies.201600062

Tsujimoto, Y., Cossman, J., Jaffe, E., & Croce, C. M. (1985). Involvement of the bcl-2 Gene in Human Follicular Lymphoma. *Science*, *228*, 1440–1443. https://www.jstor.org/stable/1695708

Tsujimoto, Y., Finger, L. R., Yunis, J., Nowell, P. C., & Croce, C. M. (1984). Cloning of the Chromosome Breakpoint of Neoplastic B Cells with the t(14;18) Chromosome Translocation. *Science*, *226*(4678), 1097–1099. https://www.jstor.org/stable/1693640

Tunyasuvunakool, K., Adler, J., Wu, Z., Green, T., Zielinski, M., Žídek, A., Bridgland, A., Cowie, A., Meyer, C., Laydon, A., Velankar, S., Kleywegt, G. J., Bateman, A., Evans, R., Pritzel, A., Figurnov, M., Ronneberger, O., Bates, R., Kohl, S. A. A., … Hassabis, D. (2021). Highly accurate protein structure prediction for the human proteome. *Nature*, *596*(7873), 590–596. https://doi.org/10.1038/s41586-021-03828-1

Uren, R. T., O'Hely, M., Iyer, S., Bartolo, R., Shi, M. X., Brouwer, J. M., Alsop, A. E., Dewson, G., & Kluck, R. M. (2017). Disordered clusters of Bak dimers rupture mitochondria during apoptosis. *ELife*, *6*, e19944. https://doi.org/10.7554/elife.19944

Willis, S. N., Chen, L., Dewson, G., Wei, A., Naik, E., Fletcher, J. I., Adams, J. M., & Huang, D. C. S. (2005). Proapoptotic Bak is sequestered by Mcl-1 and Bcl-xL, but not Bcl-2, until displaced by BH3-only proteins. *Genes & Development*, *19*(11), 1294–1305. https://doi.org/10.1101/gad.1304105

Willis, S. N., Fletcher, J. I., Kaufmann, T., Delft, M. F. van, Chen, L., Czabotar, P. E., Ierino, H., Lee, E. F., Fairlie, W. D., Bouillet, P., Strasser, A., Kluck, R. M., Adams, J. M., & Huang, D. C. S. (2007). Apoptosis Initiated When BH3 Ligands Engage Multiple Bcl-2 Homologs, Not Bax or Bak. *Science*, *315*(5813), 856–859. https://doi.org/10.1126/science.1133289

Xin, M., Li, R., Xie, M., Park, D., Owonikoko, T. K., Sica, G. L., Corsino, P. E., Zhou, J., Ding, C., White, M. A., Magis, A. T., Ramalingam, S. S., Curran, W. J., Khuri, F. R., & Deng, X. (2014). Small Molecule Bax Agonists for Cancer Therapy. *Nature Communications*, *5*(1), 4935–4935. https://doi.org/10.1038/ncomms5935

Youle, R. J., & Strasser, A. (2008). The BCL-2 protein family: opposing activities that mediate cell death. *Nature Reviews Molecular Cell Biology*, *9*(1), 47–59. https://doi.org/10.1038/nrm2308

Yuan, Z., Dewson, G., Czabotar, P. E., & Birkinshaw, R. W. (2021). VDAC2 and the BCL-2 family of proteins. *Biochemical Society Transactions*, *49*(6), 2787–2795. https://doi.org/10.1042/bst20210753

Zheng, J. H., Follis, A. V., Kriwacki, R. W., & Moldoveanu, T. (2016). Discoveries and controversies in BCL-2 protein-mediated apoptosis. *The FEBS Journal*, *283*(14), 2690–2700. https://doi.org/10.1111/febs.13527

Zhou, J., & Grigoryan, G. (2015). Rapid search for tertiary fragments reveals protein sequence–structure relationships. *Protein Science*, *24*(4), 508–524. https://doi.org/10.1002/pro.2610

Zhou, J., Panaitiu, A. E., & Grigoryan, G. (2020). A general-purpose protein design framework based on mining sequence–structure relationships in known protein structures. *Proceedings of the National Academy of Sciences of the United States of America*, *117*(2), 1059–1068. https://doi.org/10.1073/pnas.1908723117

CHAPTER 2

Paper Title: Discovery of diverse human BH3-only and non-native peptide binders of pro-apoptotic BAK indicate that activators and inhibitors use a similar binding mode and are not distinguished by binding affinity or kinetics

Authors: Fiona Aguilar[1], Stacey Yu[2,3,4], Robert Grant[1], Sebastian Swanson[1], Dia Ghose[1], Bonnie G Su[1], Kristopher A. Sarosiek[2,3,4], and Amy E. Keating[1,5,6 *]

Affiliations

[1] Department of Biology, Massachusetts Institute of Technology, Cambridge, MA, USA

[2] Laboratory of Systems Pharmacology, Harvard Program in Therapeutic Science, Department of Systems Biology, Harvard Medical School, Boston, MA, USA

[3] Program in Molecular and Integrative Physiological Sciences Program, Harvard T.H. Chan School of Public Health, Boston, MA, USA

[4] John B. Little Center for Radiation Sciences, Harvard T.H. Chan School of Public Health, Boston, MA, USA

[5] Department of Biological Engineering, Massachusetts Institute of Technology, Cambridge, MA, USA

[6] Koch Institute for Integrative Cancer Research, Massachusetts Institute of Technology, Cambridge, MA, USA

*corresponding author

bioRxiv Citation

Aguilar F, Yu S, Grant RA, Swanson S, Ghose D, Su B, Sarosiek KA, Keating AE. Discovery of diverse human BH3-only and non-native peptide binders of pro-apoptotic BAK indicate that activators and inhibitors use a similar binding mode and are not distinguished by binding affinity or kinetics. bioRxiv doi: 10.1101/2022.05.07.491048

Author Contribution

F.A. and A.E.K. conceptualized project, designed and analyzed experiments, and wrote the paper. F.A. performed all biochemical and structural experiments. S.Y. conducted cell-based assays. R.A.G. directed and assisted with crystallography. S.S. conducted peptide computational design and RMSD calculations. B.G.S. assisted with crystallography and assay development. D.G. assisted with cell-surface display experiments. K.A.S. helped with the design and interpretation of cell-based experiments.

List of Figures

Figure 1. Model of BAK activation based on previously published putative intermediate crystal structures 45
Figure 2. Three methods to obtain peptides binders of BAK 48
Figure 3. Candidate BH3-only peptides bind BAK with a range of affinities 52
Figure 4. AlphaFold structure predictions for human BAK binding proteins..... 53
Figure 5. AlphaFold Predicted Aligned Error for predicted structures of human proteins 53
Figure 6. Localization of BAK to the liposome membrane is necessary for BID BH3-triggered dye release 56
Figure 7. Dye release increases with increasing concentrations of BAK 56
Figure 8. Peptides from Bcl-2 BH3-only proteins show differences in BAK activation function 57
Figure 9. BAK contains 5 hydrophobic pockets referred to as h0, h1, h2, h3, and h4 ..59
Figure 10. Point mutations at hydrophobic positions increase the activation potency of BH3 peptides from proteins NOXA and PUMA 59
Figure 11. dM2, dF8, dM4, BNIP5, and PXT1 peptides function as BAK activators, ...61
Figure 12. Peptides dF8, dM2, and dM4 act as activators alone and in the presence of BIM-RT BH3..... 62
Figure 13. Peptides dF2, dF3, dF4, 5vx0, BK1, BimPcRT, and dF7 inhibit activation of BAK by BIM-RT..... 63
Figure 14. CASP3, TERT, and TRPM7 BH3 peptides show BAK-independent membrane disruption at high concentrations 64
Figure 15. Circular dichroism (CD) experiments do not support heterodimerzation of inhibitor peptides with BIM-RT 66
Figure 16. Diagram of BH3 profiling assay 67
Figure 17. Non-native peptides and human BNIP5 and PXT1 peptides induce membrane permeabilization cells..... 68
Figure 18. Western blot performed on 72-hour treated siRNA HeLa cells shows levels of BAK and BAX, with GAPDH as a loading control..... 69
Figure 19. dF2, dF3, and dM2 bind to BAK similarly to other inhibitor and activator BH3 peptides 72
Figure 20. Peptide inhibitors containing non-natural amino acids bind to BAK in very similar binding modes 73
Figure 21. Activator dM2 binds differently compared to BAK BH3 and Bim-RT activator peptides 74
Figure 22. Activators and inhibitors of BAK bind with no systematic differences in structure..... 76
Figure 23. Cavity sizes in BAK: peptide complexes do not correlate with function 78

Figure 24. Sequence logos of activators and inhibitors show few residue preferences 78
Figure 25. Pairwise RMSD calculations of activator vs. inhibitor peptides show an average RMSD of 1.1 79
Figure 26. Neither rate constants nor affinities are indicative of peptide activator vs. inhibitor function 80
Figure 27. Free energy diagram for BH3 peptide activation or inhibition of BAK 86
Figure 28. Free energy diagram to explain differences between activators and inhibitors of BAK 88
Figure 29. Raw liposome data of activator peptides 100
Figure 30. Raw liposome data of inhibitors 101

List of Tables

Table 1. BAK-binding signal for peptides that interact with anti-apoptotic Bcl-2 family proteins tested using yeast-surface display 49
Table 2. Energy scores for BAK:peptide complexes calculated using dTERMen and ranked from lowest (best) to highest 51
Table 3. Known and candidate BH3 motifs in human proteins 54
Table 4. AlphaFold structure predictions and BH3 accessibility 54
Table 5. Alignment of peptide sequences tested for activation 58
Table 6. Percent helical content does not correlate with functional differences between inhibitors and activators 65
Table 7. Peptide sequences used for BH3 profiling assay 67
Table 8. X-ray data collection and refinement statistics 71
Table 9. Biolayer interferometry kinetics for BH3 peptides binding to BAK show a range of affinities that do not correlate with activation function 81
Table 10. Fluorescence anisotropy measurements 81
Table 11. Affinities determined using biolayer interferometry vs. fluorescence polarization give consistent classifications of peptide binders of BAK 81

INTRODUCTION

BAK is a pro-apoptotic member of the BCL-2 protein family (Chittenden et al., 1995). It plays a key role in regulating apoptosis, a programmed form of cell death that is important for development and tissue homeostasis, and its dysregulation can lead to a range of diseases (Duque-Parra, 2005; Kerr et al., 1972; Lindsten et al., 2000; R. Singh et al., 2019). For example, BAK is implicated in hematopoietic regulation through the clearance of mature T and B lymphocytes (Takeuchi et al., 2005; Rathmell et al., 2002). Moreover, over-expression of BAK has been found in human brains from Alzheimer's patients (Kitamura et al., 1998). Age- and tissue-specific differences in expression levels of BAK and the related protein BAX give rise to differences in sensitivity to cancer therapeutics (Sarosiek et al., 2017).

In an irreversible step toward cell death, BAK and BAX promote apoptosis via mitochondrial outer membrane permeabilization (MOMP) in response to a variety of signals (Tait & Green, 2010). Structural, biochemical, and cell biological studies have illuminated some aspects of the mechanism of membrane permeabilization by BAK and BAX, yet a full understanding remains elusive due to the dynamic nature of these proteins, the lipid environment in which they function, and the complex multilayered BCL-2 network that provides regulatory control (Sandow et al., 2021; Delbridge et al., 2016). In this study, we addressed early steps in the activation of BAK in which the binding of certain BCL-2 family members to form heterodimers leads to a conformation change that is required for downstream steps including BAK dimerization and higher-order oligomerization.

The BCL-2 family can be subdivided into three groups: anti-apoptotic proteins, pro-apoptotic proteins, and BH3-only proteins. All family members contain a Bcl-2 homology 3 (BH3) motif (Aouacheria et al., 2013); the anti-apoptotic and pro-apoptotic proteins additionally contain other conserved motifs (BH1, BH2, BH4) (Youle & Strasser, 2008). Anti-apoptotic and pro-apoptotic proteins include a C-terminal transmembrane segment that can anchor them in the mitochondrial outer membrane (MOM), and 8 helices that adopt a globular fold localized to the cytoplasmic face of the membrane (Youle & Strasser, 2008). This globular domain contains a hydrophobic groove that can be bound in trans by the BH3 motif regions of other MOM-anchored BCL-2 proteins (Sattler et al., 1997). The pro-apoptotic proteins include BAK, BAX, and less-studied BOK (Moldoveanu & Czabotar, 2019). BAK and BAX are structurally and functionally very similar, although differences in the mechanistic details of their overall-similar functions have been reported (Sarosiek et al., 2013; Czabotar et al., 2013; Brouwer et al., 2014; Garner et al., 2016).

BH3-only proteins can be classified based on their functions as either 'sensitizers' or 'activators'. All known BH3-only proteins bind to anti-apoptotic proteins with high affinity ($K_d \leq 10$ nM), competitively inhibiting their engagement of BAK and BAX, and thus *sensitizing* the cell to undergo apoptosis (Willis et al., 2005; Willis et al., 2007; Zheng et al., 2016). Only three human proteins contain BH3 motifs that can bind directly to BAK and induce a conformational change that leads to BAK dimerization and then MOMP: truncated BID (tBID), BIM, and PUMA; we refer to these as 'activators' (H. Kim et al., 2009; Llambi et al., 2011; Dai et al., 2014). The sequence and structural features that distinguish a sensitizer from an activator are unknown, as is the mechanism of BH3-binding induced activation.

There is controversy in the field regarding the requirement of direct activation for BAK-dependent cell death. On one hand, there is clear evidence from biochemical studies using liposomes that BH3 peptides can directly activate both BAK and BAX (Brouwer et al., 2017; Gavathiotis et al., 2008; G. Singh et al., 2022). Adding such peptides to mitochondria or to permeabilized cells with intact mitochondria also induces MOMP (Sarosiek et al., 2013; Moldoveanu et al., 2013). The indirect activation model, on the other hand, posits that the binding of BH3 proteins to anti-apoptotic proteins localized at the mitochondria is sufficient to allow unimpeded, spontaneous activation of BAK or BAX, perhaps triggered by the mitochondrial membrane itself (K. Huang et al., 2019). In this model, activator BH3-only proteins are not required for binding to BAK or BAX. The strongest evidence for this model comes from experiments involving inducible expression of sensitizer BAD (a binder of anti-apoptotics BCL-2, BCL-X_L, and BCLW, but not BAK or BAX) in cells lacking all other BH3-only proteins and anti-apoptotic MCL-1 (K. Huang et al., 2019). In this setting, expression of BAD alone is sufficient to induce BAX-mediated MOMP (K. Huang et al., 2019). A key question is whether all activating proteins were depleted in these cell lines, or whether unknown activators might have had some role in these experiments. Also, further studies looking at BAK in addition to BAX and using physiological concentrations of protein will also help clarify the implications of this important work.

Regardless of the relative roles of direct vs. indirect BAK activation *in vivo*, direct activation is robust and well-established *in vitro* assays consisting of liposomes, recombinant protein, and BH3 peptides suggesting that it can be induced by endogenous or exogenous BH3 activators in cells, regardless of whether this is absolutely required for cell death. We will focus on this direct activation model throughout the rest of the paper.

Structures and crosslinking studies have provided a working model to describe some of the steps involved in BAK activation, i.e. the path that is taken from a membrane-tethered monomer (PDB: 2IMS) to a BH3 bound monomer (PDB: 5VX0) and ultimately a membrane-

embedded associations of dimers (**Figure 1**) (Brouwer et al., 2017; Kuwana et al., 2002; Sandow et al., 2021). Both crystal structures and crosslinking support a conformational change in which the "latch" region (α6-α8) disengages from the BAK "core" region (α2-α5) (PDB: 5VWV) (Brouwer et al., 2014). Two activated BAK monomers can then exchange BH3 helices and form stable BH3: groove homodimers (PDB:7K02) on the mitochondrial outer membrane that then associate with other dimers and ultimately give rise to MOMP (Brouwer et al., 2014; Birkinshaw et al., 2021).

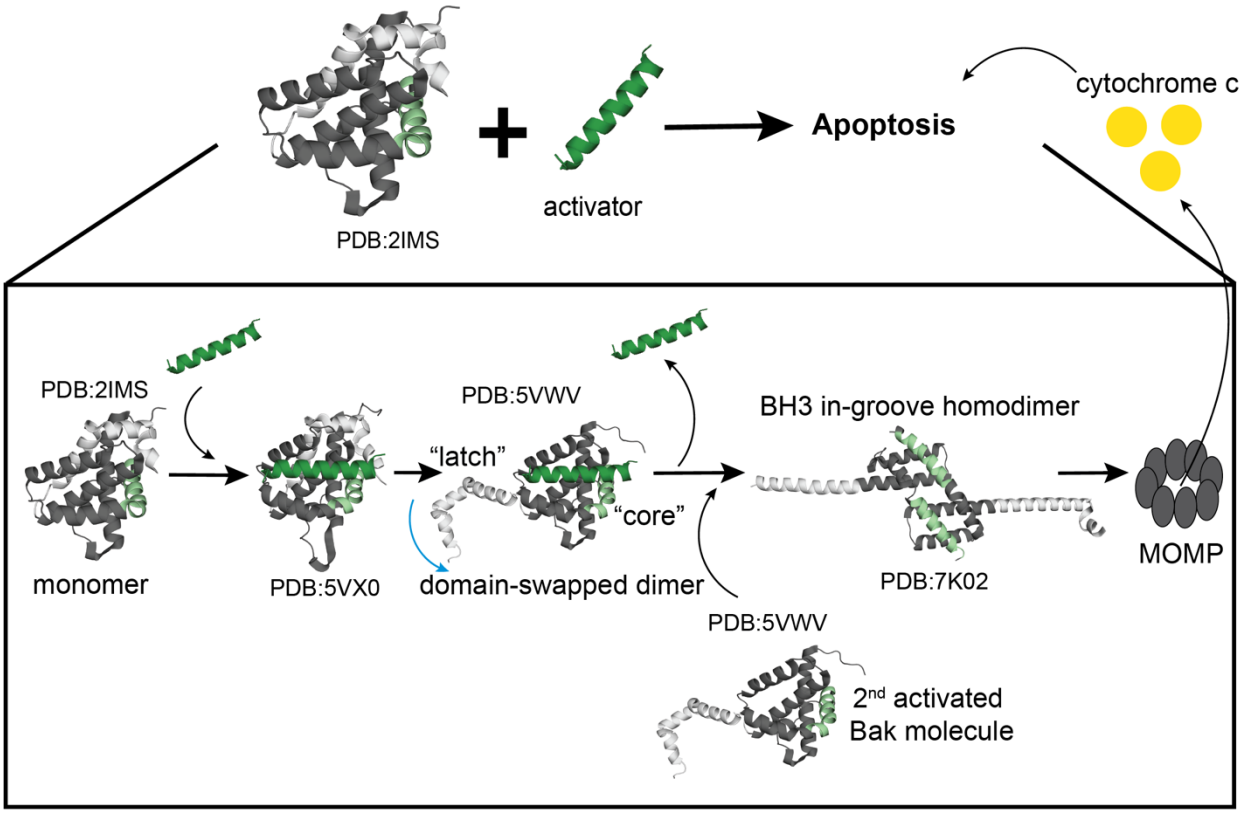

Figure 1. Model of BAK activation based on previously published putative intermediate crystal structures. The current model for BAK activation involves binding of a BH3 segment (dark green) from an activating protein to monomeric BAK (grey) (PDB:2IMS), as observed in the structure of BAK bound to a modified BIM BH3 peptide (PDB:5VX0). Binding leads to release of the BAK "latch" (α6-α8) (light grey) from the "core" (α1-α5) (dark grey) as observed in domain-swapped structures of BAK (PDB:5VWV). Subsequent conformational changes lead to a "BH3-in-groove" dimer (PDB:7K02) formed by the core regions of two BAK monomers that exchange BH3 helices (light green).

Given their therapeutic potential to treat cancer or neurodegenerative diseases, there is great interest in developing tools to both probe BAK and BAX function and understand their complex activation mechanisms (Reyna et al., 2017; Pritz et al., 2017; Niu et al., 2017; Delft et

al., 2019; Iyer et al., 2020) . For example, previous research has shown that is it possible to bind BAK and inhibit rather than activate it, using tight binding peptides containing non-natural amino acids (Brouwer et al., 2017). Conversely, antibodies targeting the α1-α2 loop of BAK can induce MOMP, demonstrating an alternative binding site to trigger activation (Iyer et al., 2016). Other groups have developed small molecules that promote or directly activate BAX (Pritz et al., 2017) as well as inhibit BAX oligomerization (Niu et al., 2017).

In this study, we explored the sequence space of peptide binders of BAK using computational structure-based design and cell surface display. We obtained novel non-native BAK-binding peptides with diverse sequences. Additionally, we discovered 9 previously unknown binders of BAK in the human proteome, two of which function as activators in liposome assays and in mitochondrial permeabilization assays. We conduct functional, biophysical, and structural studies on these peptide to dissect differences between peptide activators and inhibitors of BAK. Our results indicate that binding affinity, binding kinetics, and binding geometry are not sufficient to clearly distinguish between the two. We speculate on the energetic requirements in each case and propose an energy-landscape model to summarize our findings.

RESULTS

SECTION 1.1 STRUCTURE-BASED DESIGN AND LIBRARY SCREENING IDENTIFY NOVEL PEPTIDE BINDERS OF BAK

To discover novel binders of BAK that could function as activators or inhibitors, we used computational peptide design and cell-surface screening of candidate BH3-like peptides (**Figure 2**). **D**esign with **TERM** energies (dTERMen) is a computational method that computes statistical energies from repeating structural elements in known protein structures and has been applied to design peptide binders of anti-apoptotic BCL-2 proteins (**Table 1**) (Zhou et al., 2020; Frappier et al., 2019). Given a protein backbone structure, dTERMen mines a diverse database of known structures to identify matches to component motifs and uses the sequences of the matches to compute a Potts model that gives energy as a function of sequence. Optimizing this function rapidly provides the sequence that is predicted to be most compatible with the target structure. As input into dTERMen for BAK-binder design, we used the crystal structure of BAK in complex with BIM-h3Glg (PDB:5VX0), a peptide that contains a non-natural amino acid with a long side chain. BIM-h3Glg functions as an inhibitor of BAK activation (Brouwer et al., 2017)(**Figure 2A**). Our designed peptide, BK3, binds to BAK (see below) and, interestingly, contains lysine at position 3f, which is conserved as aspartate in native BH3 peptides and is glutamate in some other BAK binders that we studied (see below).

We identified additional BAK binders through yeast-surface display screening of previously published BH3-like peptide binders of anti-apoptotic BCL-2 family proteins (**Figure 2B and Table 1**). Based on the structural similarity of BAK to BCL-x_L, MCL-1, and BFL-1, and the fact that BH3 peptides from BIM, BID, and PUMA bind to both the pro- and anti-apoptotic BCL-2 family members, we reasoned that these designed peptides might also bind pro-apoptotic BAK. Prior work used a monovalent yeast surface-display assay (Dutta et al., 2015; Jenson et al., 2017). However, BID and BIM BH3 peptides bind to BAK much more weakly than they bind to the anti-apoptotic family members (data not shown), so we adapted the yeast-surface display framework to a multi-valent format, using pre-tetramerized BAK to enhance avidity (**Figure 2B**). We tested 28 peptides and discovered 19 that bound to tetramerized BAK on the yeast surface (**Table 1**). Binding profiles measured by Fluorescence Activated Cell Sorting (FACS) were categorized into 4 groups based on binding signal relative to peptide expression: high, medium, low, or no binding (**Figure 2B**). We performed further characterization of sequences from the high-binding group, which included designed peptide BK3, as described below.

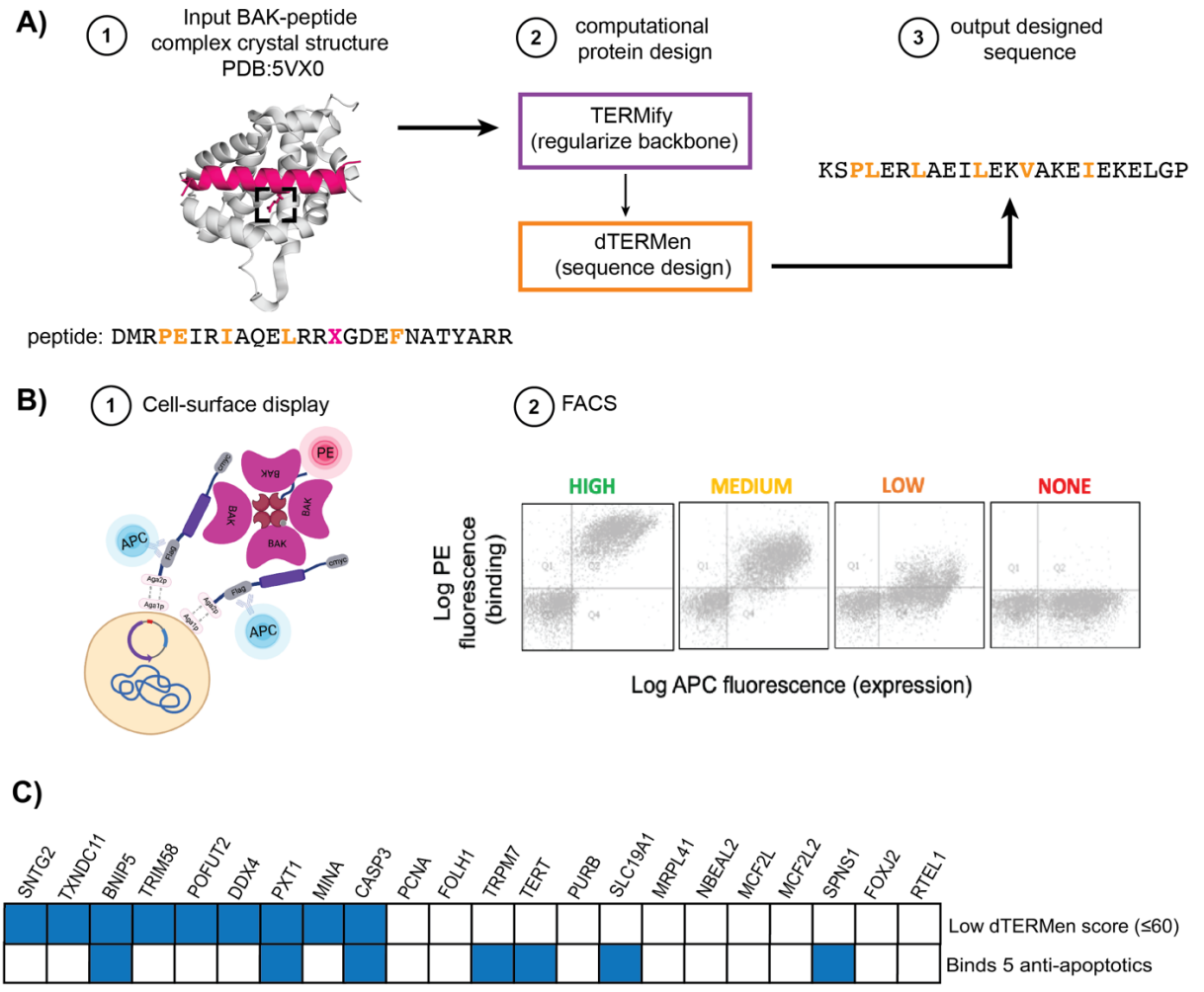

Figure 2. Three methods to obtain peptides binders of BAK. A) The structure of BAK bound to Bim-h3Glg (PDB:5VX0) was used as input for computational re-design using dTERMen to generate novel BAK binding sequence BK3. A non-natural amino acid is depicted with an X in the input peptide sequence and surrounded with a dashed box in the structure. **B)** Cartoon representation of the yeast surface display assay used to test candidate binders of BAK. Peptide expression was detected using an HA tag and binding to BAK tetramers was quantified using SAPE fluorescence. High-binding (green), medium-binding (light orange), low-binding (dark orange), and non-binding (red) peptides were determined based on binding vs. peptide expression signals using flow cytometry. Peptides were assigned manually to one of these four categories. **C)** BH3-like regions in human proteins reported by DeBartolo *et al*. were scored for binding to pro-apoptotic BAK using dTERMen. Those with favorable, low-energy scores are indicated in blue. Proteins containing peptides that bind all five of BCL-2, BCL-x_L, MCL-1, BFL-1, and BCL-W are also indicated in blue. BH3 peptides from all of the proteins that are indicated in blue were subsequently tested for binding to BAK.

Peptide name	Sequence	Source	FACS profile
	1 | 2 | 3 | 4 | 5		
	cdefgabcdefgabcdefgabcdefgabcdefg		
	h0 h1 h2 h3 h4		
dF4	---SLLEKLAEYLRQMADEINKKYVK-------	Frappier, V. *et al.*	high
dF3	---SLLEKLAEELRQLADELNKKFEK-------	Frappier, V. *et al.*	high
dF7	---SLLEKLAEELAQLADELNKKFEK-------	Frappier, V. *et al.*	high
BIM	-DMRPEIWIAQELRRIGDEFNAYYAR-------	BH3-only protein	high
dM2	--APYLEQVARTLRKIGEEINEALR--------	Frappier, V. *et al.*	high
dM3	--DKTLEEIARELAKLAEEIDKEI---------	Frappier, V. *et al.*	high
dF2	---SYIDKIADLIRKVAEEINSKLE--------	Frappier, V. *et al.*	high
BK3	--KSPLERLAEILEKVAKEIEKELGP-------	dTERMen (this work)	high
dM4	--DKTLEEIARWLARLALEIDKEI---------	Frappier, V. *et al.*	high
dF8	---SLLEKLAEYLAQMGDEINKKYVK-------	Frappier, V. *et al.*	medium
dF6	---SYIDKIADLIDKVVEEINSKLE--------	Frappier, V. *et al.*	medium
dM5	--APKEKEVARTLIKIGEEINEALK--------	Frappier, V. *et al.*	medium
dM7	--DKTLEEIARELLKLALEIDKEI---------	Frappier, V. *et al.*	medium
dM1	--APKEKEVAETLRKIGEEINEALK--------	Frappier, V. *et al.*	low
dM9	---DIEQEIAEALKEVADELSKAIED-------	Frappier, V. *et al.*	low
dM6	--APYLEQVARTLLHIGMEINEALR--------	Frappier, V. *et al.*	low
dF5	---SYVDKIADLMKKVAEKINSDLT--------	Frappier, V. *et al.*	low
MF2	--GRWIDQIAQFLRRIGDHIEKYI---------	Jenson, J.M. *et al.*	none
dM10	---DVVLSVAETLRELADRLYEEINT-------	Frappier, V. *et al.*	none
M1	--GRSELEVVQELVRIGDIVVAYF---------	Jenson, J.M. *et al.*	none
MF6	--GRRVDEIAQILRRIGDNVTTYI---------	Jenson, J.M. *et al.*	none
XF2	--GRREVWLSQSLKRIADQFQKYL---------	Jenson, J.M. *et al.*	none
M9	--GRSQYEVIQELIRIGDIVLAYF---------	Jenson, J.M. *et al.*	none
F10	--GRRVVQIAAGLRRAGDQLEKYG---------	Jenson, J.M. *et al.*	none
BAD	PNLWAAQRYGRELRRMSDEFVDSFKKGLPRPK-	BH3-only protein	none
X7	--GQPLIWFGAQLRRGADEFAAQR---------	Jenson, J.M. *et al.*	none
F4	--GQRVVHIAAGLRRTGDQLEAYG---------	Jenson, J.M. *et al.*	none
X1	--GQTLIWYGASLRRYADEFAKQR---------	Jenson, J.M. *et al.*	none
XF1	--GRRVVWIGQGLKRLADEYHKYA---------	Jenson, J.M. *et al.*	none
MX1	--GRSQIWYVQELVRGGDVNHAYR---------	Jenson, J.M. *et al.*	none
MX7	--GRSEIWYDQELVRSGDVNAAYR---------	Jenson, J.M. *et al.*	none

Table 1. BAK-binding signal for peptides that interact with anti-apoptotic Bcl-2 family proteins tested using yeast-surface display. Residues in the L-xxxx-D/E BH3 motif are highlighted are bolded.

Residues that align with positions of BIM that bind into hydrophobic pockets on BAK are in orange; residues in green are exceptions to the residue types typically found in BH3 motifs.

SECTION 1.2 DISCOVERY OF NEW HUMAN BH3-ONLY BINDERS OF BAK

In prior work, DeBartolo *et al*. scanned the human proteome to identify candidate, previously unidentified BH3-only sequences (DeBartolo et al., 2014). The survey employed structure-based scoring combined with experimental screening using SPOT arrays and identified 34 peptides that bound detectably to at least one of the five anti-apoptotic proteins MCL-1, BCL-X_L, BCL-2, BFL-1, and BCL-W (DeBartolo et al., 2014). Given the high structural similarity between pro-apoptotic BAK and the anti-apoptotic proteins, we reasoned that some of the peptides might also bind BAK (**Figure 2C)**. Using three BAK-BH3 peptide complex structures that we solved as part of this work (see below), we aligned each of the 22 human proteome candidate sequences that had affinities of $K_d \leq 500$ nM to anti-apoptotic members to the peptides in our crystal structures and calculated an energy score using dTERMen. This generated 3 different scores per candidate peptide (**Figure 2C and Table 2).** We tested binding of the top 7 ranked BH3-only peptides using fluorescence anisotropy and discovered three new binders (**Table 2 and Figure 3A**). Of the three, BNIP5 bound most tightly, with K_d = 0.4 μM. PXT1 bound with K_d = 11 μM, and TRIM58 was the weakest binder; with an estimated K_d > 20 μM (**Figure 3A**). We next expanded our test to include all of the sequences reported by DeBartolo *et al*. that bind to all 5 anti-apoptotic proteins. These included peptides from NBEAL2, SLC19A1, SPNS1, CASP3, TERT, and TRMP7 (**Figure 3B**). We discovered that all 6 sequences bound BAK weakly (K_d > 20 μM) as determined by fluorescence polarization binding assays (**Figure 3B**).

Binding of BH3 segments to BAK or anti-apoptotic BCL-2 family proteins requires that the BH3 region be accessible. Most BH3-containing proteins are intrinsically disordered and for BID, a cleavage event converts a folded structure that sequesters the BH3 motif into a shorter protein called tBID in which this region is exposed (McDonnell et al., 1999). AlphaFold structure predictions of known BH3-only activators BIM and PUMA show high levels of disorder, except for the BH3 region, which is predicted to be helical (**Figure 4**). With the exception of CASP3, there are no solved structures for any of the human BH3-containing proteins that bind BAK. Thus, we used AlphaFold to examine predicted structures and categorized the candidates into three groups based on their per-residue confidence (pLDDT) score over the BH3 region, which is typically low for disordered proteins, and the predicted accessibility of the BH3 motif (**Figures 4 and 5, Tables 3 and 4).** BNIP5 is predicted to be highly disordered, and its BH3 region is predicted to adopt an

PEPTIDE	SEQUENCE	BAK:DF2 dTERMen score	BAK:DF3 dTERMen score	BAK:DM2 dTERMen score	FINAL RANK
	1 | 2 | 3 | 4 |5				
	efgabcdefgabcdefgabcdefga				
SNTG2	NATHEEVVHLLRNAGDEVTITVEYL	53	49	48	1
TXNDC11	TRELQELARKLQELADASENLLTEN	49	53	50	2
BNIP5	DAIIQMIVELLKRVGDQWEEEQSLA	53	51	54	3
TRIM58	KSRLVQQSKALKELADELQERCQRP	48	60	61	4
POFUT2	TRRSMVFARHLREVGDEFRSRHLNS	52	58	62	5
DDX4	FSKREKLVEILRNIGDERTMVFVET	54	63	54	6
PXT1	EEIIHKLAMQLRHIGDNIDHRMVRE	56	61	56	7
MINA	TVATRRLSGFLRTLADRLEGTKELL	57	60	60	7
CASP3	SWFIQSLCAMLKQYADKLEFMHILT	62	63	62	8
PCNA	SGEFARICRDLSHIGDAVVISCAKD	61	64	64	9
FOLH1	PFDCRDYAVVLRKYADKIYSISMKH	63	69	62	10
TRPM7	FERVEQMCIQIKEVGDRVNYIKRSL	62	72	62	11
TERT	LRGSGAWGLLLRRVGDDVLVHLLAR	63	68	63	11
PURB	FKAWGKFGGAFCRYADEMKEIQERQ	69	71	73	12
SLC19A1	ACGDSVLARMLRELGDSLRRPQLRL	71	71	74	13
MRPL41	MGVLAAAARCLVRGADRMSKWTSKR	67	74	76	14
NBEAL2	AELRLFLAQRLRWLCDSCPASRATC	69	74	76	15
MCF2L	VDSIRPKCQELRHLCDQFSAEIARR	69	74	78	16
MCF2L2	ADAIRPRCVELRHLCDDFINGNKKK	80	70	82	17
SPNS1	ISSYMVLAPVFGYLGDRYNRKYLMC	75	83	81	18
FOXJ2	PAKKMTLSEIYRWICDNFPYYKNAG	79	75	82	18
RTEL1	RVCPYYLSRNLKQQADIIFMPYNYL	89	81	88	19

Table 2. Energy scores for BAK:peptide complexes calculated using dTERMen and ranked from lowest (best) to highest. The indicated sequence was scored on each of three BAK:peptide complex structures using dTERMen and energies were rounded to the nearest integer; lower energies reflect greater predicted affinity. Ranks on the different templates were consolidated into a single overall rank. Some sequences had similar energy scores and were assigned the same rank number.

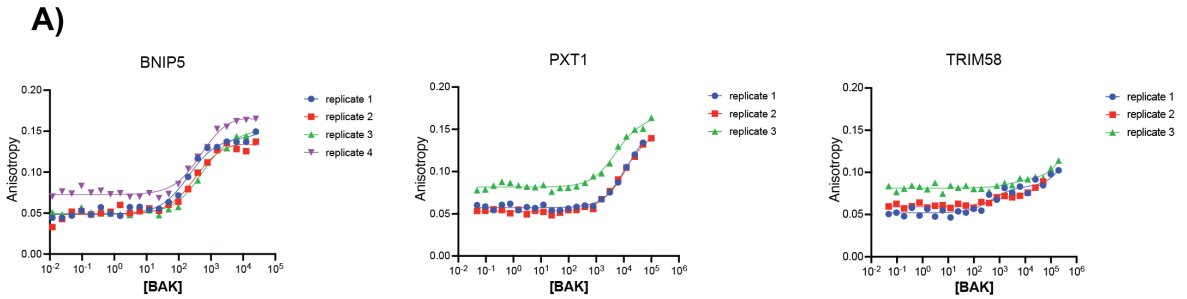

Peptide	Replicate #1	Replicate #2	Replicate #3	Replicate #4	Average Kd
BNIP5	0.2 μM	0.3 μM	0.6 μM	0.4 μM	0.4 μM +/- 0.2
PXT1	14 μM	12 μM	7 μM	-	11 μM +/- 4

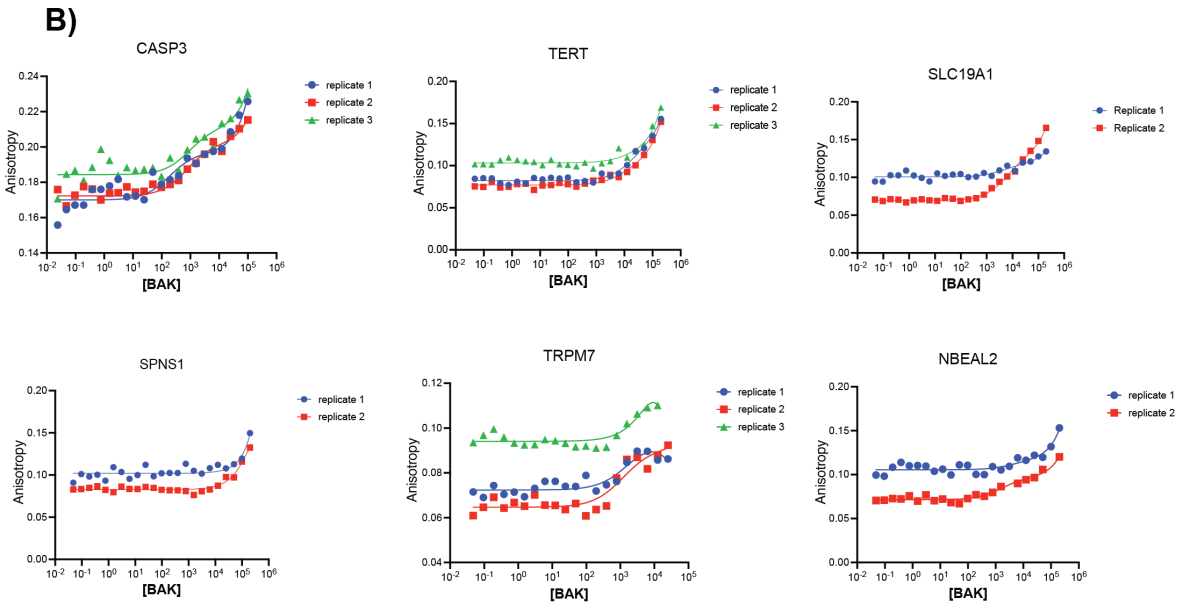

Figure 3. Candidate BH3-only peptides bind BAK with a range of affinities. Peptides that bind anti-apoptotic proteins MCL-1, BCL-x_L, BCL-2, BCL-W, and BFL-1 were tested for binding to recombinant human BAK using fluorescence polarization. **A)** BNIP5 and PXT1 showed the tightest binding with dissociation constants of 400 nM and 11 μM, respectively. **B)** CASP3, TERT, and SLC19A1 showed weak binding up to 200 μM BAK. SPNS1, TRPM7, and NBEAL2 were the weakest binders with unmeasurable affinities. SNTG2, TXDC11, POFUT2, DDX4, and Mina did not bind BAK (data not shown).

alpha helical structure with a low confidence pLDDT score. Structure gazing indicates that the BH3 region is largely accessible and solvent exposed, as it is does not form part of a tertiary

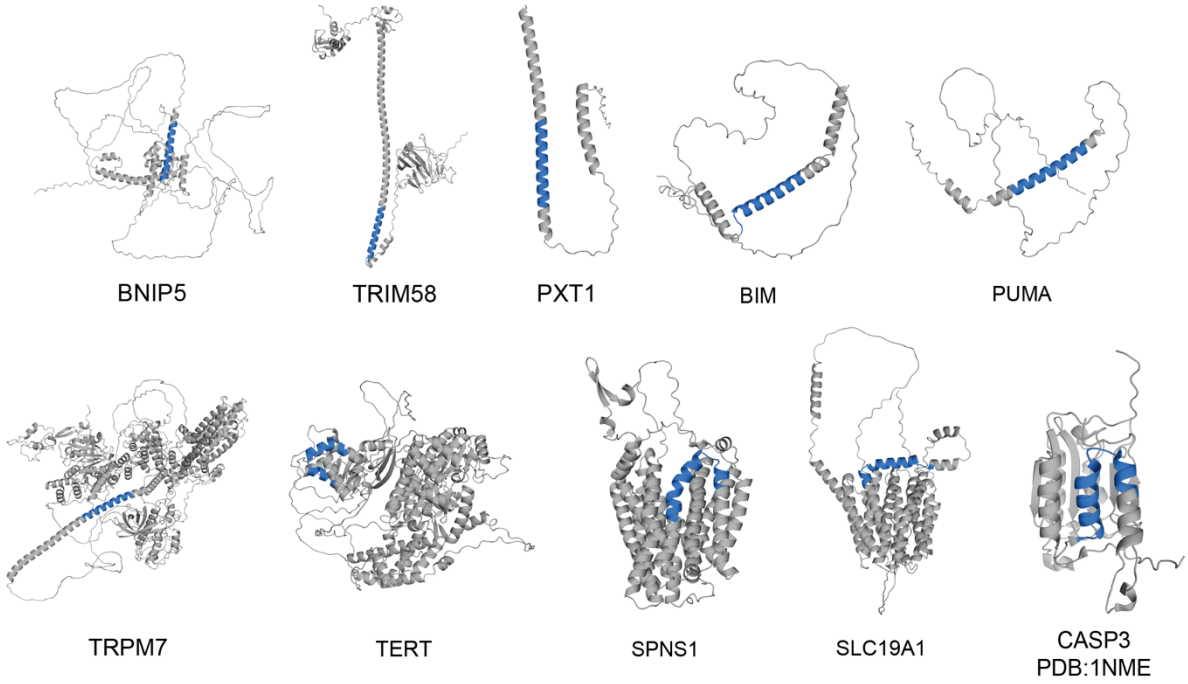

Figure 4. AlphaFold structure predictions for human BAK binding proteins. The candidate BH3 motif is highlighted in blue.

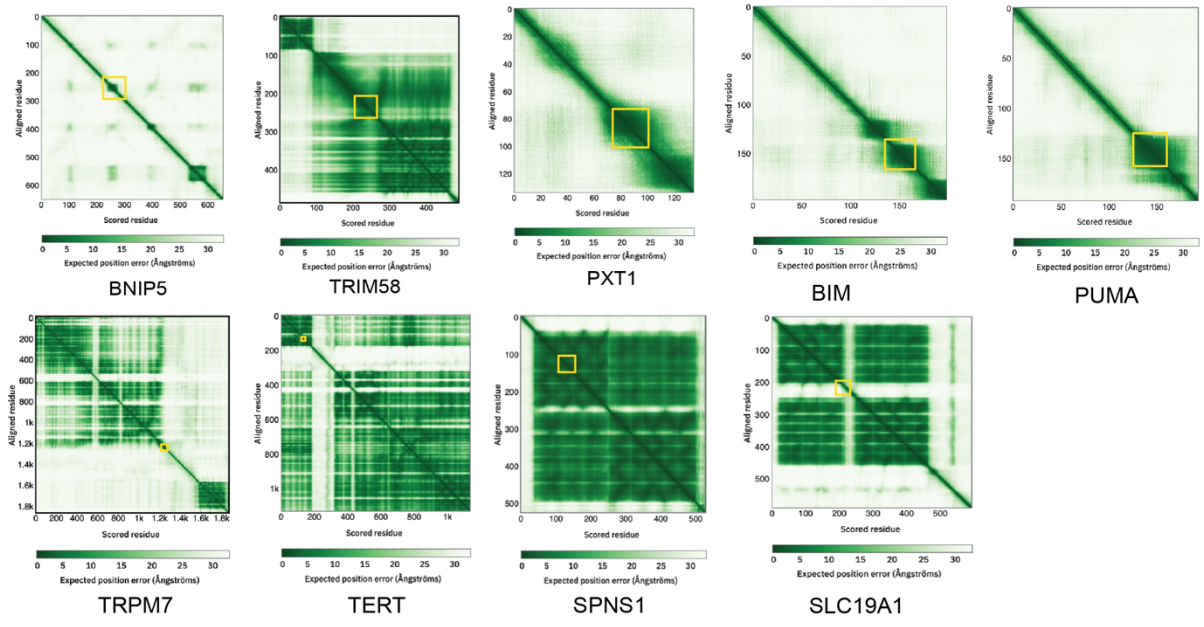

Figure 5. AlphaFold Predicted Aligned Error for predicted structures of human proteins. The candidate BH3 motif is indicated with a yellow box.

PEPTIDE	SEQUENCE	UNIPROT ID	RESIDUES
BNIP5	DAIIQMIVELLKRVGDQWEEEQSLA	P0C671	244-268
TRIM58	KSRLVQQSKALKELADELQERCQRP	Q8NG06	219-243
PXT1	EEIIHKLAMQLRHIGDNIDHRMVRE	Q8NFP0	76-100
BIM	MRPEIWIAQELRRIGDEFNAYYARR	O43521	142-166
PUMA	EQWAREIGAQLRRMADDLNAQYERR	Q9BXH1	131-155
TRPM7	FERVEQMCIQIKEVGDRVNYIKRSL	Q96QT4	1201-1225
TERT	LRGSGAWGLLLRRVGDDVLVHLLAR	O14746	131-155
SLC19A1	ACGDSVLARMLRELGDSLRRPQLRL	P41440	245-269
CASP3	SWFIQSLCAMLKQYADKLEFMHILT	P42574	213-237
SPNS1	ISSYMVLAPVFGYLGDRYNRKYLMC	Q9H2V7	105-129
NBEAL2Δ254	AELRLFLAQRLRWLCDSCPASRATC	Q6ZNJ1	n.a.

Table 3. Known and candidate BH3 motifs in human proteins. Residues in the L-x(4)-D/E BH3 motif are highlighted in red. N.a. indicates we will be update result in bioRxiv manuscript.

PEPTIDE	pLDDT SCORE OF BH3 REGION	STRUCTURE OF BH3 REGION	ACCESSIBILITY OF BH3 INTERACTION WITHIN PROTEIN
BNIP5	50-70	alpha helical/ disordered	very accessible
TRIM58	>90	alpha helical	very accessible
PXT1	>70	alpha helical	very accessible
BIM	>70	alpha helical	very accessible
PUMA	>70	alpha helical	very accessible
TRPM7	70-90	alpha helical	less accessible
TERT	>90	alpha helical	less accessible
SLC19A1	50-90	alpha helical/ disordered	less accessible
CASP3	N.A.	alpha helical	inaccessible
SPNS1	>70	alpha helical	inaccessible
NBEAL2	n.a.	n.a.	n.a.

Table 4. AlphaFold structure predictions and BH3 accessibility. pLDDT scores indicate the confidence of structural prediction and are classified as follows: >90 - very high confidence, 90>pLDDT>70 - confident, 70>pLDDT>50 - low confidence, and pLDDT<50 - very low confidence. A pLDDT <50 is predicted as disordered (Tunyasuvunakool et al., 2021). We manually classified sequences into three groups: very accessible, less accessible, and inaccessible based on the predicted structure and the predicted alignment error. *n.a. indicates we will update result in bioRxiv manuscript.

structure. We reached similar conclusions for PXT1, TRIM58, BIM, and PUMA. The candidate BH3 motifs in other proteins were more structurally constrained by surrounding residues and

showed less solvent accessibility, including TRPM7, TERT, and SLC19A1; these were classified as less accessible. The candidate BH3 motifs in CASP3 and SPNS1 were classified as inaccessible since major conformational changes would have to occur in order for a BH3-mediated interaction to occur.

SECTION 1.3 NOVEL BH3 BINDERS OF BAK FUNCTION AS ACTIVATORS OR INHIBITORS

Liposomes loaded with recombinant proteins provide a way to study BAX and BAK activation while avoiding the influence of confounding factors such as anti-apoptotic proteins (Brouwer et al., 2017; Gavathiotis et al., 2008; Hockings et al., 2015). Because recombinant full-length BAK is not soluble, we used a previously published C-terminally truncated BAK construct with a His_6 tag (BAKΔC25-His_6) (that localizes BAK to Ni^{2+}-labeled liposomes (Brouwer et al., 2017). Briefly, we made 100 nm liposomes that mimicked the composition of the mitochondrial outer membrane with encapsulated fluorescent dye DPX and quencher ANTS. In this assay, dye release reports on membrane permeabilization as a proxy for MOMP. In initial experiments performed with a membrane-localized activating peptide from BID (His_6-SUMO-BID), BAKΔC25-His_6 but not BAK ΔN22 ΔC25 C166S (which lacks the membrane-localizing His_6 tag) showed a response to activator (**Figure 6**). We used BAKΔC25-His_6 in all subsequent liposome-based experiments. BAK activation involves BAK oligomerization (Cosentino et al., 2022), and we confirmed that this process is concentration dependent: 500 nM BAKΔC25-His_6 showed greater activation than 150 nM BAKΔC25-His_6 (**Figure 7**).

We used this assay to test activation by a range of soluble 22-35 residue peptides (**Figure 8 and Table 5**). BH3 peptides from BAK activators BID and BIM gave concentration dependent activation, consistent with prior reports (Brouwer et al., 2017; Hockings et al., 2015; G. Singh et al., 2022). Our data shows that PUMA and HRK peptides give minimal activation compared to BID and BIM BH3 peptides at 2.5 μM and 5 μM. NOXA and BAD peptides did not activate up to concentrations of 5 μM.

The canonical binding groove of pro-apoptotic proteins BAK and BAX contains 5 hydrophobic pockets referred to as h0, h1, h2, h3, and h4 (**Figure 9**). Numerous structures of BAK and BAX complexes have shown that specific positions within the BH3 peptide engage these hydrophobic pockets, and mutations to pocket-binding residues can disrupt function (Czabotar et al., 2013; Brouwer et al., 2017). To probe the sensitivity of BAK to mutations in BH3 activators, we focused on mutations previously shown to affect activation of BAX (**Figure 10**) (Czabotar et al., 2013). A 26-residue PUMA BH3 peptide showed weak activation at 20 μM. Substitution of

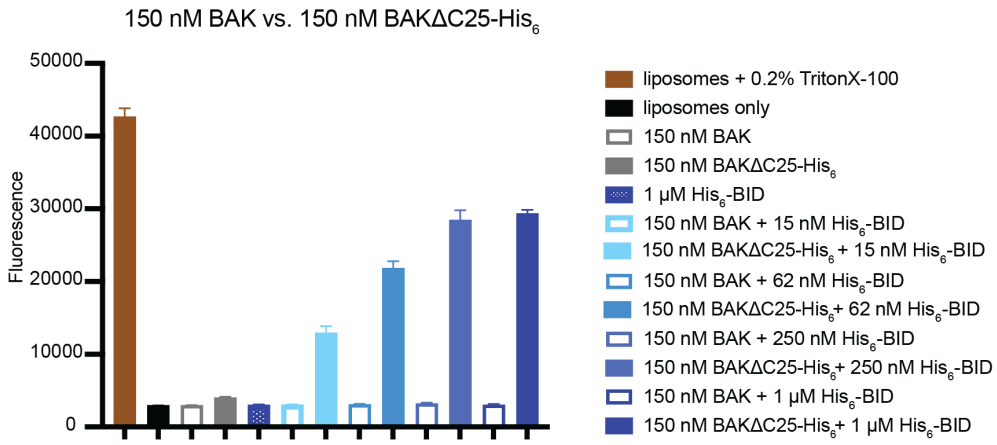

Figure 6. Localization of BAK to the liposome membrane is necessary for BID BH3-triggered dye release. Liposomes containing ANTS/DPX dye and 18:1 DGS-NTA (Ni^{2+}) lipid were incubated with either 150 nM of BAK ΔN22 ΔC25 C166S (indicated as BAK) or 150 nM of BAKΔC25-His_6 and increasing concentrations of His_6-SUMO-BID BH3 (indicated as His_6-BID). Whereas BAKΔC25-His_6 showed BID concentration-dependent dye release, BAK without a His_6 tag did not lead to dye release even when treated with 1 μM His_6-BID. 0.2% Triton X-100 detergent (brown) was included as a positive control for dye release. Plots show the fluorescence signal at 1 hour, for experiments run in triplicate, with error bars representing standard deviations.

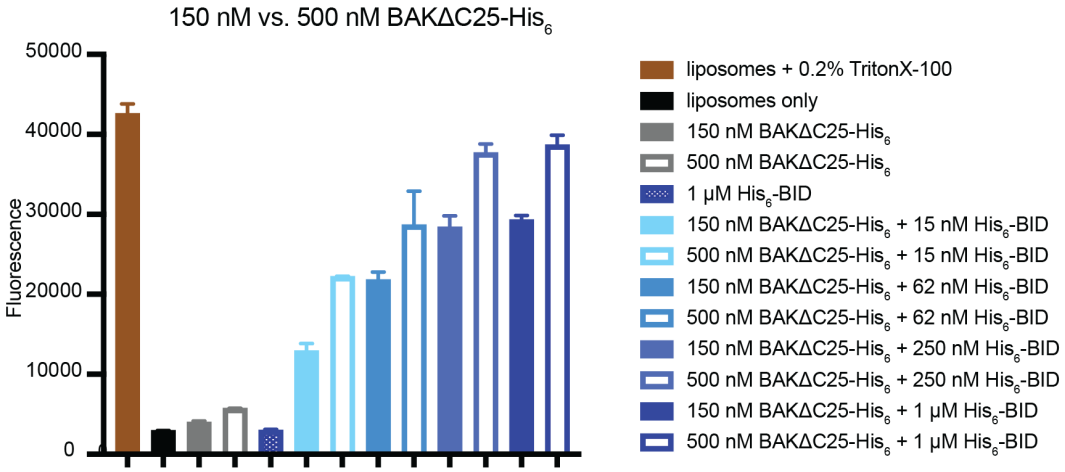

Figure 7. Dye release increases with increasing concentrations of BAK. For all tested concentrations of His-SUMO-BID BH3 (indicated as His_6-BID), greater dye release was observed for 500 nM vs. 150 nM BAKΔC25-His_6. No dye release was observed for BAKΔC25-His_6 in the absence of His_6-BID at either 150 or 500 nM. Plots show the fluorescence signal at 1 hour for experiments run in triplicate, with error bars representing standard deviations.

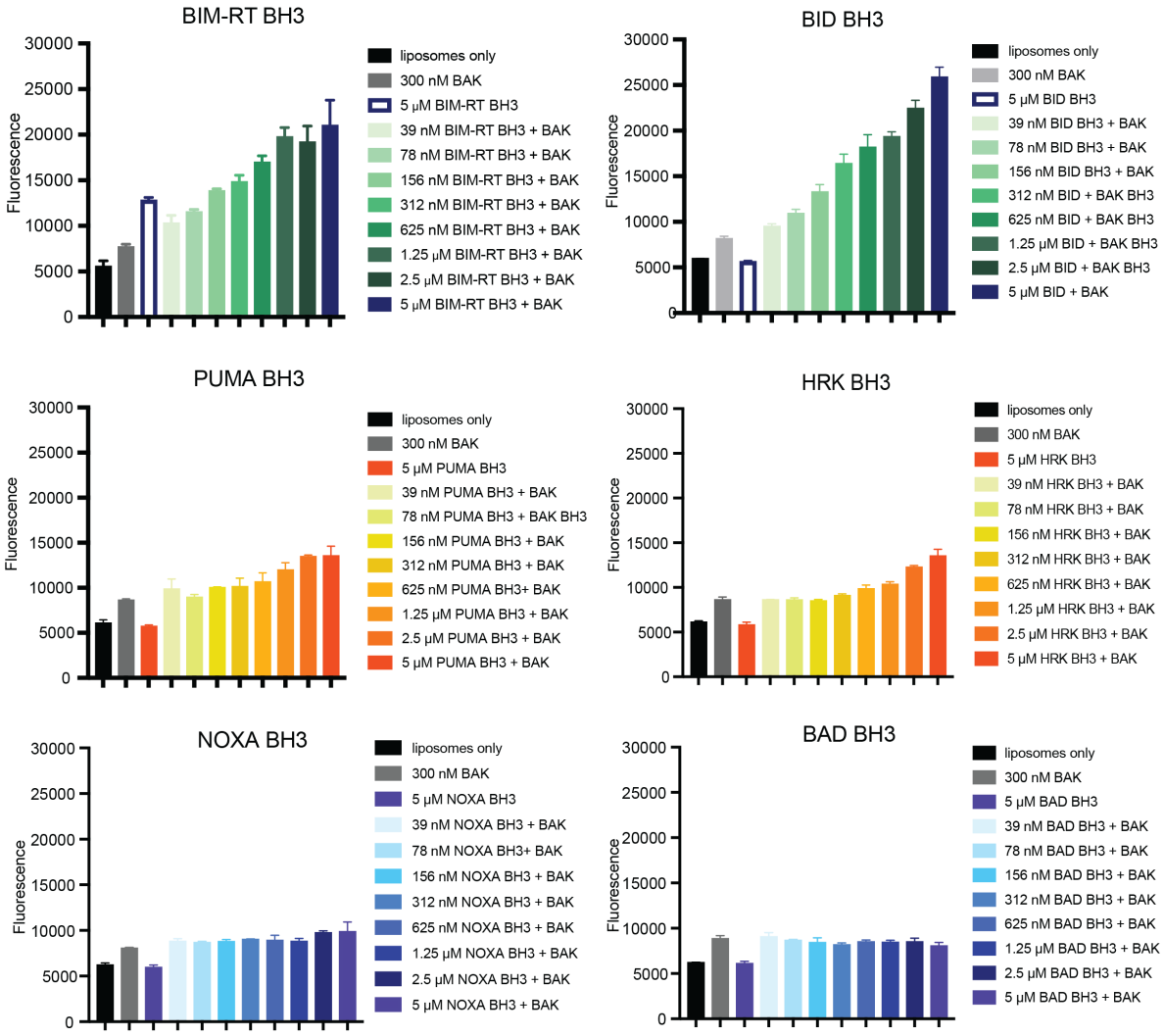

Figure 8. Peptides from Bcl-2 BH3-only proteins show differences in BAK activation function. BH3 peptides BID, BIM, PUMA, HRK, Y-NOXA, and BAD were tested for activation. 300 nM BAKΔC25-His_6 (indicated as BAK in the figure) was incubated with BH3 peptides at concentrations ranging from 39 nM to 5 μM. BH3 peptides were grouped into activators (green), weak activators (orange) and non-activators (blue). Plots show the fluorescence signal at 1.5 hours for experiments run in triplicate, with error bars representing standard deviations. Peptide sequences are in **Table 5.**

PEPTIDE	SEQUENCE	FUNCTION
	1 | 2 | 3 | 4 |5	
	abcdefgabcdefgabcdefgabcdefgabcdef	
	h0 h1 h2 h3 h4	
BIM-RT	----DMRPEIRIAQELRRIGDEFNATYARR-----	Activator
Y-BID	YSESQEDIIRNIARHLAQVGDSMDRSIPPGLVNGL	Activator
PUMA M3DI	-----EQWAREIGAQLRRIADDLNAQYERRRQEEQ	Activator
dF8	------SLLEKLAEYLAQMGDEINKKYVK------	Activator
dM4	-----DKTLEEIARWLARLALEIDKEI--------	Activator
dM2	-----APYLEQVARTLRKIGEEINEALR-------	Activator
BNIP5	-----DAIIQMIVELLKRVGDQWEEEQSLA-----	Activator
PXT1	-----EEIIHKLAMQLRHIGDNIDHRMVRE-----	Activator
Y-NOXA	---YPAELEVECATQLRRFGDKLNFRQKLL-----	Weak activator
Y-NOXA C2dI	---YPAELEVEIATQLRRFGDKLNFRQKLL-----	Weak activator
PUMA	-----EQWAREIGAQLRRMADDLNAQYERRRQEEQ	Weak activator
BAD	---PNLWAAQRYGRELRRMSDEFVDSFKKG-----	Non-activator
HRK	-LGLRSSAAQLTAARLKALGDELHQR---------	Non-activator
dF2	------SYIDKIADLIRKVAEEINSKLE-------	Inhibitor
Y-dF7	------SLLEKLAEELAQLADELNKKFEK------	Inhibitor
dF3	-------LLEKLAEELRQLADELNKKFEK------	Inhibitor
dF4	------SLLEKLAEYLRQMADEINKKYVK------	Inhibitor
BK3	-----KSPLERLAEILEKVAKEIEKELGP------	Inhibitor
BIMh3PcRT	----DMRPEIRIAQELRRXGDEFNATYARR-----	Inhibitor

Table 5. Alignment of peptide sequences tested for activation. Residues are colored according to **Table 1**.

native methionine 144 with isoleucine gave greater BAK activation compared to WT. Similarly, substitution of native cysteine to isoleucine in NOXA gave greater BAK activation.

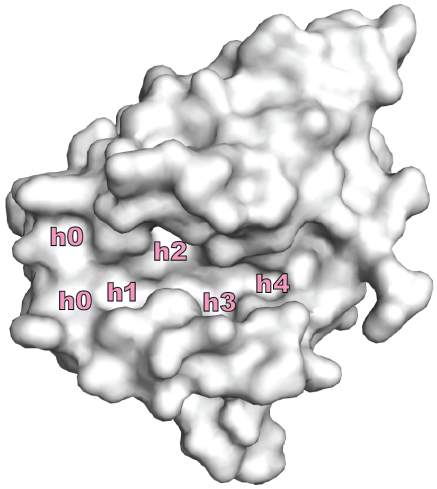

Figure 9. BAK contains 5 hydrophobic pockets referred to as h0, h1, h2, h3, and h4. Surface representation of BAK (PDB:5VX0) with hydrophobic pockets in the canonical peptide binding groove labeled in pink.

	Sequence
	1 | 2 | 3 | 4 | 5
	cdefgabcdefgabcdefgabcdefgabc
	h0 h1 h2 h3 h4
PUMA	EEQWAREIGAQLRRMADDLNAQYERR
PUMA M3dI	EEQWAREIGAQLRRIADDLNAQYERRR
NOXA	PAELEVECATQLRRFGDKLNFRQKLL
NOXA C2dI	YPAELEVEIATQLRRFGDKLNFRQKLL

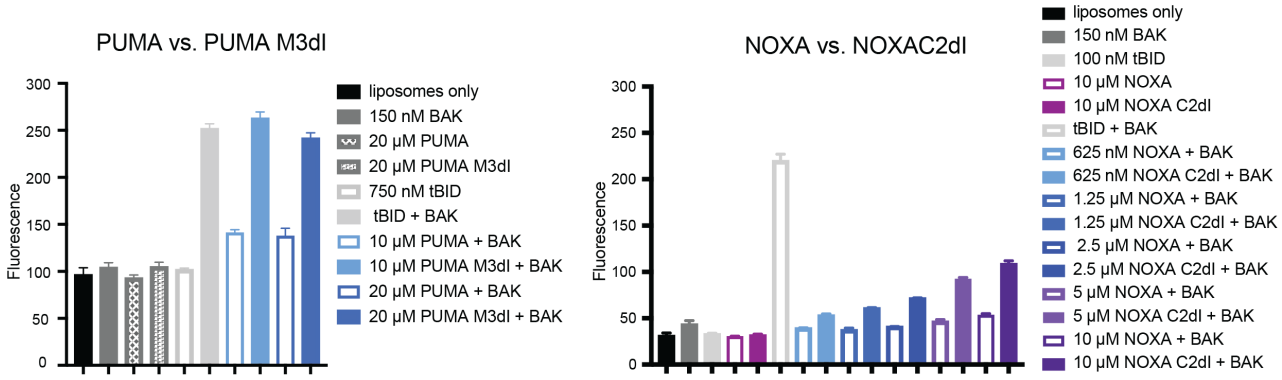

Figure 10. Point mutations at hydrophobic positions increase the activation potency of BH3 peptides from proteins NOXA and PUMA. Using heptad notation, peptide residues 1g and 2, 2d, 3a, 3d and 4a bind to hydrophobic pockets h0, h1, h2, h3, and h4, respectively. Substitution of Met to Ile in Puma BH3 peptide (PUMA M3dI) and Cys to Ile in NOXA BH3 peptide (NOXA C2dI) increased activation potency. Dye containing liposomes were incubated with 150 nM BAKΔC25-His_6 (indicated as BAK) and peptides with concentrations ranging from 625 nM to 10 μM. Plots show the fluorescence signal at 1 hour for experiments run in triplicate, with error bars representing standard deviations.

We tested our newly discovered BAK-binding peptides for BAK activation using the liposome assay (see **Appendix Figure 1** for raw data). Three peptides previously designed to bind to anti-apoptotic proteins (dF8, dM2, and dM4) are very different from one another and from known activators BIM, BID, and PUMA, yet all showed an increase in fluorescence signal compared to negative controls at 1.5 h, indicating BAK activation (**Figure 11A**). A BIM BH3 peptide with solubilizing mutations (BIM-RT) was used as a positive control. dF8 and dM4 were more potent activators than BIM-RT at 1.25 μM. dM2 peptide, on the other hand, showed weaker activation compared to BIM-RT. Peptides from human proteins BNIP5 and PXT1 activated 300 nM BAKΔC25-His_6 (**Figure 11B**). At 250 nM, BNIP5 showed greater activation than PXT1, using positive control BIM-RT at 500 nM as a reference, indicating BNIP5 is a more potent activator. To test whether our new activating peptides act synergistically or in competition with BIM BH3, we incubated 300 nM of BAKΔC25-His_6 with 200 nM BIM-RT and increasing concentrations of dF8, dM2, or dM4 peptides. Addition of 500 nM dF8 or dM4 to 200 nM BIM-RT resulted in greater activation than observed for BIM-RT alone; this was also true but to a smaller extent for dM2 (**Figure 12**).

Not all BAK-binding peptides functioned as activators in our assay. Specifically, dF2, dF3, dF4, and BK3 peptides did not result in dye release at 300 nM BAKΔC25-His_6 with 5 μM (dF3, dF4, and dF2) (**Figure 13A**) or 10 μM (dF7) peptide (**Figure 13B**) (see **Appendix Figure 2** for raw data). We postulated that BAK-binding peptides that do not activate may function as inhibitors, so we tested dF2, dF3, dF4, BK3, and dF7 with 300 nM BAKΔC25-His_6 and varying concentrations of BIM-RT (**Figure 13**). Given the limitations of the *in vitro* assay, including liposome variability from batch to batch as well as a plateau reached at high activation levels (loss of activation resolution), we first picked a concentration of BIM-RT at which approximately half maximal dye release is observed (200 nM for experiments in **Figure 13A** and 625 nM for experiments in **Figure 13B**). We subsequently conducted experiments with 300 nM BAKΔC25-His_6 and varying concentrations of candidate inhibitor peptides that were mixed with BIM-RT at the established half-maximal concentration. Peptides dF2, dF3, dF4, BK3, and dF7 showed concentration-dependent inhibition of BAK activation by BIM-RT. dF2 was the most potent inhibitor, with approximately full BAK inhibition reached at 1.25 μM. Computationally designed BK3 gave complete inhibition at 5 μM. We also tested previously published BIM-h3Pc-RT, an inhibitor peptide that contains a non-natural amino acid (Brouwer et al., 2017), and noted that all four of our peptides were more potent inhibitors in this assay.

The candidate BH3 peptide from human TRIM58 with measured K_d > 20 μM did not function as an activator or inhibitor of BAK. NBEAL2, SLC19A1, and SPNS1 peptides are not soluble in water and we did not test this further, whereas CASP3, TRPM7, and TERT showed BAK-independent dye release from liposomes (**Figure 14**).

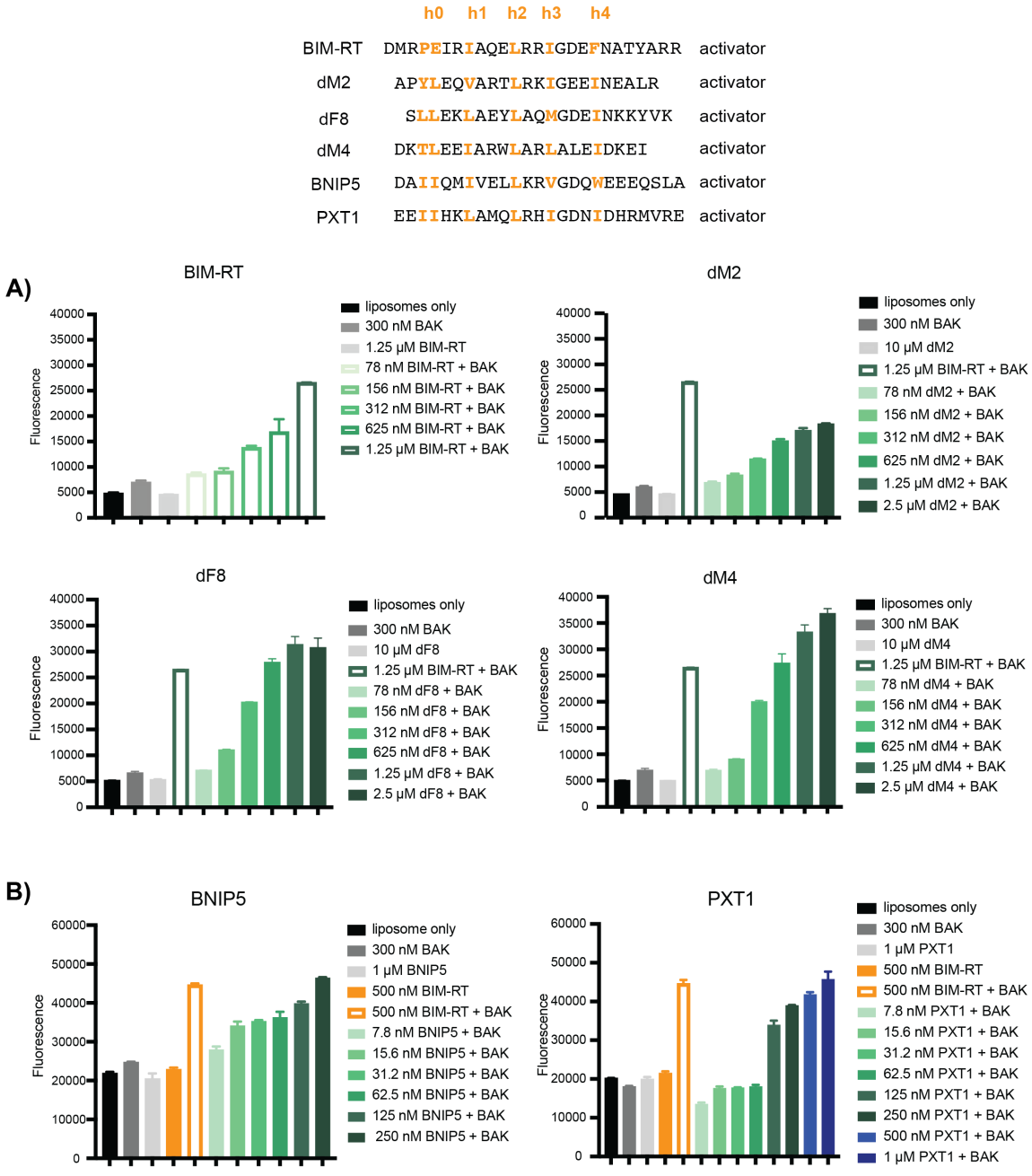

Figure 11. dM2, dF8, dM4, BNIP5, and PXT1 peptides function as BAK activators. Dye containing liposomes were incubated with 300 nM BAKΔC25-His_6 (indicated as "BAK" in figure panels) and newly identified BAK-binding peptides. **A)** Synthetic peptide concentrations from 78 nM to 2.5 μM were tested in

comparison to 1.25 μM BIM-RT as a positive control (open bars). Plots show fluorescence signal at 1.5 hours. **B)** Peptides from BNIP5 and PXT1 were tested at concentrations ranging from 7.8 nM to 250 nM (BNIP5) or 7.8 nM to 1 μM (PXT1) compared to 500 nM BIM-RT as a positive control (open bars). Plots shows show fluorescence signal at 1 hour. In all panels, error bars indicate standard deviations over three replicates.

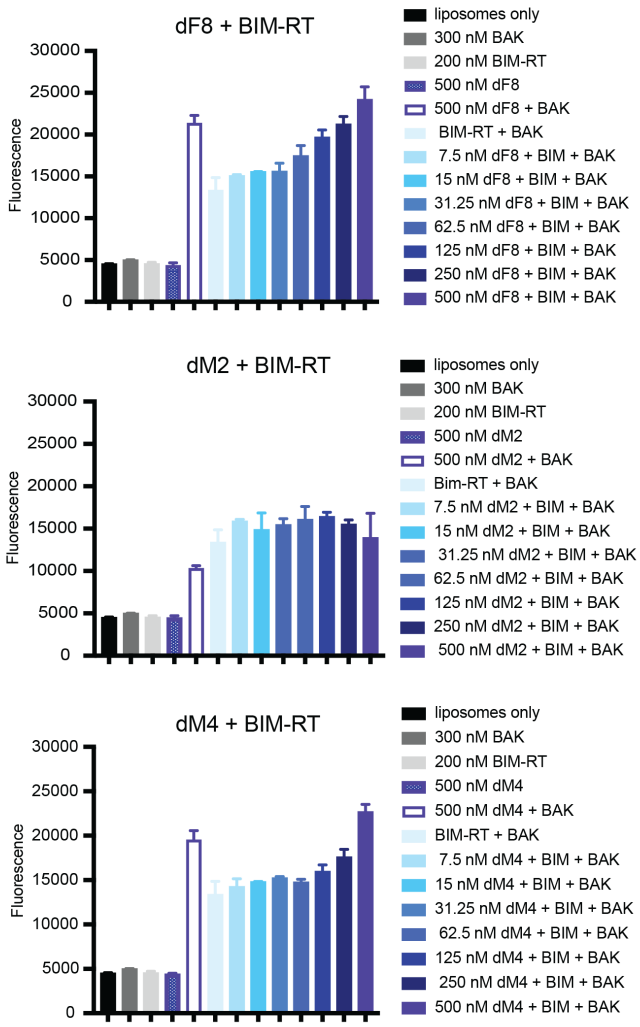

Figure 12. Peptides dF8, dM2, and dM4 act as activators alone and in the presence of BIM-RT BH3. Liposomes containing dye were incubated with 300 nM BAKΔC25-His_6 (indicated as BAK in the figure), 200 nM BIM-RT (activator), and 7.5 – 500 nM dF8, dM2, or dM4 peptides. Plots show the fluorescence signal at 2 hours. All peptide combinations displayed greater fluorescence compared to 300 nM BAKΔC25-His6 and either 200 nM BIM-RT or 500 nM dF8, dM2, or dM4 peptide alone.

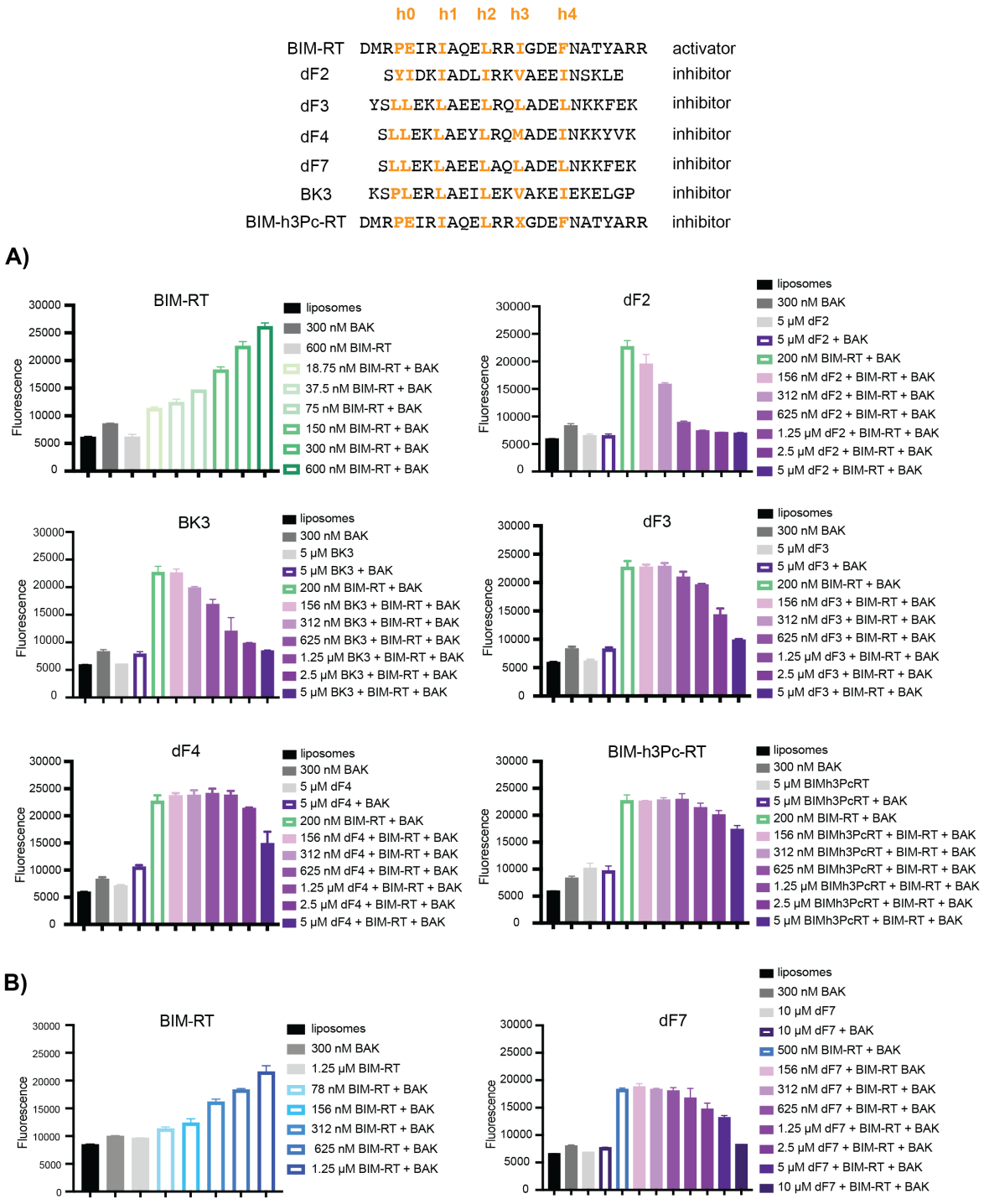

Figure 13. Peptides dF2, dF3, dF4, BK3, BIM-h3-PcRT, and dF7 inhibit activation of BAK by BIM-RT. Liposomes containing dye were incubated with BIM-RT at a range of concentrations and then with BIM-RT plus candidate peptide inhibitors. **A)** Liposomes with 300 nM BAKΔC25-His_6 (shown as BAK in the figure) plus 200 nM BIM-RT were incubated with dF2, BK3, dF3, or dF4. Previously published BIM-h3Pc-RT peptide served as a positive control for inhibition (Brouwer et al., 2017). Plots show fluorescence signal at

1.5 hours. **B)** Liposomes with 300 nM BAKΔC25-His_6 (shown as BAK in figure) plus 500 nM BIM-RT were incubated with dF7 at increasing concentrations. Plots show fluorescence signals at 1.5 hours. In all panels, error bars indicate standard deviations over three replicates. More replicates in progress.

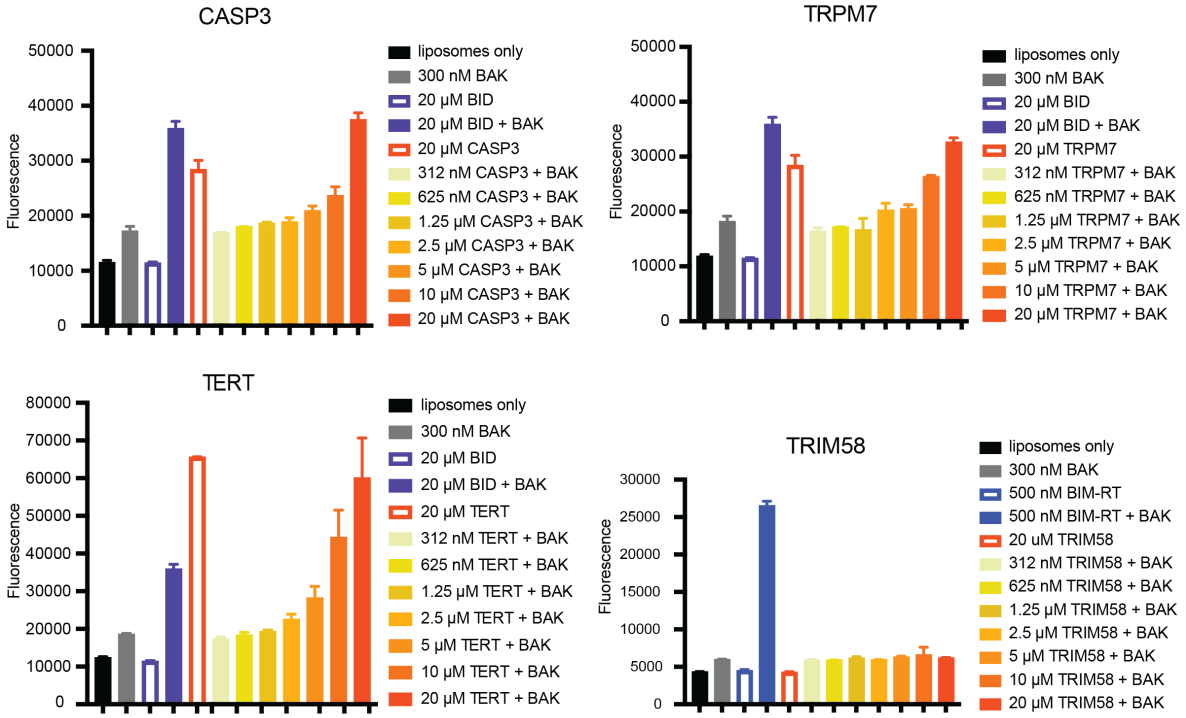

Figure 14. CASP3, TERT, and TRPM7 BH3 peptides show BAK-independent membrane disruption at high concentrations. BID-Y 25mer is a positive control showing concentration dependent activation in the presence of 300 nM BAKΔC25-His_6 (indicated as BAK in figure). CASP3, TERT, and TRPM7 peptides show membrane disruption at concentrations greater than 5 μM, 2.5 μM, and 5 μM, respectively. TRIM58 does not show activation at 20 μM.

Amphipathic helical peptides can associate into coiled coils or other helical-assembly structures (Truebestein & Leonard, 2016). To test whether BH3-like peptides that functioned as inhibitors bind to BIM-RT or Y-BID, as well as to BAK, and whether this might contribute to the observed inhibition, we conducted circular dichroism (CD) experiments to test for peptide hetero-association, comparing the helicity of peptides alone vs. in a hetero-mixture (**Table 6 and Figure 15**). The lowest peptide concentration at which we were able to obtain a low-noise CD signal was 15 μM, which is greater than the concentration used in our liposome assay. However, even at this high peptide concentration, no association was observed between any of dF2, dF3, and BK3 and BIM-RT or Y-BID. Previous biophysical and structural evidence has shown that BIM BH3 peptides can self-associate to form tetramers (Assafa et al., 2021). To test whether our peptides contained

significant amount of alpha helical content, possibly due to self-association, we calculated the mean residue ellipticity (MRE) and found that activators and inhibitors both exhibited a range of helicities (**Table 6**). Inhibitor peptides dF2 and dF3 showed 28% and 83% helicity, respectively, while activator peptides BIM-RT and PumaM3dI showed helicities of 5% and 50%, respectively. Given that short peptides typically have very low helicity as monomers, we anticipate that the high-helicity signals at 15 μM likely result from peptide self-assembly, although we did not pursue this further.

Peptide	Sequence	N	MRE at 222 nm deg*cm^2*(10dmol*N)$^{-1}$	Temperature (°C) at 222 nm	% helical content	Function
BIM-RT	DMRPEIRIAQELRRIGDEFNATYAR	26	-2353	24	5	activator
Y-NOXA C2dI	YPAELEVEIATQLRRFGDKLNFRQKLL	27	-7280	24	17	activator
Y-BID	YSESQEDIIRNIARHLAQVGDSMDRSIPPGLVNGL	35	-6945	25	17	activator
Y-BAX BH3	YPQDASTKKLSECLKRIGDELDSNMELQRMIA	32	-10862	24	26	activator
dF8	SLLEKLAEYLAQMGDEINKKYVK	23	-11667	25	27	activator
dF2	SYIDKIADLIRKVAEEINSKLE	22	-12240	25	28	inhibitor
dM2	APYLEQVARTLRKIGEEINEALR	23	-14975	23	34	activator
dM4	DKTLEEIARWLARLALEIDKEI	22	-15820	23	36	activator
PUMA M3dI	EQWAREIGAQLRRIADDLNAQYERRRQEEQ	32	-20890	24	50	activator
Y-BK3	KSPLERLAEILEKVAKEIEKELGP	25	-28848	25	67	inhibitor
Y-dF3	SLLEKLAEELRQLADELNKKFEK	23	-35916	25	83	inhibitor

Table 6. Percent helical content does not correlate with functional differences between inhibitors and activators. 15 μM of peptide was used in each experiment. N indicates the number of residues in the sequence. MRE stands for mean residue ellipticity.

SECTION 1.4 HUMAN PROTEOME BNIP5 AND PXT1 BH3 PEPTIDES AND NON-NATIVE PEPTIDES ACTIVATE BAK IN CELLS

Testing for activation function in cells is complicated by the presence of many different BCL-2 family members including BAK and BAX, pro-apoptotic BH3-only proteins, and anti-apoptotic proteins. Inhibiting anti-apoptotic proteins can lead to MOMP through an indirect sensitization mechanism (Chen et al., 2005; Willis et al., 2007). Nevertheless, to look for evidence of function of our newly discovered activators in cells we used permeabilized, siRNA-treated HeLa cells, which express human BAK and BAX and low levels of anti-apoptotic proteins compared to other cell lines (Placzek et al., 2010). We tested for peptide-induced release of cytochrome c, as previously published (Fraser et al., 2019) (**Figure 16, Figure 17, and Table 7**). We compared cytochrome-c release across WT, BAK only, BAX only, and BAK/BAX **d**ouble **k**nock**o**ut (DKO) cells using BID, BIM, and PUMA BH3 activating peptides as positive controls and PUMA2A peptide as a negative control (**Table 7 and Figure 17**). Western blots confirmed effective siRNA

knockdowns of BAK and BAX (**Figure 18**), and DKO cells were resistant to peptide-induced MOMP for BID, BIM, PUMA, and negative control peptide PUMA2A (**Figure 17**) (Fraser et al., 2019). We were able to corroborate the previously published observations that BIM preferentially activates BAX and BID preferentially activates BAK (Sarosiek et al., 2013). Using this assay, we compared the mitochondrial functions of new peptides that activate BAK in liposome assays with established activators BIM and BID.

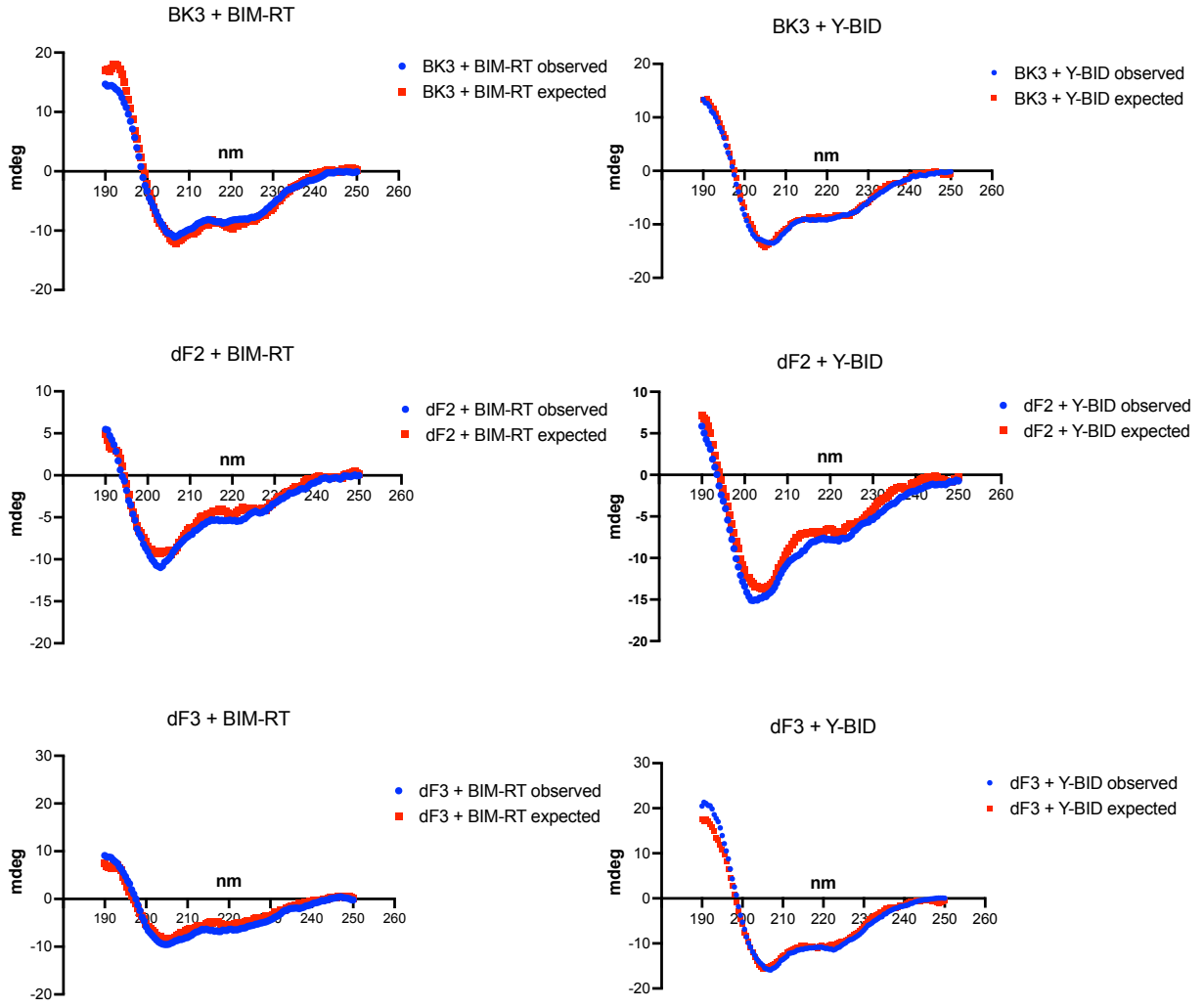

Figure 15. Circular dichroism (CD) experiments do not support hetero-dimerzation of inhibitor peptides with BIM-RT. CD spectra were collected for each peptide at a concentration of 15 μM. Summing the CD signals for the indicated peptides gave the expected spectra, which are plotted in red. For comparison with the signal expected from a physical mixture of two non-interacting peptides, 15 μM BIM-RT or Y-BID was mixed with 15 μM BK3, dF2, or dF3 to obtain the observed CD spectra, which are plotted

in blue. The observed spectra (blue) showed minimal differences from the spectra expected for non-interacting peptides (red).

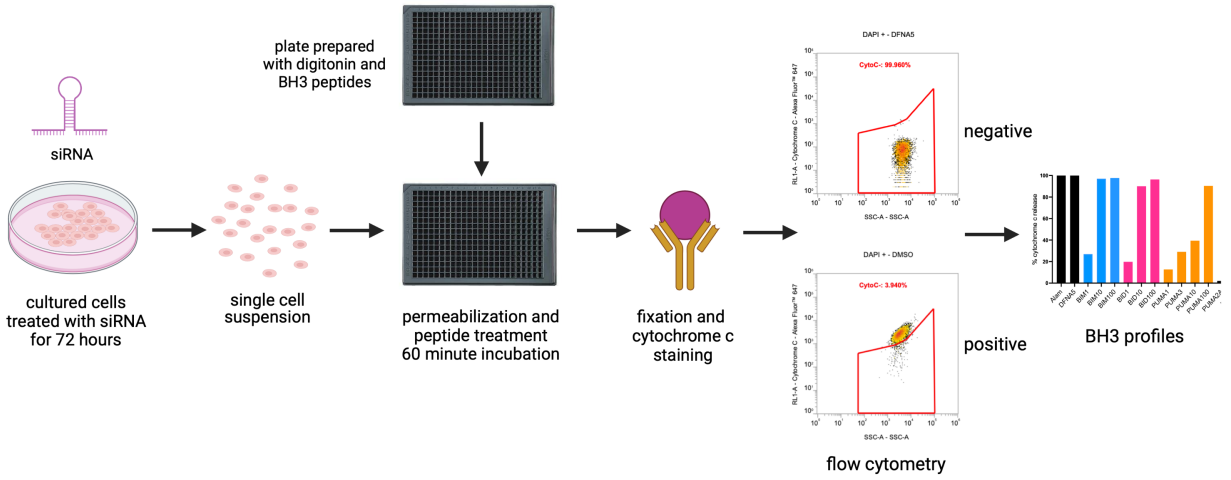

Figure 16. Diagram of BH3 profiling assay.

Peptide	N-termini	Sequence	C-termini
Y-PXT1	Ac	YEEIIHKLAMQLRHIGDNIDHRMVRED	NH2
BNIP5	Ac	DAIIQMIVELLKRVGDQWEEEQSLAS	NH2
Y-TRIM58	Ac	YKSRLVQQSKALKELADELQERCQRPA	NH2
dM2	Ac	APYLEQVARTLRKIGEEINEALR	NH2
dM4	Ac	DKTLEEIARWLARLALEIDKEI	NH2
dF8	Ac	SLLEKLAEYLAQMGDEINKKYVK	NH2
BID-Y	Ac	EDIIRNIARHLAQVGDSMDRY	NH2
BIM	Ac	MRPEIWIAQELRRIGDEFNA	NH2
PUMA	Ac	EQWAREIGAQLRRMADDLNA	NH2
PUMA2A	Ac	EQWAREIGAQARRMAADLNA	NH2

Table 7. Peptide sequences used for BH3 profiling assay.

Our results show that BNIP5, PXT1, dM2, dF8, and dM4 induce release of cytochrome c, consistent with our results showing that these peptides activate BAK in liposome assays (**Figure 17 and Figure 11**). Interestingly, BNIP5 strongly activates BAX as indicated by full cytochrome c release at 1 μM. Moreover, PXT1 activates both BAK and BAX with similar potency and less so than BNIP5. Furthermore, we observed that dM2, dF8, and dM4 preferentially induce MOMP in the BAX knock-down cells but not the BAK knock-down cells, consistent with selective activation of BAK.

A)

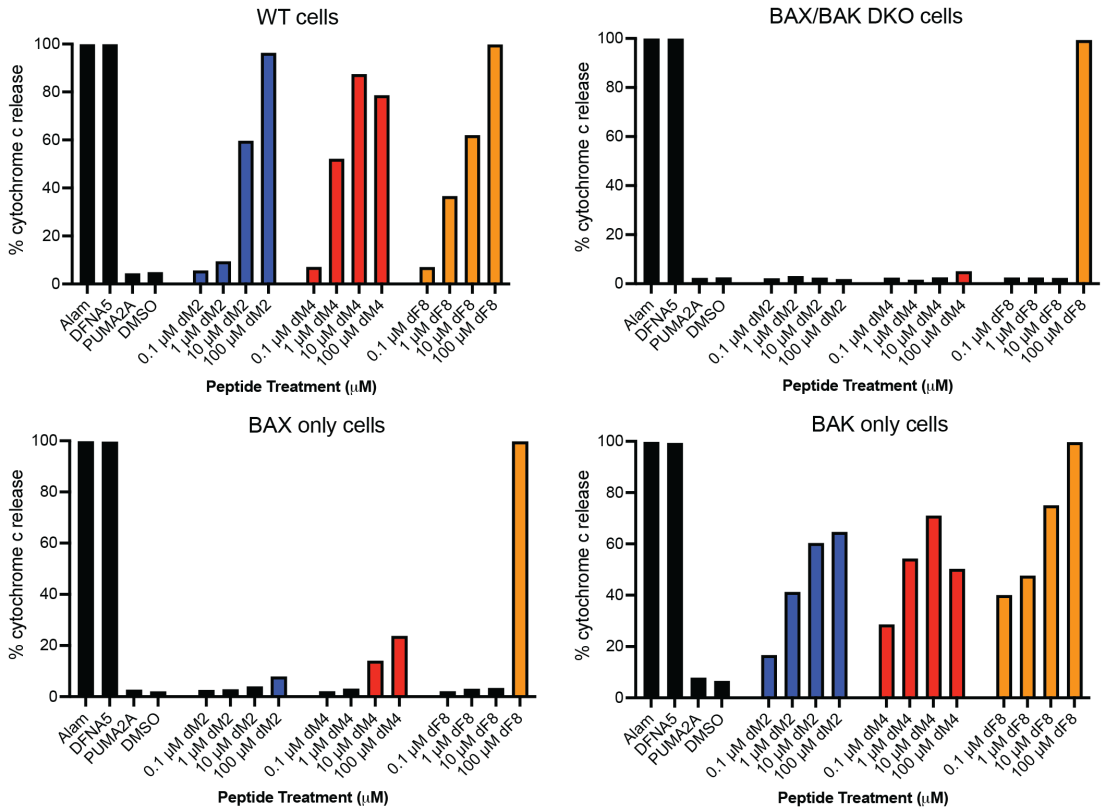
WT cells
BAX/BAK DKO cells
BAX only cells
BAK only cells
% cytochrome c release
Peptide Treatment (μM)
Alam
DFNA5
PUMA2A
DMSO
0.1 μM dM2
1 μM dM2
10 μM dM2
100 μM dM2
0.1 μM dM4
1 μM dM4
10 μM dM4
100 μM dM4
0.1 μM dF8
1 μM dF8
10 μM dF8
100 μM dF8

B)

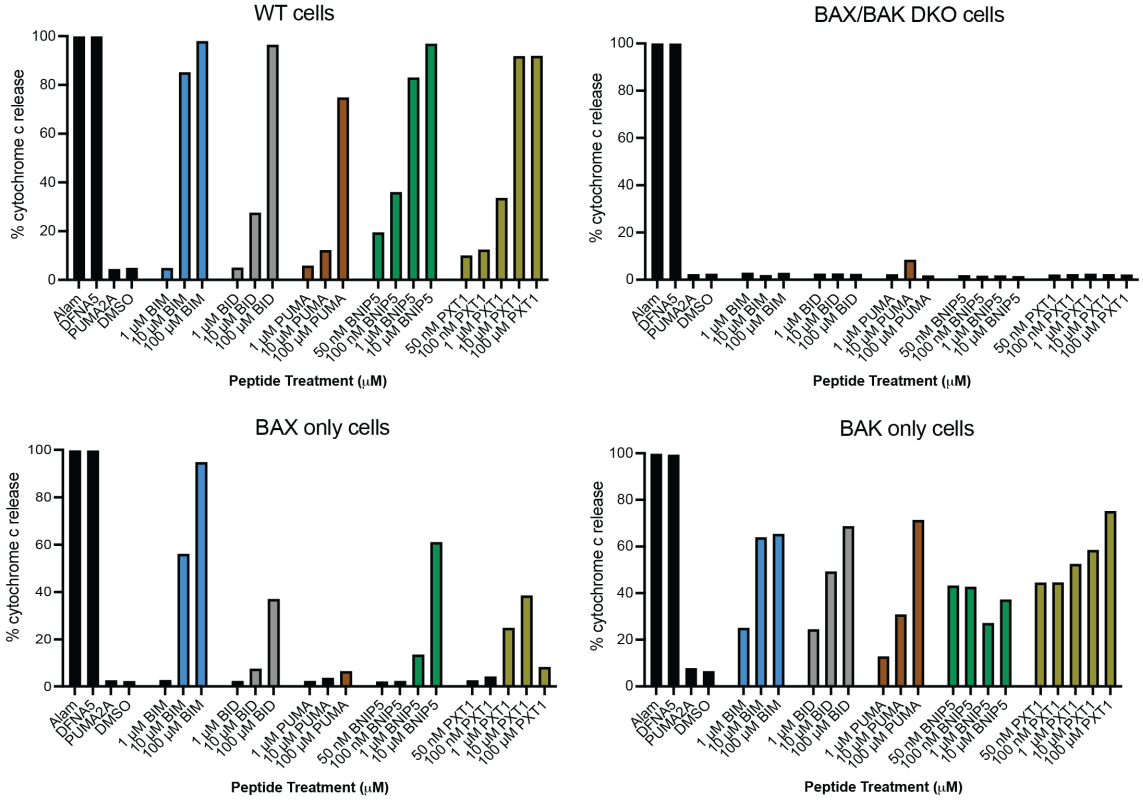
WT cells
BAX/BAK DKO cells
BAX only cells
BAK only cells
% cytochrome c release
Peptide Treatment (μM)
Alam
DFNA5
PUMA2A
DMSO
1 μM BIM
10 μM BIM
100 μM BIM
1 μM BID
10 μM BID
100 μM BID
1 μM PUMA
10 μM PUMA
100 μM PUMA
50 nM BNIP5
100 nM BNIP5
1 μM BNIP5
10 μM BNIP5
50 nM PXT1
100 nM PXT1
1 μM PXT1
10 μM PXT1
100 μM PXT1

Figure 17. Non-native peptides and human BNIP5 and PXT1 peptides induce membrane permeabilization cells. Percent cytochrome-c release was measured through BH3 profiling in permeabilized HeLa cells including WT, BAK only, BAX only, and BAK/BAX DKO cells. **A)** Non-native peptides dM2 (navy blue), dM4 (red), and dF8 (orange) were tested. **B)** Known activators BIM, BID, and PUMA were tested in addition to BNIP5 and PXT1. Data are from a single experiment (replicates are in progress).

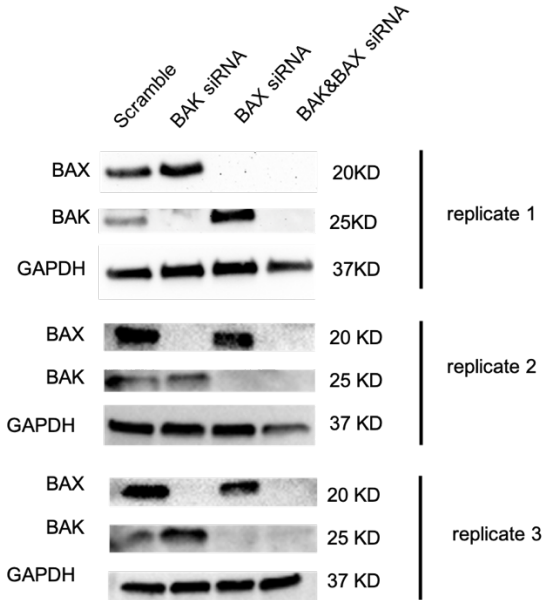

Figure 18. Western blot performed on 72-hour treated siRNA HeLa cells shows levels of BAK and BAX, with GAPDH as a loading control.

SECTION 1.5 ACTIVATORS AND INHIBITORS BIND BAK WITH SIMILAR BINDING MODES

To address what sequence or structural features may distinguish activators from inhibitors, we solved crystal structures of examples of each type of peptide bound to monomeric BAK and carried out a systematic comparison of these new structures and other complexes already available from prior work (**Figure 19A and Table 8**).

To compare inhibitor complexes, we resolved a 1.3 Å structure of BAK (grey) bound to dF2 (purple) and a 1.99 Å structure of BAK bound to dF3 (light pink) (**Figure 19A**). Superposition based on the highly similar structure of BAK in these two complexes showed that dF2 and dF3 bind very similarly, with no notable differences in the peptide backbone or the positioning of BAK-contacting side chains (**Figure 19B**). BAK complexes with inhibitor peptides BIM-h0-h3Glt, BIM-h3Glg, and BIM-h3Pc-RT, previously solved by Brouwer et al., include both BAK monomers and

core-latch domain-swapped BAK dimers bound to peptides that include a non-native amino acid that binds deep in the BAK domain core (Brouwer et al., 2017). The two core-latch dimer complexes, with BAK bound to either BIM-h0-h3Glt (raspberry red) (PDB:5VWX) or BIM-h3Pc-RT (salmon) (PDB:5VWY) differ in sequence at only a single peptide residue and are highly structurally similar, so we chose PDB:5VWY as a representative structure (**Figure 20**). We compared this core-latch dimer to monomeric BAK bound to BIM-h3Glg (hot pink) (PDB:5VX0) and once again observed no significant differences between the two (**Figure 20**). Finally, we compared monomeric BAK bound to BIM-h3Glg (hot pink) (PDB: 5VX0) and BIM-h3Pc-RT (light magenta) (PDB:5VWZ) to our novel inhibitors (**Figure 19B**). Overall, we did not see any significant differences in the structure of BAK, nor in the peptide backbone or side-chain arrangements, leading us to the conclude that our inhibitors adopt the same binding mode as previously published peptides that contain long, non-natural amino acids that make interactions not accessible to native residues.

To compare our novel activator dM2 to previously published activator complexes, we obtained a 1.3 Å structure of dM2 bound to monomeric BAK (**Figure 19A**). Other structures of activator peptides include mutants of native activator BID such as W3W5_BID (PDB: 7M5A), which contains Trp residues at positions 3d and 4e, and M3W5_BID (PDB:7M5B), with Met and Trp at these positions (**Figure 19C**) (G. Singh et al., 2022). Singh et al. do not classify W3W5_BID as an activating peptide, but we do so here on the basis of data demonstrating that it induces robust activation, similar to that of BID and BIM BH3 peptides, when used at a concentration of 1 μM in a liposome assay (G. Singh et al., 2022). Superposition of BAK bound to dM2 (pale green), W3W5_BID (forest green), and M3W5_BID (lime green) reveals high similarity and excellent structural alignment with no observable distinctions among the three peptides, with the exception of two side-chain rotamers (**Figure 19C**).

We also compared BAK-bound activator dM2 with crystal structures of core-latch domain-swapped dimers of BAK bound to BAK BH3 (PDB: 7M5C) and BIM-RT (PDB:5VWV), which are both activating peptides (G. Singh et al., 2022). Comparison of BAK structures indicates that the BAK BH3-bound binding groove opens up less, compared to the BAK dM2 binding groove (**Figure 21**). A slight divergence at the N-terminus of superimposed dM2 (pale green) and BAK BH3 (deep teal) peptides also leads to differences in polar contacts between the two peptides (**Figure 21**). Specifically, BAK BH3 forms additional polar contacts with BAK H99 and Q98 (**Figure 21A**). Another distinction is observed when superimposing complexes of BAK bound to dM2 (pale green) and BIM-RT (sky blue) (**Figure 21B**). A small difference at the C-terminus of the peptides is associated with a difference in polar contacts. **Figure 21B** shows a top view of dM2 (yellow

	DM2	DF2	DF3
Resolution range	38.07 - 1.3 (1.347 - 1.3)	44.29 - 1.3 (1.347 - 1.3)	40.35 - 1.99 (2.061 - 1.99)
Space group	C 1 2 1	C 1 2 1	P 1 21 1
Unit cell	102.13 41.04 47.02 90 93.644 90	94.13 41.08 56.39 90 122.001 90	48.29 65.26 111.57 90 102.117 90
Total reflections	320911	289866	160024
Unique reflections	46424 (3181)	43727 (2462)	43172 (4019)
Multiplicity	6.91(100.88)	6.63(117.73)	3.7(39.81)
Completeness (%)	96.66 (91.73)	96.6 (73.5)	92.3 (82.8)
Mean I/sigma(I)	17.30(1.29)		6
Wilson B-factor	20.24	15.75	22.26
R-merge	.04(1.71)	.03(0.58)	0.15(0.71)
R-meas	.04(1.85)	0.36(0.65)	0.17(0.82)
R-pim			
CC1/2	1(0.7)	1(0.87)	0.99(0.79)
Reflections used in refinement	46366 (4360)	43706 (3441)	43044 (4010)
Reflections used for R-free	2006 (188)	2006 (159)	1988 (178)
R-work	0.1782 (0.3845)	0.1615 (0.3179)	0.2456 (0.3342)
R-free	0.1982 (0.3849)	0.1822 (0.3799)	0.2758 (0.3808)
Number of non-hydrogen atoms	1646	1692	6322
RMS(bonds)	0.02	0.02	0.004
RMS(angles)	1.6	1.57	0.62
Ramachandran favored (%)	100	98.37	99.45
Ramachandran allowed (%)	0	1.63	0.55
Ramachandran outliers (%)	0	0	0
Rotamer outliers (%)	1.26	0	0.65
Clashscore	3.3	1.32	4.42
Average B-factor	34.83	24.61	28.46
Number of TLS groups	8	0	0

Table 8. X-ray data collection and refinement statistics. Values in parentheses are for the highest-resolution shell.

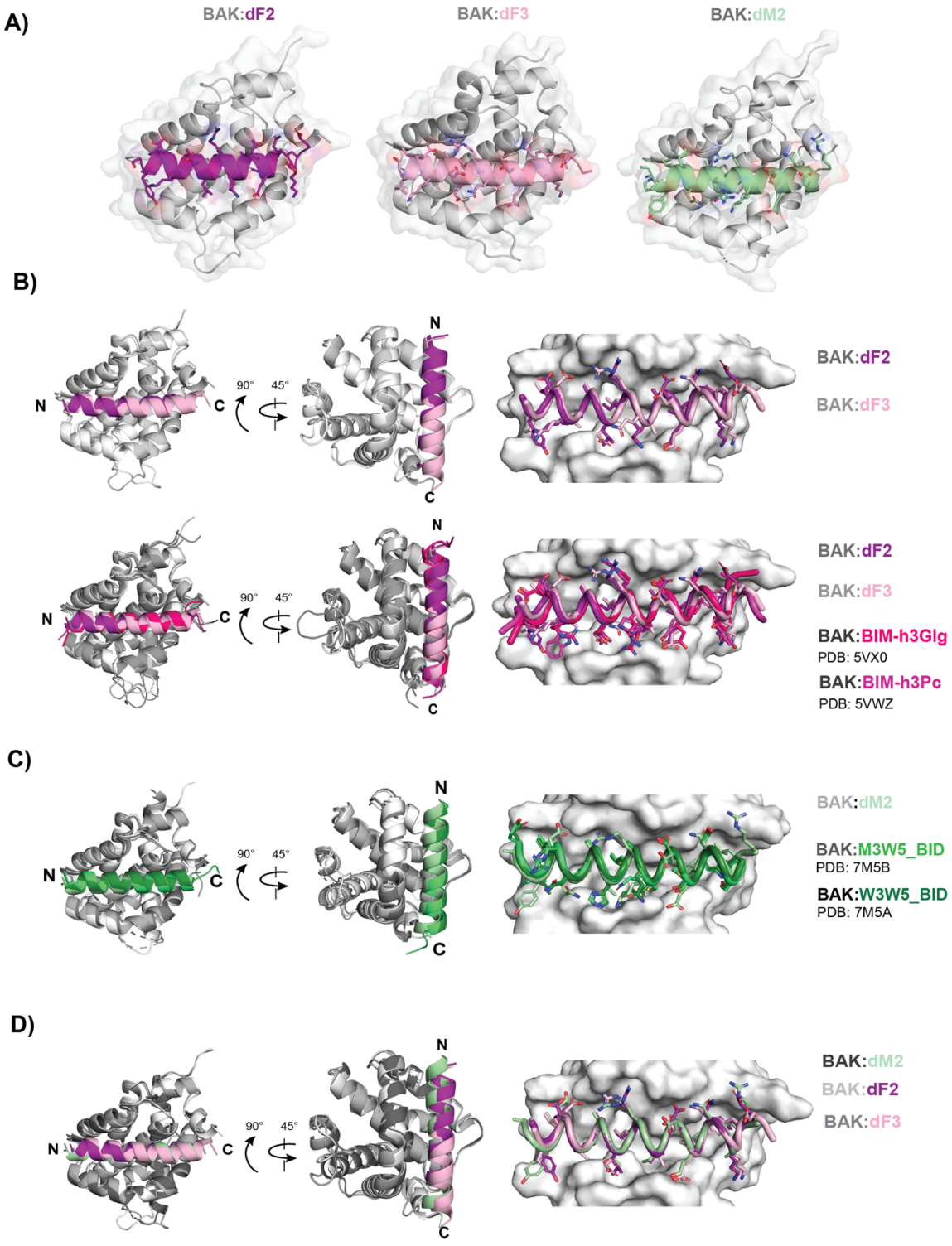

Figure 19. dF2, dF3, and dM2 bind to BAK similarly to other inhibitor and activator BH3 peptides. A) Structures of BAK (grey) bound to dM2 (pale green, dF2 (purple), and dF3 (light pink). Inhibitors are shown in shades of purple and pink and activators are shown in shades of green. **B)** (Top) Superimposed representations of BAK bound to dF2 and dF3 inhibitors (left side). BAK-contacting residues in the peptide

are shown with sticks (right side). (Bottom) Superposition of BAK bound to inhibitors containing non-natural amino acids including BIM-h3Glg (hot pink, PDB:5VX0) and BIM-h3Pc (light magenta, PDB:5VWZ) compared with newly solved dF2 and dF3 complex structures. **C)** Superposition of BAK complexes including activator peptides: dM2 (light green) and previously published activators M3W5_BID (lime green, PDB:7M5B) and W3W5_BID (forest, PDB:7M5A). **D)** Superimposed cartoon representations of dM2 (activator), dF2 (inhibitor), and dF3 (inhibitor). Further comparisons are included in **Figure 20 and 21.**

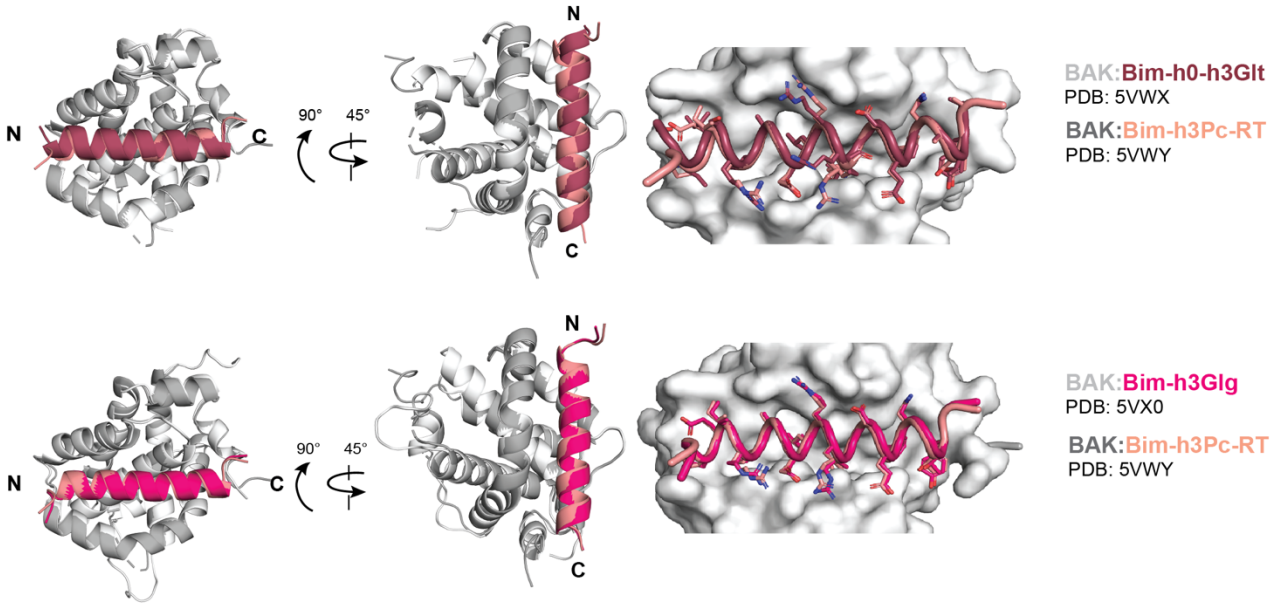

Figure 20. Peptide inhibitors containing non-natural amino acids bind to BAK in very similar binding modes. Structures are from (Brouwer et al., 2017). The inhibitor peptide sequences are the same, except for the non-natural amino acid at the 3d position that binds in the h3 pocket. Top) Comparison of inhibitors bound to domain-swapped core-latch BAK dimer structures: Bim-h0-h3Glt (raspberry, PDB: 5VWX) and BIM-h3Pc-RT (salmon, PDB: 5VWY). Bottom) Comparison of inhibitors bound to monomeric BAK (PDB:5VX0) and core-latch dimer BAK (PDB: 5VWY). BIM-h3Glg is in hot pink and BIM-h3Pc-RT is in salmon.

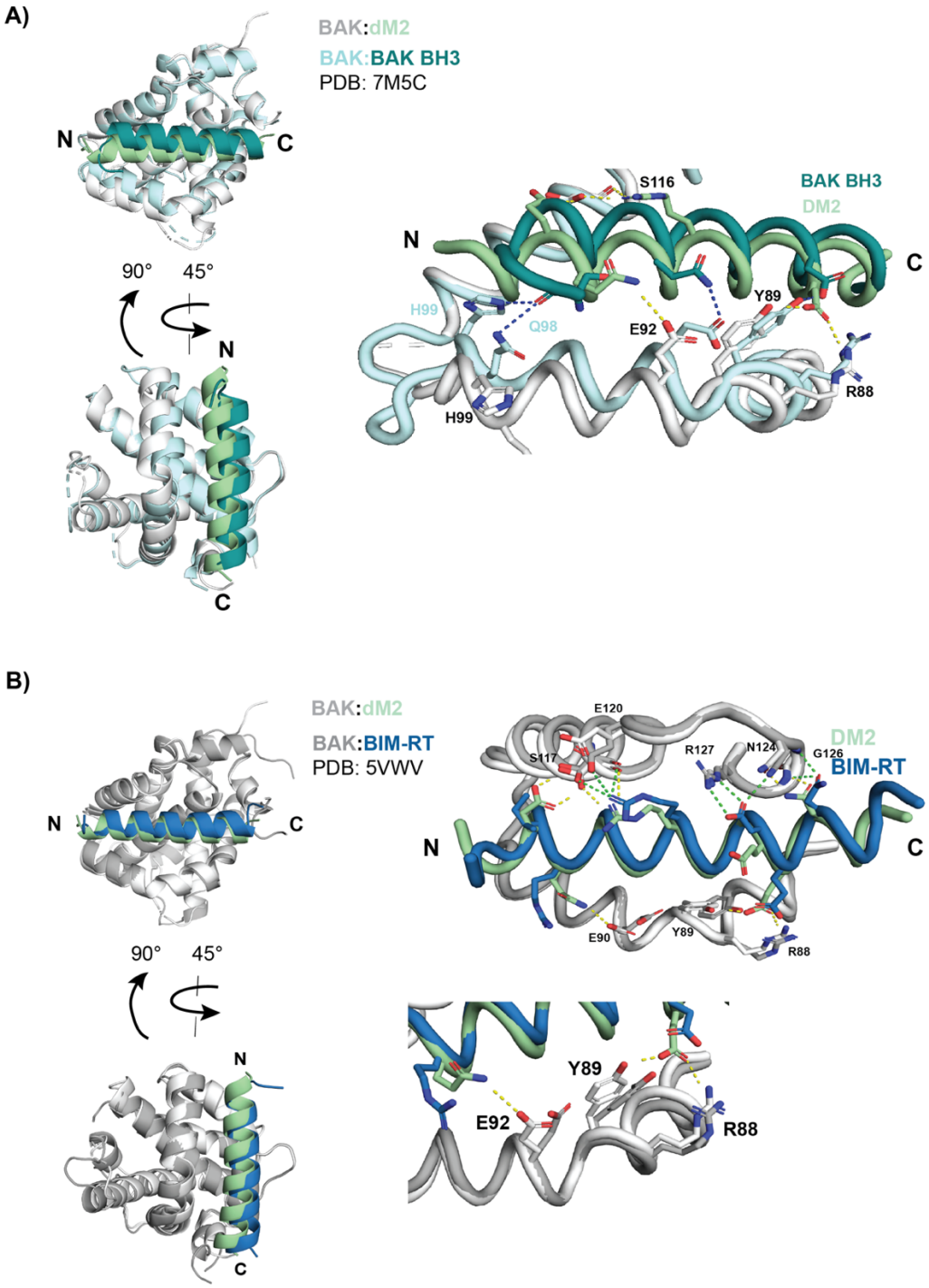

Figure 21. Activator dM2 binds differently compared to BAK BH3 and BIM-RT activator peptides. A) Comparison of dM2 (pale green) with BAK BH3 (deep teal) shows a shift of the N-terminus of the BAK BH3 peptide and the BAK α3 helix that forms part of the binding site. This difference in peptide binding mode is accompanied by a difference in polar contacts (yellow for DM2 and navy blue for BIM-RT). Specifically, BAK BH3 peptide forms contacts with H99 and Q98 on BAK that are not made by dM2. **B)** Superimposed crystal structures of dM2 (pale green) and BIM-RT (sky blue) show slightly different positioning of the C-

termini of the peptides. This difference allows dM2 to make polar contacts with residues E92, Y89, and R88 on BAK.

contacts) and BIM-RT (green contacts) hydrogen bonding networks. The biggest variation is observed at residues E92, Y89, and R88 on BAK that can form interactions with dM2, but not BIM-RT. This gain of contacts, however, does not prevent dM2 from functioning as an activator, although dM2 is a weaker activator compared to BIM-RT at 1.25 μM peptide (**Figure 13**). Overall, we concluded that structures of activators display more differences among them compared to inhibitors, based on structures solved so far.

Finally, to compare structural differences between activators and inhibitors, we compared our three new structures of BAK complexes bound to inhibitors dF2 (purple), dF3 (light pink), and activator dM2 (pale green) (**Figure 19)**. Interestingly, peptide dM2 engages BAK using the same geometry as the inhibitor peptides dF2 and dF3; it is not distinguished by a unique binding mode nor by any difference in the BAK structure. We extended our analysis by incorporating another inhibitor BAK:BIM-h3Glg (hot pink), and the activators BAK: BAK BH3 (deep teal) and BAK:BIM-RT (sky blue) into this comparison (**Figure 22**). With the exception of BAK: BAK BH3, which is an outlier, the peptides bound very similarly in the groove, with little variation in positioning or axial rotation (**Figure 22A**). Given the previously noted importance of residues at hydrophobic positions, we carefully examined the hydrophobic residues that engage the hydrophobic pockets of BAK and found that, in agreement with the similar binding modes, all activators and inhibitors aligned well at the hydrophobic positions (**Figure 22B**). Singh et al. have reported the presence of an electrostatic network that includes α1 helix and involves residues R42, E46, D90, N86, Y89, R137 in BAK (G. Singh et al., 2022). We found that the BAK:BAK BH3 complex shows differences in this network compared to the 5 other BAK complexes (**Figure 22B**). For example, side chains D90, R137, N86 showed alternative rotamer placements. However, the five related activator and inhibitor structures share a similar network in this region, dissimilar to that observed for BAK:BAK BH3, indicating that this local structure is not a characteristic of activators generally. Overall, our structural analyses did not reveal consistent differences in binding mode or residue interaction networks that could distinguish structures of BAK bound to activators vs. inhibitors.

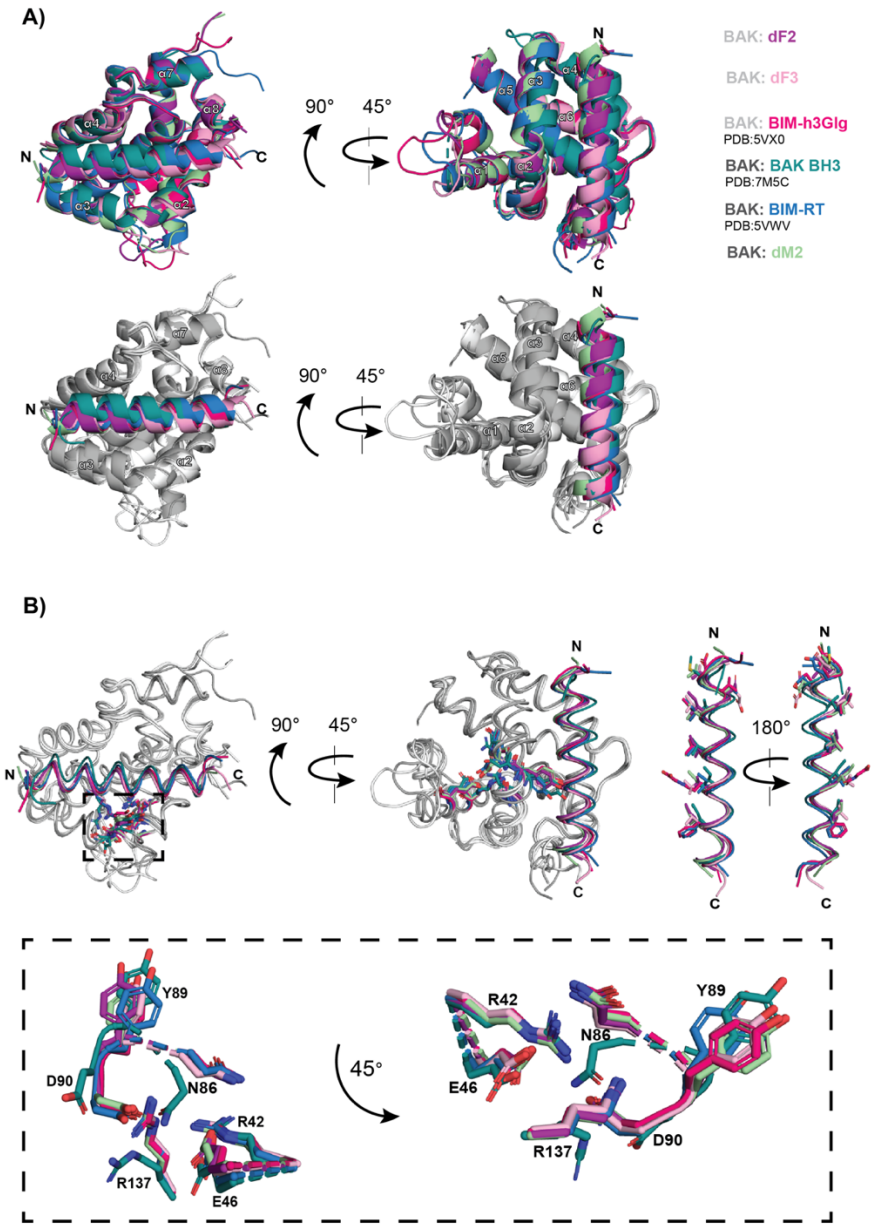

Figure 22. Activators and inhibitors of BAK bind with no systematic differences in structure. A) Superposition of complexes of BAK bound to activators (BAK BH3, BIM-RT, and dM2 peptides) and inhibitors (dF2, dF3, and BIM-h3Glg peptides). BAK BH3 (deep teal, PDB: 7M5C) shows the greatest deviation compared to the rest of the structures, with a shift of the N terminus of the peptide and the α3 helix of BAK. (Top) BAK and corresponding peptide shown in the same color. (Bottom) Same figure as in top, but with BAK colored in shades of grey for clearer visualization. **B)** (Left) Ribbon representation of cartoon in A). Residues involved in a previously reported electrostatic network are depicted with sticks and enclosed in a dotted rectangle. A closer look at the electrostatic network involving residues N86, Y89, D90,

R42, E46, and R137 viewed from two different perspectives differing by 45°. (Right) All six peptides are superimposed with hydrophobic residues depicted with sticks.

Previous groups have reported the presence of a cavity at the protein-peptide interface of complexes of BAK and BAX bound to BH3 peptides, and it has been suggested that this is important for BH3-induced destabilization and activation (Czabotar et al., 2013; Brouwer et al., 2017; G. Singh et al., 2022). The BAK:BIM-RT peptide complex cavity is located between BAK α1, α2, α3, and α5 helices with an estimated volume of 435 Å^3, while the BAX:BID peptide complex is located between BAX helices α2, α5, and α8 with an estimated volume of 140 Å^3 (Brouwer et al., 2017; Czabotar et al., 2013). Inhibitor peptides with non-natural amino acids occupy this cavity in BAK (Brouwer et al., 2017), suggesting that stabilizing this region of BAK may be important for inhibition.

We measured differences in cavity size across BAK:peptide complexes for activators and inhibitors and found no clear associations between cavity volume and peptide function (**Figure 23**). The activator BAK:BIM-RT complex (PDB:5VWV) had the largest cavity, with a volume of 404 Å^3, while the second-largest was found in the inhibitor BAK:dF2 complex with a cavity volume of 343 Å^3. Activator complexes BAK:M3W5_BID (PDB: 7M5A) and BAK:BAK BH3 (PDB: 7M5C) showed the smallest cavities, with volumes of 68 Å^3 and 104 Å^3.

We generated peptide sequence logos and pairwise RMSD calculations to compare activators and inhibitors (**Figure 24 and 25**). Sequence logos showed that both inhibitors and activators display the canonical L-xxx-G/A-D/E motif in addition to a preference for hydrophobic residues at the BAK hydrophobic pocket positions. However, activators showed more sequence variability at the site that binds the h0 pocket. For example, a negatively charged glutamate is present at position 2a in activator BIM, but not in any of the other activators. Furthermore, inhibitors appear to show a strong preference at positions 2b, 2c, 2f for negatively, positively, and negatively charged residues, respectively. However, inspection of BAK:peptide complex structures shows that these residues are solvent exposed and do not form significant contacts with BAK. Similarly, lysine residues in inhibitors at positions 4c do not display polar make contacts with BAK. Lastly, both activator and inhibitor peptides contain a negatively charged glutamate at position 3g that forms a salt bridge with arginine 88 on BAK. Overall, we did not see any consistent differences in peptide sequences that were indicative of activator or inhibitor function.

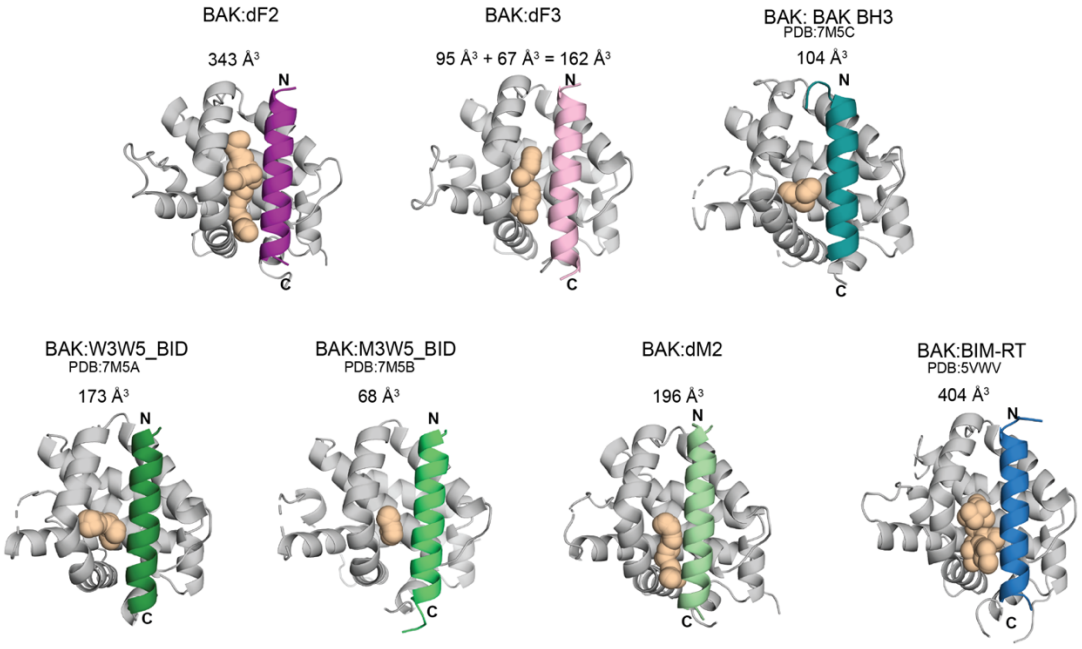

Figure 23. Cavity sizes in BAK: peptide complexes do not correlate with function. The program F-pocket was used to detect and quantify cavity volumes (indicated with wheat-colored spheres) using a minimum probe radius of 3.4 Å and a maximum probe radius of 6.2 Å. Inhibitor peptides are shown in purple and pink, and activator peptides are shown in shades of green and blue.

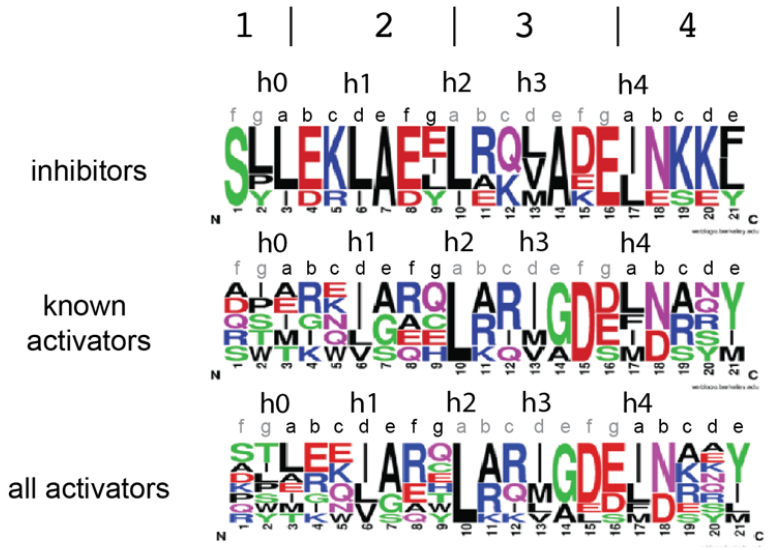

Figure 24. Sequence logos of activators and inhibitors show few residue preferences. Peptide sequence logos were generated for inhibitors (dF2, dF3, BK3, dF4, dF7), known activators (BID, BIM, PUMA, BAK, and BAX BH3 regions), and all activators (BID, BIM, PUMA, BAK, BAX, dM2, dF8, and dM4).

To further our structural analysis, we computed pairwise RMSD values between all peptides of BAK:peptide complexes including those of inhibitors dF2, dF3, and BIM-h3Glg as well as activators dM2 and BIM-RT. We did not include the BAK:BAK BH3 complex (PDB:7M5C) in our analysis given that this structure contains clear differences in the BAK opening, making it an unfair candidate for comparison across peptides. Our pairwise comparisons of activator vs. inhibitor peptides gave an average RMSD value of 1.2 Å, indicating no significant distinction between the two groups.

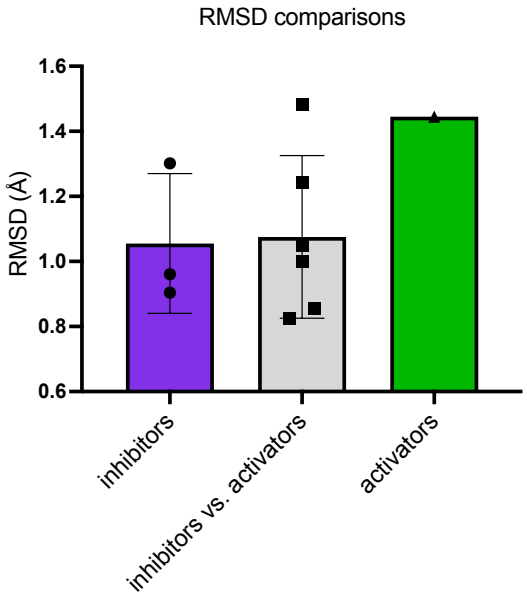

Figure 25. Pairwise RMSD calculations of activator vs. inhibitor peptides show an average RMSD of 1.1 Å. Crystal structures of BAK:peptide complexes were aligned based on BAK and then difference between peptide binding geometries were compared based on the all-backbone-atom RMSD values for inhibitors vs. inhibitors (purple), inhibitors vs. activators (grey), or activators vs. activators (green). Structures used for analysis included (BAK:dF2, BAK:dF3, BAK:BIM-h3Glg - PDB:5VX0, BAK:BIM-RT - PDB:5VWV, and BAK:dM2).

SECTION 1.6 BINDING AFFINITIES AND KINETICS DO NOT DISTINGUISH ACTIVATORS AND INHIBITORS OF BAK

To test whether activator vs. inhibitor peptides might bind to BAK with systematically different affinities or kinetics, we conducted experiments using bio-layer interferometry (BLI) (**Figure 26**). Briefly, b-His_6-BAK_{16-186} was purified and immobilized on streptavidin coated tips and

binding and dissociation of His_6-SUMO-peptide fusions was measured. We examined trends in affinities, k_{on}, and k_{off} values for 5 inhibitors and 3 activators (**Figure 26** and **Table 9**). We were unable to measure BLI affinities for activators dM4 and PXT1, given their weak binding and fast kinetics. However, we were able to measure steady state affinities through fluorescence anisotropy (**Table 10**) that were in agreement with our BLI measurements (**Table 11**). Although in general the activators were weaker binders than the inhibitors, this was not consistent across all peptides. For example, inhibitors dF4, dF3, dF2, and BK3 bound more tightly compared to activators dF8 and dM2, but tight binding activator BNIP5 BH3 was an exception to this trend.

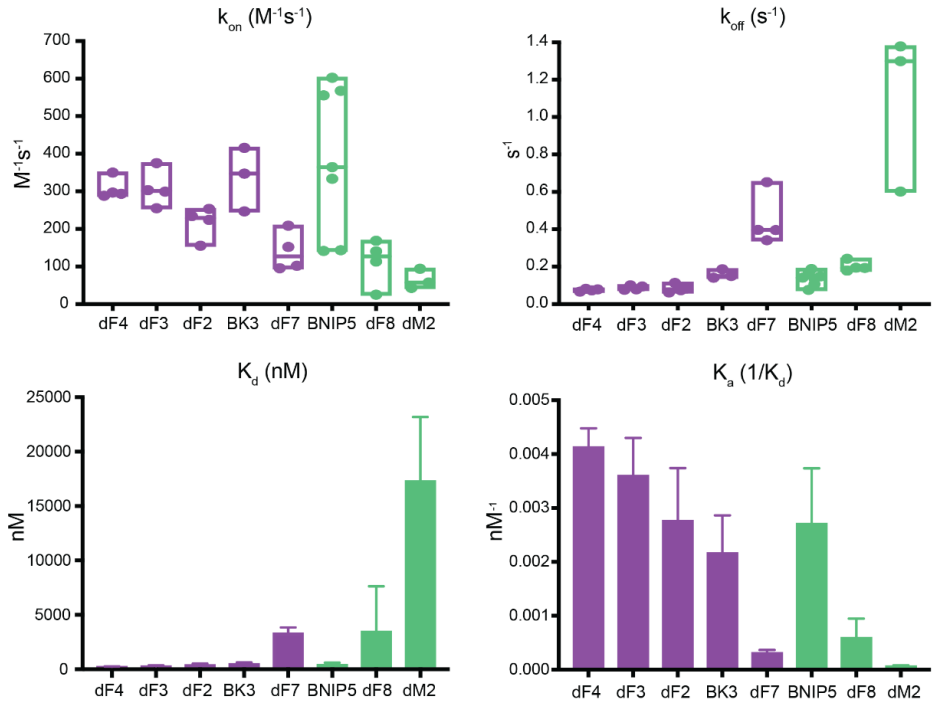

Figure 26. Neither rate constants nor affinities are indicative of peptide activator vs. inhibitor function. Replicates consisted of dF4 n=4, dF3 n=4, dF2 n=4, BK3 n=3, dF7 n=4, BNIP5 n=7, dF8 n=4, and dM2 n=3. Inhibitors are in purple and activators are in green. Biotinylated b-His_6-BAK_{16-186} was immobilized on streptavidin-coated tips and tested for binding to recombinantly expressed and purified His_6-SUMO-peptides. At least three replicate measurements for each peptide are indicated as points on the box plots. K_d values were computed as the ratio of k_{off}/k_{on}.

Peptide	Function	k_{off} (s^{-1})	stdev k_{off} (s^{-1})	k_{on} ($M^{-1}s^{-1}$)	stdev k_{on} (s^{-1})	Kd (nM)	stdev Kd (nM)
dF4	inhibitor	7.5E-02	6.8E-03	3.1E-04	2.9E-05	244	2.1E+01
dF3	inhibitor	8.7E-02	1.2E-02	3.1E-04	5.0E-05	288	6.9E+01
dF2	inhibitor	8.3E-02	2.2E-02	2.2E-04	4.3E-05	394	1.2E+02
BK3	inhibitor	1.6E-01	2.4E-02	3.4E-04	8.5E-05	493	1.4E+02
dF7	inhibitor	4.0E-01	1.4E-01	1.3E-04	5.3E-05	3294	5.5E+02
BNIP5	activator	1.6E-01	2.6E-02	5.8E-04	2.4E-05	424	1.8E+02
dF8	activator	2.0E-01	2.8E-02	1.1E-04	6.2E-05	3462	4.2E+03
dM2	activator	1.1E+00	4.3E-01	6.5E-05	2.6E-05	17296	5.9E+03

Table 9. Bio-layer interferometry kinetics for BH3 peptides binding to BAK show a range of affinities that do not correlate with activation function. Peptides were made as His_6-SUMO-BH3 fusions and immobilized on tips for binding to soluble BAK as described in the methods. Binding kinetics were too fast to fit for dM4 (activator) and PXT1 (activator) peptides.

Peptide	Function	K_d (nM)	Stdev K_d (nM)
dF4	inhibitor	547	7.0+01
dF3	Inhibitor	594	1.7E+02
dF2	Inhibitor	155	8.2E+01
BK3	Inhibitor	151	3.1E+01
dF7	Inhibitor	1813	4.7E+02
BNIP5	activator	411	1.7E+02
dF8	activator	916	5.3+0.2
dM2	activator	1480	5.9E+02
dM4	activator	5307	2.0E+02
PXT1	activator	10823	3.8E+03

Table 10. Fluorescence anisotropy measurements. Peptides tested were those listed in **Table 9**.

Peptide	Function	BLI Kd (nM)	FP Kd (nM)	Classification
dF4	inhibitor	244 ± 2.1E+01	547 ± 7.0+01	tight binder
dF3	Inhibitor	288 ± 6.9E+01	594 ± 1.7E+02	tight binder
dF2	Inhibitor	394 ± 1.2E+02	155 ± 8.2E+01	tight binder
BK3	Inhibitor	493 ± 1.4E+02	151 ± 3.1E+01	tight binder
dF7	Inhibitor	3294 ± 5.5E+02	1813 ± 4.7E+02	medium binder
BNIP5	activator	424 ± 1.8E+02	411 ± 1.7E+02	tight binder
dF8	activator	3462 ± 4.2E+03	916 ± 5.3+0.2	medium binder
dM2	activator	17296 ± 5.9E+03	1480 ± 5.9E+02	medium binder
dM4	activator	n.a.	5307 ± 2.0E+02	weak binder
PXT1	activator	n.a.	10823 ± 3.8E+03	weak binder

Table 11. Affinities determined using bio-layer interferometry vs. fluorescence polarization give consistent classifications of peptide binders of BAK. Peptides were grouped into tight (< 800 nM), medium (800 nM – 3 μM) , and weak (> 3 μM) binders for comparison to account for variability among methods. We were unable to measure affinities of weak binders dM4 and PXT1 by BLI. Fast kinetics for dM2 made it difficult to determine accurate k_{off} and k_{on} rate constants.

Our results also did not reveal consistent differences in kinetics. For example, we found that activators dF8 and BNIP5 had similar k_{off} rate constants to inhibitor BK3. Activators dF8 and dM2 showed slower association compared to inhibitors dF4, dF3, dF2, and BK3; but inhibitor dF7 bound with similar kinetics as activator dF8. Activator dM2 displayed fast binding kinetics, making it difficult to determine k_{on} with confidence, even at low peptide concentrations. In conclusion, 4 out of 5 inhibitors showed higher affinities compared to 2 out of 3 activators, although the number of activators for which we could get reproducible data was smaller than that of inhibitors. (Singh et al., 2022). Measurements for other peptides, reported in the literature, further support the absence of an affinity requirement for activation or inhibition, as discussed below.

DISCUSSION

Pro-apoptotic BAK is a key regulator that directly disrupts the mitochondrial outer membrane upon cell death stimulus (Chittenden et al., 1995). This irreversible step is regulated by BH3-only proteins binding to membrane localized BAK, which triggers a series of conformational changes that lead to BAK homodimerization and subsequent higher order cluster formation and MOMP (H. Kim et al., 2009). We sought to elucidate features that allow some, but not all, BH3-only proteins to activate pro-apoptotic BAK. With the goal of further deciphering the complex activation mechanism that governs BAK function, we focused our studies on the initial binding event that triggers the cascade of subsequent conformational changes.

Seeking a broad panel of BAK binders, we used peptide screening and computational design to discover 19 non-native peptide binders of BAK. These peptides displayed a range of profiles in yeast surface-display experiments, and we tested 10 peptides with strong binding signals in a liposome assay that serves as a proxy for MOMP. We found that 5 peptides functioned as inhibitors and 5 peptides functioned as activators of BAK in liposome permeabilization assays. To our knowledge, previous groups have only tested point mutations of previously known activators. Our results dramatically expand the sequence space that has been tested for BAK-regulating function and reveals that this space includes both activators and inhibitors that could serve as the basis for developing BAK-modulating therapeutics. Notably, inhibitor peptides BK3, DF2, and DF3 are more potent in liposome assays than the previously reported BAK-inhibitor peptide BIM-h3PcRT yet are composed entirely of native amino acids (Brouwer et al., 2017). However, we did not compare our peptides to other tighter variations of BIM-h3PcRT containing other non-natural amino acids (NNAs) at the 3d position engaging with the BAK h3 pocket.

To our knowledge, only five native BH3 peptides are consistently reported to bind and activate BAK including BID, BIM, PUMA, the BH3 sequence within BAK itself, and the corresponding region in BAX (Moldoveanu et al., 2013; Sarosiek et al., 2013; Hockings et al., 2015; Llambi et al., 2011). In this work, we discovered 9 previously unidentified human proteins that contain BH3-like regions that directly interact with BAK, most of which are predicted to be structurally accessible in the context of the full-length protein **(Table 4)**, and two of which showed potent induction of MOMP in cells. BNIP5 (also referred to as C6orf222) and PXT1 bound BAK with different affinities (nanomolar vs. low micromolar) but both induced BAK-dependent membrane permeabilization cells. BNIP5 and PXT1 were more potent than BID, BIM, and PUMA in this profiling assay. Also, BNIP5 was more potent than PXT1, consistent with our biochemical data. Interestingly, BNIP5 and PXT1 retained high potency at 10 μM in BAK depleted cells,

indicating that both induce BAX-mediated MOMP. Both BNIP5 and PXT1 bind all five anti-apoptotic BCL-2-family proteins with nanomolar affinities (DeBartolo et al., 2014), which means that the function of these proteins as activators vs. sensitizers likely depends on the relative expression levels and localizations of pro- vs. anti-apoptotic proteins. BNIP5 has unknown function, though transcript levels are high in colon, small intestine, pancreas, and stomach cells as characterized in haematopoietic cells (Luck et al., 2020). Peroxisomal testis-specific 1 (PXT1) is expressed in male germ cells, where overexpression induces apoptosis of spermatocytes (Kaczmarek et al., 2011). Our work indicates that that BNIP5 and PXT1 are two additional BH3-only activator proteins that may have unexplored biological implications in the apoptotic regulatory network.

The features that make a peptide an activator vs. an inhibitor of BAK are not known. Prior to our study, others had shown that a single-residue substitution at a BAK-binding hydrophobic position could convert an activator to an inhibitor (Brouwer et al., 2017), suggesting that minimal sequence differences are sufficient to alter BAK function. Furthermore, consistent with a previous report for BAX (Czabotar et al., 2013), we find differences in activation potency among BH3-only peptides that establish that an amphipathic peptide with a BH3 motif including L-x(4)-D/E (x = any amino acid) is not sufficient to activate BAK. Single-residue substitutions in BH3 peptides can increase BAK activation activity and convert a non-activator (NOXA) to a weak activator and a moderate activator to a more potent activator (PUMA), as has previously been observed for BAX. Clearly, as-yet unknown sequence and structural features drive varying functional outcomes.

A possible mechanistic explanation for activation could be that activators vs. inhibitors engage BAK with different binding modes, in distinct geometries. Dissociation of the BAK “latch” (α6-α8) from the core (α2-α5) is an early step in activation, and it is plausible that some peptides bind in a way that induces a conformational change that is propagated to the latch via a pathway of allosteric communication. Supporting this possibility, Singh et al. showed a BAK BH3 peptide docks into the binding groove of a BAK monomer in a distinct pose that is accompanied by a rearrangement of a BAK salt-bridging network (G. Singh et al., 2022). However, our analysis of multiple crystal structures of BAK-peptide complexes, including three structures that we solved in this work, showed that 3 inhibitors and 3 activators bind with very similar geometry and contacts. Peptides in these two functional groups cannot be structurally distinguished by any criterion that we could discern. The re-arranged BAK residues in the BAK:BAK BH3 complex appear to be specific to that interaction, and not characteristic of activators more broadly.

Considering other mechanisms, we reasoned that activators vs. inhibitors might differ in their binding kinetics. Association of activators with BAK is transient, and the groove in which

activator and inhibitor BH3 peptides bind re-shapes to form the groove that is occupied by the BH3 helix of a partner BAK molecule in the so-called "BH3:groove homodimer" that is critical for membrane poration. Following BH3 binding that induces a change in BAK, which may correspond to core-latch dissociation, dimerization requires activator peptide dissociation followed by a rearrangement in which two neighboring BAK monomers exchange BH3 helices. Peptide dissociation may therefore set up a competition between activator or inhibitor BH3 peptide re-binding vs. BAK dimerization via BH3 exchange. In this model, peptides that re-bind more slowly than BAK dimerization would function as activators, whereas those that re-bind quickly and continue to occupy the canonical groove would function as inhibitors. Although we found that most of the activator peptides in our study bound more slowly to BAK than did most of the inhibitors, this was not consistent across all peptides. Specifically, activator BNIP5 had the greatest k_{on} rate constant (5.8E-04 $M^{-1}s^{-1}$) compared to the 5 inhibitors and 3 activators that were tested. Furthermore, inhibitors did not necessarily dissociate more slowly. For example, inhibitor dF7 has a greater k_{off} rate constant (0.4 s^{-1}) compared to activators BNIP5 (0.16 s^{-1}) and dF8 (0.2 s^{-1}). Overall, our kinetic data indicate that k_{on} and k_{off} rate constants measured using bio-layer interferometry do not determine whether or not a peptide activates or inhibits BAK.

Another possibility is that activators and inhibitors vary in their affinity for BAK. This model is supported by the increase in BAK-binding affinity of BIM when position 3d is substituted with a pentyl-carboxylate (h3Pc) and its variants Glg and Glt. These substitutions increase the affinity of BIM to K_d = 1.3 μM, 21 μM and 1 μM, relative to weakly binding BIM (with an affinity that is too weak to measure using BLI), and also convert BIM from an activator to an inhibitor (Brouwer et al., 2017). Peptides that bind tightly to BAK monomers and stabilize that inactive state would be expected to act as inhibitors. This is the general trend that is observed in our data (**Figure 26**), but there are exceptions. For example, BNIP5 is an activator and tight binder, with an affinity of 424 nM. A more recent study also shows that tight-binding peptides M(3)W(5) BID BH3 (K_d = 690 nM) and M(3)W(5) BID BH3 (K_d =250 nM) can activate BAK in liposomes at 1 μM (G. Singh et al., 2022)., Leshchiner et al. have also shown that stapled BID SAHB peptides with low nanomolar affinities for binding to murine full-length BAK activate in liposome-based assays (Leshchiner et al., 2013).

We propose a modification of the affinity model that reconciles all of our observations as well as other data in the literature. In **Figure 27**, we use a free energy landscape diagram to illustrate how BH3 peptides may act as *catalysts* of activation by binding differentially to the BAK ground-state monomer and to the transition state for BAK activation. In the figure, we represent BAK tethered to the mitochondrial outer membrane as an inactive monomer. Following activation,

BAK forms the lower energy BH3-in-groove dimer (PDB: 7K02). Between the monomer and the dimer, on this pathway, BAK must pass through a transition state of unknown structure. In the context of this free energy landscape model, activators and inhibitors differ in their affinities for distinct BAK conformational states. As for enzyme-catalyzed reactions, tighter binding of a BH3 peptide to the activation transition state vs. the monomer ground state will lower the energy barrier and promote activation. In contrast, tighter binding to the ground state than to the transition state will inhibit activation.

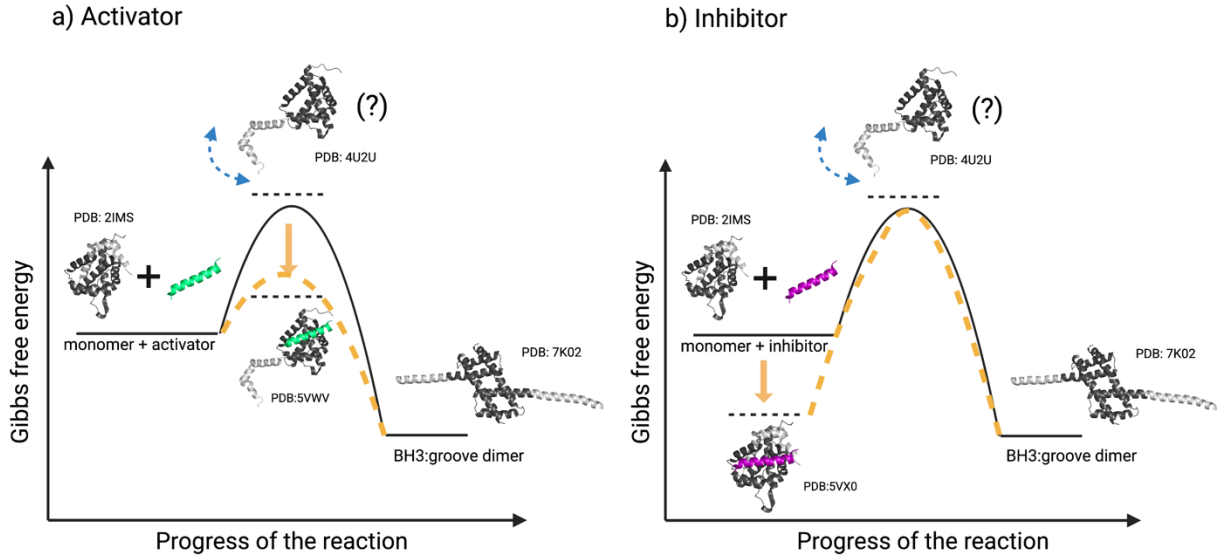

Figure 27. Free energy diagram for BH3 peptide activation or inhibition of BAK. Crystal structures of the BAK monomer and putative intermediates are used to illustrate steps in activation, with the BAK core in dark grey and the latch in light grey. Monomeric BAK (PDB: 2IMS) is placed at a higher energy compared to the BH3:groove homodimer (PDB:7K02), which is presumed to be embedded in the outer mitochondrial membrane (not shown). The structure or nature of the transition state is not known, and is labeled with a question mark, but may resemble an unlatched conformation of BAK as discussed in the text (here represented using PDB:4U2U). **A)** Illustrates stabilization of a putative transition state of BAK by binding of an activator (green). **B)** Illustrates stabilization of monomeric BAK in the presence of an inhibitor (purple).

Multiple conformational changes of BAK need to occur in order to reach the dimeric state, including core-latch dissociation and dimerization via exchange of BH3 helices. Several groups have reported exposure of the BH3 region as an indicator of activation (Moldoveanu et al., 2006). Because existing structures of domain-swapped dimers with dissociated latch regions do not exhibit any rearrangements of the BH3 region, we assume that this step follows latch dissociation, as illustrated in **Figure 28**. Existing data do not establish which conformational change corresponds to the rate-limiting step. However, all of our peptides – both activators and inhibitors

– can bind to the monomer state, and our model requires that at least the activators also bind to the transition state. Activators and inhibitors are similar in sequence and structure, and peptides that differ by just two mutations can differ in their function (inhibitor dF4 and activator dF8). These arguments suggest that the monomer and the transition state share structural similarities and therefore that the transition state is "early" in the pathway leading to dimer formation. For this reason, and because we expect there to be a large energy cost for latch dissociation that disrupts stabilizing intradomain interactions, we speculate that disengagement of the latch from the core is the rate-limiting step, and we use the core-latch dissociated structure (PDB: 4U2U) as a model for the transition state in **Figure 27** and **Figure 28**. However, our data do not rule out other scenarios – such as rate-limiting dissociation of the BH3 helix from the BAK core, following latch dissociation – which can also be considered.

Notably, it is easy to incorporate the effects of many peptides, and even non-peptide binders into this model. BIM peptide variants with non-natural amino acids at position 3d stabilize the monomeric ground state more than the transition state, whereas stapled BID SAHB peptides with low nanomolar affinities to murine full-length BAK stabilize the transition state in preference to the monomer (Brouwer et al., 2017; Leshchiner et al., 2013). In addition to binding the canonical hydrophobic groove, it is possible to bind other regions within BAK and induce activation. For example, antibody 7D10 triggers BAK activation by binding the α1-α2 loop. In the context of our model, this implies that the structure of this region differs between the monomer state and the transition state, and that antibody binding preferentially stabilizes the transition state, lowering the energy barrier to the conformational changes that are required for MOMP to occur.

Our finding that just a few mutations in BH3-like helices can give rise to BAK activators would seem to pose a risk that evolutionary drift in BH3 sequences might lead to unregulated cell death. However, anti-apoptotic BCL-2 members play a key role in restraining activation, by sequestering the exposed BH3 region of pro-apoptotic members BAK and BAX at some point after core unlatching. Nanomolar affinities of the BAK BH3 region for anti-apoptotic BCL-2 family members (K_d = 53 nM for BCL-x_L and 20 nM for MCL-1) allows for an affinity buffer that can tolerate such mutations. That is, mutated BH3-like helices must bind both BAK and the partner anti-apoptotic protein with an affinity greater than that of the BAK BH3 region in order to induce MOMP. Furthermore, the role of mitochondrial membrane channel VDAC2 in restraining BAK must also be taken into consideration (Yuan et al., 2021).

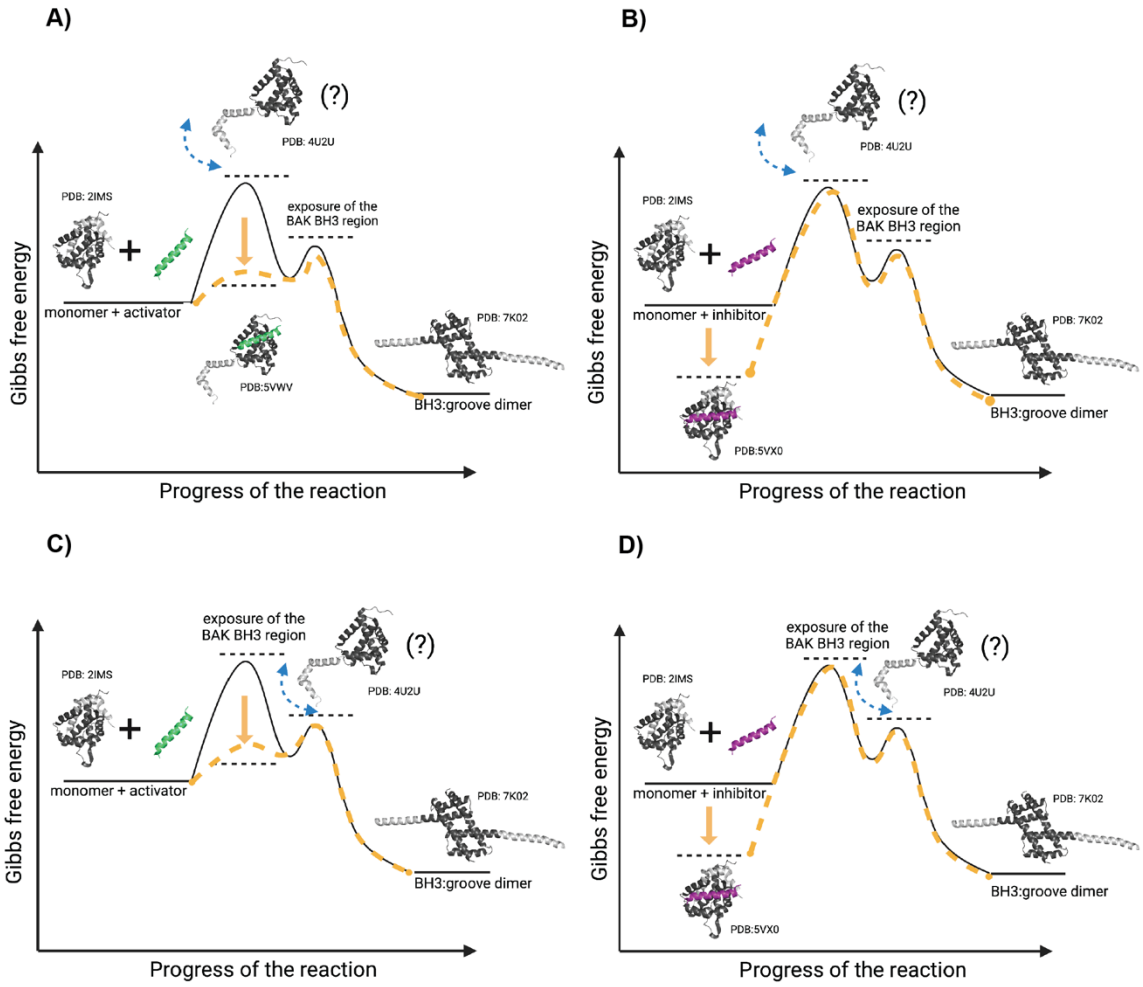

Figure 28. Free energy diagram to explain differences between activators and inhibitors of BAK. Depicted are putative intermediate crystal structures of BAK with the core in dark grey and the latch in light grey as described for **Figure 28**. Exposure of the BAK BH3 is depicted as occurring **top)** after release of the latch from the core and **bottom)** before release of the latch from the core.) **A)** and **C)** illustrate BAK activators stabilizing the transition state. **B)** and **D)** illustrate BAK inhibitors stabilizing the ground state.

Overall, we have discovered two new human and eight non-native peptide binders of BAK with diverse sequences and function. These included human proteins BNIP5 and PXT1, which activate BAK in cells. We solved 3 crystal structures of BAK:peptide complexes including 2 inhibitors and 1 activator and found that all three peptides bound in the canonical hydrophobic groove of BAK with a shifted binding mode when superimposed with BIM BH3 peptide. Surprisingly, the binding mode of both inhibitors is highly similar to that of the activator, despite their different functions. In addition, our kinetic data shows that neither peptide binding kinetics

nor affinity for BAK are sufficient to distinguish activators from inhibitors. This work highlights the complexities associated with binding to the BAK BH3-binding groove and the resulting allosteric regulatory network that regulates BAK function. We speculate on the energetic requirements for peptide activation vs. inhibition functions and propose a model to summarize our findings.

METHODS

Peptide synthesis, purification, and concentration determination

Peptides were synthesized in the Swanson Biotechnology Center Biopolymers and Proteomics Core. All peptides were amidated at the C terminus; peptides used for fluorescence assays were labeled at the N terminus using a 5-Carboxyfluorescein, single isomer (5-FAM); peptides used for liposomes and crystallography were acetylated at the N terminus. Non-natural amino acid Fmoc-AsuOtbu-OH was purchased from ChemImpex. Crude peptides were purified by HPLC on a C18 column using a linear gradient of water/acetonitrile and masses were verified using MALDI mass spectrometry. Synthesized peptides used in liposome assays were dissolved in water. Absorbance at 280 nm (A_{280}) was measured in Edelhoch buffer (7 M guanidine-HCl + 0.1 M potassium phosphate buffer pH 7.4) using a NanoDrop UV spectrophotometer and then peptide concentration (C) was determined based on Beer's law with the extinction coefficient calculated based on the number of tyrosines (1490 $M^{-1}cm^{-1}$) and tryptophans (5500 $M^{-1}s^{-1}$) in the peptide using the ProtParam tool in ExPasy https://web.expasy.org/protparam/. Synthesized peptides used in cell-based assays were dissolved in DMSO. Peptide concentration was also determined using Beer's Law, however extinction coefficients were re-calculated based on controls tested in DMSO, giving values of 2287 $M^{-1}s^{-1}$ and 6650 $M^{-1}s^{-1}$ for tyrosine and tryptophan, respectively.

Fluorescence anisotropy binding assays

Fluorescence anisotropy assays were performed in 25 mM Tris, 50 mM NaCl, 1 mM EDTA, 20 mM HEPES at pH 8.0, with 5% DMSO (FP buffer), in Corning 96-well, black, polystyrene, nonbinding surface plates. Two-fold serial dilution of b-His_6-BAK_{16-186} to generate 24 points was done in Eppendorf tubes and then protein solutions were transferred to plates. A solution of 100 nM peptide in 50% DMSO and 50% FP buffer was prepared, and 5 μl of this mixture was added to each well to give a final concentration of 10 nM peptide in 5% DMSO. Plates were incubated for 2 hours at room temperature to reach equilibrium and subsequently read at 25 °C in a SpectraMax M5 Multi-Mode microplate reader. Five replicate titrations were performed for each peptide, and the dissociation constant was estimated by fitting each curve to a 1:1 binding model as in Roehrl *et al*. using Python (Roehrl et al., 2004).

Yeast surface-display

Peptides in **Table** 2 were constructed as described in Frappier et al. (Frappier et al., 2019). Briefly, synthetic DNA encoding peptides was amplified and cloned into the yeast surface display plasmid pCTCON2 between Xho1 and Nhe1 restriction digest sites using homologous

recombination (Chao et al., 2006). The construct contained a carboxy-terminal FLAG tag after the peptide. Sequences were transformed into yeast strain EBY100 using a Frozen-EZ yeast transformation II kit. Sequence-verified yeast clones were stored in glucose media SD + CAA media (5 g/L casamino acids, 1.7 g/L yeast nitrogen base, 5.3 g/L ammonium sulfate, 10.2 g/L Na_2HPO_4-•$7H_2O$ and 8.6 g/L NaH_2PO_4-•H_2O, 2% glucose) + 20% glycerol. To induce expression of peptides on yeast, the previously published protocol of Reich *et al.* was adapted (Reich et al., 2016). Plated cells were grown overnight in 5 ml of SD + CAA media at 30 °C. Cells were then diluted to OD600 of 0.05 in 5 ml of SD + CAA media and grown for approximately 8 hours at 30 °C. Once again, cells were diluted to an OD600 of 0.005 and left to grow until reaching an OD of 0.1-0.4. To induce peptide expression, cells were diluted to an OD600 of 0.025 in 5 ml of galactose media (SG + CAA media: 5 g/L casamino acids, 1.7 g/L yeast nitrogen base, 5.3 g/L ammonium sulfate, 10.2 g/L Na2HPO4-•7H2O and 8.6 g/L NaH2PO4-•H2O, 2% galactose) and grown to an OD600 of 0.2–0.5 (approx. 20 hours) at 30 °C.

Peptide-displaying yeast cells were prepared for sorting in low protein-binding 96-well 0.45 µm filter plates. A volume of 50 µl per well at a concentration of $1*10^7$ cells/ml was used. Based on an estimate that an OD600 = 1 corresponds to $3*10^7$ cells/ml, the required volume of cells was pelleted at 14,000 g for 5 minutes. Supernatant was aspirated and cells were washed twice in BSS buffer (50 mM Tris, 100 mM NaCl, 1 mg/ml BSA, pH 8.0). Cells were resuspended to a final density of $1*10^7$ cells/ml in BSS buffer. Then 50 µl of cells per well plus a final concentration of 2.4 µM of pre-tetramerized BAK monomer (see protein expression and purification section) were incubated for 1.5 - 2 hours at room temperature (~25 °C). Cells were filtered with a vacuum and washed twice with pre-chilled BSS buffer. 20 µl of primary anti-HA antibody (mouse, Roche, Indianapolis, IN, RRID:AB_514505) diluted 1:100 was added to the mixture and incubated for 15 minutes at 4 °C in BSS buffer. Cells were filtered and washed twice with BSS buffer. Next, 20 µl of APC-conjugated secondary antibody (rat anti-mouse; CD45 Clone 30-F11, RUO from BrandBD Pharmingen) was added at 1:40 dilution and incubated at 4 °C for 15 minutes. Cells were filtered and washed twice with BSS. Finally, cells were resuspended in BSS and transferred to a second 96-well plate for fluorescence activated cell sorting (FACS) and analyzed for BAK binding using a FACSCanto II HTS-1.

Liposome assay

Large unilamellar vesicles (LUVs) mimicking the outer mitochondrial membrane were made using Avanti Polar Lipids, Inc. lipids dissolved in chloroform including 1-palmitoyl-2-oleoyl-glycero-3-phosphocholine (Avanti: 850457C 16:0-18:1 PC (POPC)), 1,2-dioleoyl-sn-glycero-3-

phosphoethanolamine (Avanti: 850725C 18:1 (Δ9-Cis) PE (DOPE)), L-α-phosphatidylinositol (Liver, Bovine) (sodium salt) (Avanti: 840042C Liver PI), 1,2-dioleoyl-sn-glycero-3-phospho-L-serine (sodium salt) (Avanti: 840035C 18:1 PS (DOPS)), 1,2-dioleoyl-sn-glycero-3-phospho-L-serine (sodium salt) (Avanti: 790404C 18:1 DGS-NTA(Ni)), 1',3'-bis[1,2-dioleoyl-sn-glycero-3-phospho]-glycerol (sodium salt) (Avanti: 710335C 18:1 Cardiolipin) at a (43:27:11:10:4:5) molar ratio. The lipid mixture was dispensed into borosilicate glass test tubes (13 x 100 mm, Fisherbrand) in 15 mg aliquots. Lipid films were made by evaporating the chloroform in the tubes with nitrogen gas using a glass Pasteur pipet in a fume hood. The film was further dried overnight in a flask connected to a vacuum pump. Lipid films in tubes were individually sealed in plastic pouches filled with nitrogen gas and kept in the freezer at -80 °C.

To form liposomes encapsulating dye molecules, 14 mg of 8-aminonaphthalene-1,3,6-trisulfonic acid, disodium salt (ANTS) dye (Biotium #90010) and 40 mg of p-xylene-bis(N-pyridinium bromide) DPX fluorescent quencher (Biotium #80012) were added to a test tube containing lipid film and hydrated with 500 μl of buffer A (200 mM KCl, 10 mM HEPES, 1 mM $MgCl_2$ pH 7.5). The tube was vortexed for 1 minute to completely dissolve the lipid film. The solution was then transferred to an Eppendorf tube. The lipid/dye emulsion was then subjected to 17 freeze-thaw cycles using liquid nitrogen and room temperature water. Subsequently, the resulting multilamellar vesicles were extruded up to 21 times through two sheets of polycarbonate membrane and a filter with 100-nm sized pores (Avanti Polar Lipids), until the solution could be pushed from one extrusion syringe to the other without much resistance. The resulting liposomes were separated from free ANTS/DPX dye using a disposable Sephadex G-25 in PD-10 desalting column (GE Healthcare 17-0851-01) using buffer A to flow the solution through the column. The resulting solution was collected manually in Eppendorf tubes every 10 drops. Translucent fractions were selected for dynamic light scattering (DLS) to verify the size of the liposomes. Fractions corresponding to average distributions of 100 nm diameter particles were subsequently used for experiments. Liposomes were kept covered and at 4 °C until use. Liposomes were made fresh for all experiments performed that same day.

The liposome activation assay was performed in a Corning 384-well plate (#CLS3573). Briefly, 30 μl of buffer A, 10 μl of liposomes, 5 μl of peptide, 5 μl of BAK ΔN22 ΔC25 C166S with a C-terminal His_6 tag (BAKΔC25-His_6) were added, in that order. The final volume in each well was 50 μl. Peptide and BAKΔC25-His_6 were added at 10x the desired final concentration in the well. 0.2% Triton X-100, added without peptide or BAK protein, was used as a positive control for dye release. The plate was immediately put in either a Tecan Spark Multimode or a

SpectraMax M5 Multi-Mode microplate reader and read at room temperature for 1-2 hours.

Protein expression and purification

b-His6-$_{BAK16-186}$ was cloned into vector pDW363 and transformed into BL21 (DE3) E. coli cells. 8 L of cells were grown in TB media with ampicillin. Absorbance was monitored until an OD600 of 0.6 was reached, at which point 15 mg of biotin and 1 M IPTG (final concentration 1 mM) were added. Cells were then transferred to 16 °C for overnight growth. Cells were spun down the next morning at 7000 g for 15 minutes. Pellets were transferred to falcon tubes and kept on ice. 25 mL of Ni-NTA binding buffer (20 mM Tris, 500 mM NaCl, 5 mM imidazole, pH 8.0) per liter of growth and 50 μL of PMSF at 100 mM to a final concentration of 0.2 mM per L of growth were added. Pellets were resuspended by pipetting up and down and vortexing and subsequently sonicated for a total of 3 minutes of 20 s on/20 s off at ~60 power duty cycle ~5 output control. Lysed cell cultures were centrifuged at 12,000 rpm for 30 mins and filtered through a 0.22 μm filter. Ni-NTA resin washed with Ni-NTA binding buffer was incubated with filtered supernatant for 1 hour at 4 °C. Protein-bound resin was poured through a disposable column and washed three times with Ni-NTA binding buffer. BAK protein was eluted with Ni-NTA elution buffer (20 mM Tris, 500 mM NaCl, and 300 mM imidazole, pH 8.0). Eluted sample was purified by gel filtration using a Superdex 75 26/60 column in TBS buffer pH 7.5. For yeast surface display, b-His_6-BAK_{16-186} was pre-tetramerized by incubating with streptavidin conjugated to R-phycoerythrin (SAPE) (Thermo Fisher Scientific #S866 at 1 mg/ml concentration) at a 4 BAK:1 SAPE molar ratio and incubated on ice for 15 minutes, shielded from light.

His_6-SUMO-peptide: Peptides fused to SUMO domains contained a His_6 tag and short flexible linker sequences: His_6-GSGSG-yeastSUMO-GSGSGSG-peptide sequence. Peptides were expressed and purified as described for b-His_6-BAK_{16-186}.

BAK ΔN22 ΔC25 C166S and BAKΔC25-His_6 constructs in pGEX 6P3 and pTYB1 vectors, respectively, that encoded expression as a fusion to glutathione S-transferase (GST) were obtained from Peter Czabotar, Walter and Eliza Hall Institute of Medical Research. The plasmid was transformed into BL21 (DE3) *E. coli* cells and grown in 4 L of TB media plus ampicillin and induced with IPTG (final concentration 1 mM) upon reaching an OD600 of 0.5-1.0. Cells were grown overnight at 16 °C. The next morning, cells were lysed and centrifuged at 7000 g for 15 mins. Pellets were transferred to falcon tubes and kept on ice. 25 mL of cold GST buffer (100 mM Tris, 50 mM NaCl, 1 mM EDTA, pH 7.5) per liter of growth and 50 μL of 100 mM PMSF were added per liter of growth media. Pellets were resuspended by pipetting up and down and vortexing

and subsequently sonicated for 3 mins total - 20s on/20s off at ~60 power duty cycle ~5 output control. Lysed cell cultures were centrifuged at 12,000 rpm for 30 min and filtered through a 0.22 μm filter. A bed volume of 5 ml of glutathione resin (GenScript L00207) was used, washed with 50 ml of cold PBS buffer at 4 °C. Supernatant was added to the column, maintaining a flow rate of 10-15 cm/h. The column was washed with 20x bed volume of GST buffer. The GST tag was cleaved with 200 units of PreScission protease (GE Healthcare, 27-0843-0) for 2 days on the column. Eluted cleaved protein was collected and further purified by gel filtration, using a Superdex 75 26/60 column in TBS buffer pH 7.5.

Bio-layer Interferometry

Bio-layer interferometry (BLI) experiments were performed on a Sartorius Octet RED96 instrument using streptavidin tips. b-His_6-BAK_{16-186} in optimized freshly made BLI buffer (PBS buffer (137 mM NaCl, 2.7 mM KCl, 10 mM Na_2HPO_4, 1.8 mM KH_2PO_4,) plus 0.005% Tween-20, 1% BSA, 2% DMSO, pH 7.5) was immobilized on streptavidin tips until a signal of around 0.6 nm was reached. Control His_6-tagged SUMO-peptide constructs were subtracted from the raw data using the BLI analysis software.

For kinetic analysis, curves for the dissociation portion of the curve only were fit to a One Phase Decay model using PRISM:

$$Y = (Y_0 - P) \exp(-k_{off}\ t) + P$$

Where t is time in seconds, Y is the receptor binding signal, Y_0 is Y at time 0 (the initial maximal binding signal that decreases to the plateau signal P), and k is the dissociation rate constant in units of s^{-1}. The dissociation constant k_{off} was constrained to be a single value for all peptide concentrations. Given the fit value for k_{off}, k_{on} was obtained by fitting the association portion of the data to an exponential equation using a global fit in PRISM:

$$Y=A\{1-\exp[-(k_{on}\ [peptide] + k_{off})\ t]\}$$

Where Y is the receptor binding signal and A is a constant. The dissociation constant K_d was calculated as k_{off}/k_{on}.

For steady-state analysis, the data were also fit to a one-site binding equation described in Roehrl *et al.*, using Python for comparison (Roehrl et al., 2004).

Crystallography

BAK:dF3 crystals were obtained by mixing 250 μM of BAK ΔN22 ΔC25 C166S in TBS buffer pH 7.5 with 250 μM of peptide (dissolved in water) in a 30 μl volume. Hanging drop crystals were grown at 4°C in polyethylene glycol (PEG) 3350 (20% w/v) and calcium acetate 0.2 M. BAK:dF2 crystals were obtained by mixing 250 μM of BAK ΔN22 ΔC25 C166S in TBS buffer pH 7.5 with 250 μM of peptide (dissolved in water) in a 30 μl volume. Hanging drop crystals were grown at 25 °C in 1.2 M disodium malonate, 0.1 M Tris, pH 8.5. BAK:dM2 crystals were obtained by mixing 250 μM of BAK ΔN22 ΔC25 C166S in TBS buffer pH 7.5 with 250 μM of peptide (dissolved in water) in a 30 μl volume. Hanging drop crystals were grown at 25°C in 3.5 M sodium formate. BAK:dF3, BAK:dF2, and BAK:dM2 crystals were frozen in the well solution and X-ray data were collected at Argon National Laboratories. Images were processed with HKL2000 or XDS and the structure was solved by molecular replacement with PHASER, searching for BAK monomer (PDB: 5VX0) without peptide. The final model was produced by rounds of building in COOT and refinement using PHENIX. PDB IDs will be updated in bioRxiv manuscript.

CD measurements

Peptide helicity was measured using an JASCO Circular Dichroism Spectrometer at 25 °C (unless indicated otherwise in **Table 6**. A single scan with speed of 50 nm/min at 0.5 nm increments (190 nm to 250 nm wavelengths) was recorded. The baseline signal for a buffer control (no peptide) was subtracted. Peptide samples were prepared in 10 mM sodium phosphate pH 7.0, with a final peptide concentration of 15 μM. The unfolded peptide concentration was determined by UV absorption in 6.0 M guanidine hydrochloride aqueous solution. As in (Shepherd et al., 2005) ellipticity [θ] was calculated as the mean residue ellipticity (MRE) in the units of deg $cm^2(10*dmol\ residue)^{-1}$ according to this equation:

$$[\theta]=[\theta]_{obs}/(10000*l*c*n)$$

where $[\theta]_{obs}$ is the measured ellipticity in millidegrees [mdeg], **c** is the peptide concentration [mol L^{-1}]), **n** is the number of residues, and **l** is path length (0.1 cm). The fractional helical content was calculated from the MRE at 222 nm and the number of backbone amides using the equation as in (Araghi et al., 2016):

$$\text{percent helical content} = [[\theta]_{222}/(-44000 + 250\ T)(1-3/n)]*100$$

where n is the number of amino-acid residues in the peptide and T is the temperature in degrees Celsius.

Structure-based design of BH3-only binders of BAK

We used the structure-based computational method dTERMen to design peptide binders of BAK (Zhou et al., 2020), following the approach of Frappier *et al.* (Frappier et al., 2019). In this work, we used version 35 of the dTERMen energy function and the same database of known structures as Zhou et. al (Zhou et al., 2020). To design BK3, we used BAK bound to BIM-h3Glg (PDB: 5VX0) as a template; BIM-h3Glg contains a non-native amino acid. Prior to peptide sequence design, we regularized the backbone of the peptide using the protocol TERMify, to improve compatibility with native amino-acid sequences. TERMify makes small adjustments to the backbone of a given structure to maximize similarity to common structural motifs in known proteins. A single cycle of the protocol consists of the following steps. First, the backbone structure is divided into overlapping fragments. Each fragment is then searched against a database of known structures to identify the top *N* matches, ranked by lowest RMSD. Finally, the method Fuser is used to update the coordinates of the original backbone to maximize similarity to the structural matches (Swanson et al., 2022). This process can be repeated to introduce progressively larger changes to the backbone, but in practice we have found that after ~50 cycles only minor structural changes are observed between cycles. We defined single-residue and residue-pair fragments from the structure at the beginning of every cycle. For each residue in the peptide, r_i, we defined a self-fragment consisting of r_i as well as flanking residues r_{i-1} and r_{i+1}. For each residue r_j with the potential to contact r_i, we defined a pair fragment consisting of the contacting residues and the residues flanking them $(r_{i-1}, r_i, r_{i+1}, r_{j-1}, r_j, r_{j+1})$. Residues were considered to have the potential to make a contact if their contact degree was greater than 0.01 (Holland et al., 2018). We searched a database of 12,657 non-redundant known structures for matches to the fragments using FASST, which guarantees that all structural matches within a given RMSD cutoff are identified and returned (Zhou & Grigoryan, 2015). We used a size and topology dependent function to define the RMSD cutoff used in structural searches, as in Zhou et al. (Zhou et al., 2020). We modified TERMify to account for the fixed structure and amino-acid sequence of BAK, so that only the peptide backbone geometry was updated. Single-residue fragments were defined from peptide residues only, and pair fragments were defined only for peptide-peptide and peptide-protein potential contacts. We used the sequence of BAK as an additional constraint when searching for structural matches. Specifically, for a pair fragment involving a peptide residue r_i and protein residue r_j, we required that the residue corresponding

to r_j in the match have the same amino acid as BAK. As in Swanson et. al, we fixed the structure of BAK when applying Fuser, so that only the structure of the peptide backbone was updated. When using TERMify to relax the structure of the peptide in PDB: 5VX0, we searched for 10 matches to each fragment in each of 100 cycles. The code detailing the TERMify procedure is provided at https://github.com/Grigoryanlab/Mosaist.

dTERMen scoring of human proteome sequences

BH3-containg sequences from the human proteome were scored using solved crystals structures of BAK:peptide complexes and dTERMen version 35. Because energy scores are not directly comparable between structures, we first ranked sequences according to their energy scores generated with the same structure and then compared rank order among all three structures to obtain an overall rank position.

Cavity detection

Cavities were detected and measured using F-pocket (Guilloux et al., 2009) available at: https://github.com/Discngine/fpocket.

siRNA transfection

24 hours before siRNA transfection, HeLa cells were seeded in 6-well plates and incubated overnight at 37°C. Cells were transfected with siRNA (final amount per well 25pmol) using Lipofectamine RNAiMAX (ThermoFisher 13778075) according to manufacturer's instructions. Cells were collected 72 hours later for BH3 profiling and western blotting.

BAX siRNA: ThermoFisher Silencer® Select, siRNA ID s1888

BAK siRNA: ThermoFisher Silencer® Select, siRNA ID s1881

Scramble siRNA: Dharmacon Horizon Discovery, ON-TARGETplus Non-targeting Control Pool (D-001810-10-05)

BH3 profiling

For each siRNA transfection sample, 2 million cells were centrifuged at 400g for 5 minutes and subjected to BH3 profiling as previously described (Fraser et al., 2019). In short, BH3 peptides in mannitol experimental buffer (MEB) (10 mM HEPES pH 7.5, 150 mM mannitol, 50 mM KCl, 0.02 mM EGTA, 0.02 mM EDTA, 0.1% BSA, 5 mM succinate) with digitonin were deposited into each well in a 96 well plate. Single cells were resuspended in MEB and added to each treatment well and incubated for 60 minutes at 28°C. Peptide exposure was terminated with formaldehyde and

cells were stained overnight with AF647 conjugated cytochrome c antibody (BioLegend 612310) and DAPI. Cytochrome c positivity was measured on ThermoFisher Scientifice Attune NxT Flow Cytometer.

Immunoblotting

Protein lysates were obtained by cell lysis in RIPA buffer (Boston BioProducts 115) with protease inhibitor (Roche 11697498001) and phosphatase inhibitor (ThermoFisher A32957). Protein loading was measured by BCA Protein Assay (ThermoFisher 23227). Protein samples were electrophoretically separated in precast gels (BioRad Mini-PROTEAN TGX Gels). Protein was transferred to PVDF membrane using Bio-Rad Trans-blot Semi-Dry transfer cell, blocked with 5% milk, and incubated overnight with primary antibody (BAX: Cell Signaling 2772S, BAK: Millipore Sigma 06-536, GAPDH: Cell Signaling 2118L). Secondary antibody (Peroxidase-linked anti-Rabbit: Cytiva Lifescience NA934) incubation and Pico development (ThermoFisher 34579) was performed before imaging on (Invitrogen iBright FL1500 Imaging System).

Acknowledgements and Funding

This work was funded by the National Institute of General Medical Sciences (NIGMS) award R01 GM110048 to A.E.K., MIT School of Science Fellowship in Cancer Research award to F.A., and the John W. Jarve (1978) Seed Fund for Science Innovation (MIT) award to F.A. and A.E.K. Part of this work is based upon research conducted at the Northeastern Collaborative Access Team beamlines, which are funded by the NIGMS (P30 GM124165). The Eiger 16M detector on 24-ID-E is funded by NIH-ORIP HEI grant S10OD021527. This research used resources of the Advanced Photon Source, a U.S. Department of Energy (DOE) Office of Science User Facility operated for the DOE Office of Science by Argonne National Laboratory under Contract No. DE-AC02-06CH11357. This work was supported in part by the Koch Institute Support (core) Grant P30-CA14051 from the National Cancer Institute. We thank the Koch Institute's Robert A. Swanson (1969) Biotechnology Center for technical support, specifically the Biopolymers and Proteomics Facility and the Flow Cytometry Core Facility. We also thank the MIT Structural Biology Core Facility, under the leadership of R.A.G., and we thank Molly Carney for her assistance with binding assays.

Author Contribution

F.A. and A.E.K. conceptualized project, designed and analyzed experiments, and wrote the paper. F.A. performed all biochemical and structural experiments. S.Y. conducted cell-based assays. R.A.G. directed and assisted with crystallography. S.S. conducted peptide computational design and RMSD calculations. D.G. assisted with cell-surface display experiments. B.G.S. assisted with crystallography and assay development. K.A.S. helped with the design and interpretation of cell-based experiments.

Competing Interests

The authors declare no competing interests.

APPENDIX

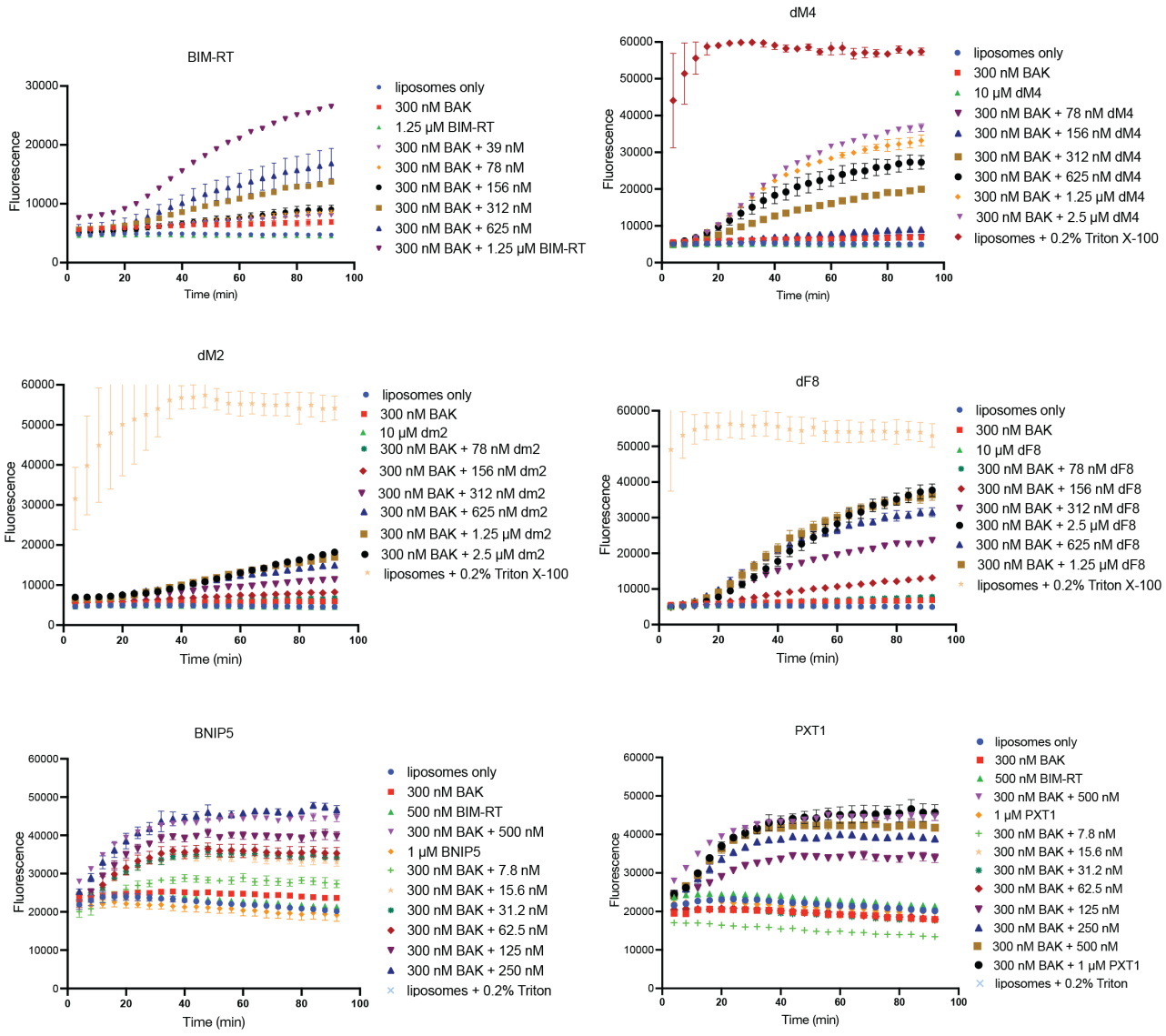

Figure 29. Raw liposome data of activator peptides.

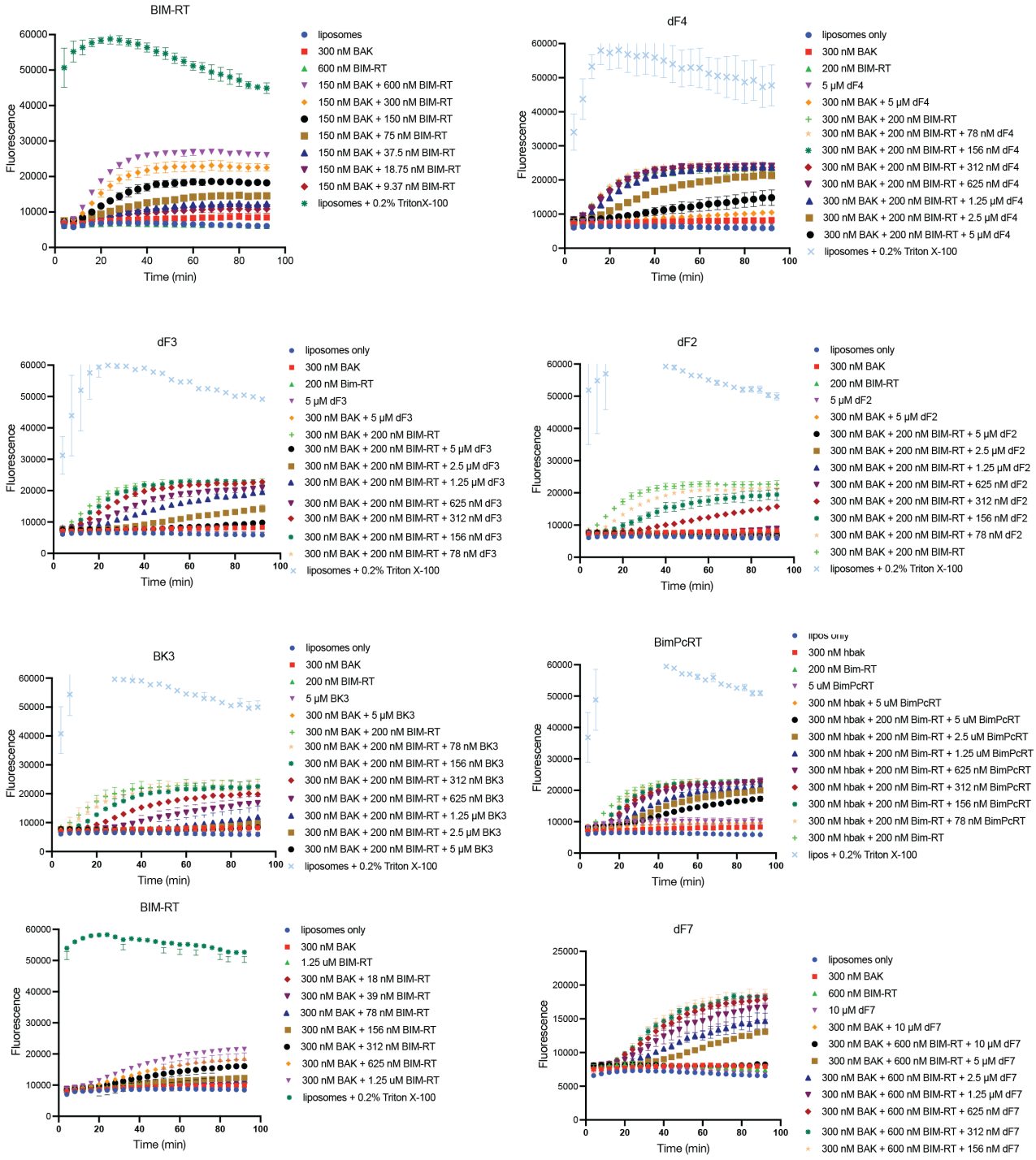

Figure 30. Raw liposome data of inhibitors

REFERENCES

Aouacheria, A., Laval, V. R. de, Combet, C., & Hardwick, J. M. (2013). Evolution of Bcl-2 homology motifs: homology versus homoplasy. *Trends in Cell Biology*, *23*(3), 103–111. https://doi.org/10.1016/j.tcb.2012.10.010

Araghi, R. R., Ryan, J. A., Letai, A., & Keating, A. E. (2016). Rapid Optimization of Mcl-1 Inhibitors using Stapled Peptide Libraries Including Non-Natural Side Chains. *ACS Chemical Biology*, *11*(5), 1238–1244. https://doi.org/10.1021/acschembio.5b01002

Assafa, T. E., Nandi, S., Śmiłowicz, D., Galazzo, L., Teucher, M., Elsner, C., Pütz, S., Bleicken, S., Robin, A. Y., Westphal, D., Uson, I., Stoll, R., Czabotar, P. E., Metzler-Nolte, N., & Bordignon, E. (2021). Biophysical Characterization of Pro-apoptotic BimBH3 Peptides Reveals an Unexpected Capacity for Self-Association. *Structure*, *29*(2), 114-124.e3. https://doi.org/10.1016/j.str.2020.09.002

Birkinshaw, R. W., Iyer, S., Lio, D., Luo, C. S., Brouwer, J. M., Miller, M. S., Robin, A. Y., Uren, R. T., Dewson, G., Kluck, R. M., Colman, P. M., & Czabotar, P. E. (2021). Structure of detergent-activated BAK dimers derived from the inert monomer. *Molecular Cell*, *81*(10), 2123-2134.e5. https://doi.org/10.1016/j.molcel.2021.03.014

Brouwer, J. M., Lan, P., Cowan, A. D., Bernardini, J. P., Birkinshaw, R. W., Delft, M. F. van, Sleebs, B. E., Robin, A. Y., Wardak, A., Tan, I. K., Reljic, B., Lee, E. F., Fairlie, W. D., Call, M. J., Smith, B. J., Dewson, G., Lessene, G., Colman, P. M., & Czabotar, P. E. (2017). Conversion of Bim-BH3 from Activator to Inhibitor of Bak through Structure-Based Design. *Molecular Cell*, *68*(4), 659-672.e9. https://doi.org/10.1016/j.molcel.2017.11.001

Brouwer, J. M., Westphal, D., Dewson, G., Robin, A. Y., Uren, R. T., Bartolo, R., Thompson, G. V., Colman, P. M., Kluck, R. M., & Czabotar, P. E. (2014). Bak Core and Latch Domains Separate during Activation, and Freed Core Domains Form Symmetric Homodimers. *Molecular Cell*, *55*(6), 938–946. https://doi.org/10.1016/j.molcel.2014.07.016

Chao, G., Lau, W. L., Hackel, B. J., Sazinsky, S. L., Lippow, S. M., & Wittrup, K. D. (2006). Isolating and engineering human antibodies using yeast surface display. *Nature Protocols*, *1*(2), 755–768. https://doi.org/10.1038/nprot.2006.94

Chen, L., Willis, S. N., Wei, A., Smith, B. J., Fletcher, J. I., Hinds, M. G., Colman, P. M., Day, C. L., Adams, J. M., & Huang, D. C. S. (2005). Differential Targeting of Prosurvival Bcl-2 Proteins by Their BH3-Only Ligands Allows Complementary Apoptotic Function. *Molecular Cell*, *17*(3), 393–403. https://doi.org/10.1016/j.molcel.2004.12.030

Chittenden, T., Harrington, E. A., O'Connor, R., Remington, C., Lutz, R. J., Evan, G. I., & Guild, B. C. (1995). Induction of apoptosis by the Bcl-2 homologue Bak. *Nature*, *374*(6524), 733–736. https://doi.org/10.1038/374733a0

Cosentino, K., Hertlein, V., Jenner, A., Dellmann, T., Gojkovic, M., Peña-Blanco, A., Dadsena, S., Wajngarten, N., Danial, J. S. H., Thevathasan, J. V., Mund, M., Ries, J., & Garcia-Saez,

A. J. (2022). The interplay between BAX and BAK tunes apoptotic pore growth to control mitochondrial-DNA-mediated inflammation. *Molecular Cell*. https://doi.org/10.1016/j.molcel.2022.01.008

Czabotar, P. E., Westphal, D., Dewson, G., Ma, S., Hockings, C., Fairlie, W. D., Lee, E. F., Yao, S., Robin, A. Y., Smith, B. J., Huang, D. C. S., Kluck, R. M., Adams, J. M., & Colman, P. M. (2013). Bax Crystal Structures Reveal How BH3 Domains Activate Bax and Nucleate Its Oligomerization to Induce Apoptosis. *Cell*, *152*(3), 519–531. https://doi.org/10.1016/j.cell.2012.12.031

Dai, H., Pang, Y.-P., Ramirez-Alvarado, M., & Kaufmann, S. H. (2014). Evaluation of the BH3-only Protein Puma as a Direct Bak Activator*. *Journal of Biological Chemistry*, *289*(1), 89–99. https://doi.org/10.1074/jbc.m113.505701

DeBartolo, J., Taipale, M., & Keating, A. E. (2014). Genome-Wide Prediction and Validation of Peptides That Bind Human Prosurvival Bcl-2 Proteins. *PLoS Computational Biology*, *10*(6), e1003693. https://doi.org/10.1371/journal.pcbi.1003693

Delbridge, A. R. D., Grabow, S., Strasser, A., & Vaux, D. L. (2016). Thirty years of BCL-2: translating cell death discoveries into novel cancer therapies. *Nature Reviews Cancer*, *16*(2), 99–109. https://doi.org/10.1038/nrc.2015.17

Delft, M. F. van, Chappaz, S., Khakham, Y., Bui, C. T., Debrincat, M. A., Lowes, K. N., Brouwer, J. M., Grohmann, C., Sharp, P. P., Dagley, L. F., Li, L., McArthur, K., Luo, M.-X., Chin, H. S., Fairlie, W. D., Lee, E. F., Segal, D., Duflocq, S., Lessene, R., … Kile, B. T. (2019). A small molecule interacts with VDAC2 to block mouse BAK-driven apoptosis. *Nature Chemical Biology*, *15*(11), 1057–1066. https://doi.org/10.1038/s41589-019-0365-8

Duque-Parra, J. E. (2005). Note on the origin and history of the term “apoptosis.” *The Anatomical Record Part B: The New Anatomist*, *283B*(1), 2–4. https://doi.org/10.1002/ar.b.20047

Dutta, S., Ryan, J., Chen, T. S., Kougentakis, C., Letai, A., & Keating, A. E. (2015). Potent and Specific Peptide Inhibitors of Human Pro-Survival Protein Bcl-xL. *Journal of Molecular Biology*, *427*(6), 1241–1253. https://doi.org/10.1016/j.jmb.2014.09.030

Frappier, V., Jenson, J. M., Zhou, J., Grigoryan, G., & Keating, A. E. (2019). Tertiary Structural Motif Sequence Statistics Enable Facile Prediction and Design of Peptides that Bind Anti-apoptotic Bfl-1 and Mcl-1. *Structure*, *27*(4), 606-617.e5. https://doi.org/10.1016/j.str.2019.01.008

Fraser, C., Ryan, J., & Sarosiek, K. (2019). BCL-2 Family Proteins, Methods and Protocols. *Methods in Molecular Biology*, *1877*, 61–76. https://doi.org/10.1007/978-1-4939-8861-7_4

Garner, T. P., Reyna, D. E., Priyadarshi, A., Chen, H.-C., Li, S., Wu, Y., Ganesan, Y. T., Malashkevich, V. N., Almo, S. S., Cheng, E. H., & Gavathiotis, E. (2016). An Autoinhibited Dimeric Form of BAX Regulates the BAX Activation Pathway. *Molecular Cell*, *63*(3), 485–497. https://doi.org/10.1016/j.molcel.2016.06.010

Gavathiotis, E., Suzuki, M., Davis, M. L., Pitter, K., Bird, G. H., Katz, S. G., Tu, H.-C., Kim, H., Cheng, E. H.-Y., Tjandra, N., & Walensky, L. D. (2008). BAX Activation is Initiated at a Novel Interaction Site. *Nature*, *455*(7216), 1076–1081. https://doi.org/10.1038/nature07396

Guilloux, V. L., Schmidtke, P., & Tuffery, P. (2009). Fpocket: An open source platform for ligand pocket detection. *BMC Bioinformatics*, *10*(1), 168–168. https://doi.org/10.1186/1471-2105-10-168

Hockings, C., Anwari, K., Ninnis, R. L., Brouwer, J., O'Hely, M., Evangelista, M., Hinds, M. G., Czabotar, P. E., Lee, E. F., Fairlie, W. D., Dewson, G., & Kluck, R. M. (2015). Bid chimeras indicate that most BH3-only proteins can directly activate Bak and Bax, and show no preference for Bak versus Bax. *Cell Death & Disease*, *6*(4), e1735. https://doi.org/10.1038/cddis.2015.105

Holland, J., Pan, Q., & Grigoryan, G. (2018). Contact prediction is hardest for the most informative contacts, but improves with the incorporation of contact potentials. *PLoS ONE*, *13*(6), e0199585. https://doi.org/10.1371/journal.pone.0199585

Huang, K., O'Neill, K. L., Li, J., Zhou, W., Han, N., Pang, X., Wu, W., Struble, L., Borgstahl, G., Liu, Z., Zhang, L., & Luo, X. (2019). BH3-only proteins target BCL-xL/MCL-1, not BAX/BAK, to initiate apoptosis. *Cell Research*, *29*(11), 942–952. https://doi.org/10.1038/s41422-019-0231-y

Iyer, S., Anwari, K., Alsop, A. E., Yuen, W. S., Huang, D. C. S., Carroll, J., Smith, N. A., Smith, B. J., Dewson, G., & Kluck, R. M. (2016). Identification of an activation site in Bak and mitochondrial Bax triggered by antibodies. *Nature Communications*, *7*(1), 11734. https://doi.org/10.1038/ncomms11734

Iyer, S., Uren, R. T., Dengler, M. A., Shi, M. X., Uno, E., Adams, J. M., Dewson, G., & Kluck, R. M. (2020). Robust autoactivation for apoptosis by BAK but not BAX highlights BAK as an important therapeutic target. *Cell Death & Disease*, *11*(4), 268. https://doi.org/10.1038/s41419-020-2463-7

Jenson, J. M., Ryan, J. A., Grant, R. A., Letai, A., & Keating, A. E. (2017). Epistatic mutations in PUMA BH3 drive an alternate binding mode to potently and selectively inhibit anti-apoptotic Bfl-1. *ELife*, *6*, e25541. https://doi.org/10.7554/elife.25541

Kaczmarek, K., Studencka, M., Meinhardt, A., Wieczerzak, K., Thoms, S., Engel, W., & Grzmil, P. (2011). Overexpression of peroxisomal testis-specific 1 protein induces germ cell apoptosis and leads to infertility in male mice. *Molecular Biology of the Cell*, *22*(10), 1766–1779. https://doi.org/10.1091/mbc.e09-12-0993

Kerr, J. F. R., Wyllie, A. H., & Currie, A. R. (1972). Apoptosis: A Basic Biological Phenomenon with Wideranging Implications in Tissue Kinetics. *British Journal of Cancer*, *26*(4), 239–257. https://doi.org/10.1038/bjc.1972.33

Kim, H., Tu, H.-C., Ren, D., Takeuchi, O., Jeffers, J. R., Zambetti, G. P., Hsieh, J. J.-D., & Cheng, E. H.-Y. (2009). Stepwise Activation of BAX and BAK by tBID, BIM, and PUMA Initiates Mitochondrial Apoptosis. *Molecular Cell*, *36*(3), 487–499. https://doi.org/10.1016/j.molcel.2009.09.030

Kuwana, T., Mackey, M. R., Perkins, G., Ellisman, M. H., Latterich, M., Schneiter, R., Green, D. R., & Newmeyer, D. D. (2002). Bid, Bax, and Lipids Cooperate to Form Supramolecular Openings in the Outer Mitochondrial Membrane. *Cell*, *111*(3), 331–342. https://doi.org/10.1016/s0092-8674(02)01036-x

Leshchiner, E. S., Braun, C. R., Bird, G. H., & Walensky, L. D. (2013). Direct activation of full-length proapoptotic BAK. *Proceedings of the National Academy of Sciences*, *110*(11), E986–E995. https://doi.org/10.1073/pnas.1214313110

Lindsten, T., Ross, A. J., King, A., Zong, W.-X., Rathmell, J. C., Shiels, H. A., Ulrich, E., Waymire, K. G., Mahar, P., Frauwirth, K., Chen, Y., Wei, M., Eng, V. M., Adelman, D. M., Simon, M. C., Ma, A., Golden, J. A., Evan, G., Korsmeyer, S. J., … Thompson, C. B. (2000). The Combined Functions of Proapoptotic Bcl-2 Family Members Bak and Bax Are Essential for Normal Development of Multiple Tissues. *Molecular Cell*, *6*(6), 1389–1399. https://doi.org/10.1016/s1097-2765(00)00136-2

Llambi, F., Moldoveanu, T., Tait, S. W. G., Bouchier-Hayes, L., Temirov, J., McCormick, L. L., Dillon, C. P., & Green, D. R. (2011). A Unified Model of Mammalian BCL-2 Protein Family Interactions at the Mitochondria. *Molecular Cell*, *44*(4), 517–531. https://doi.org/10.1016/j.molcel.2011.10.001

Luck, K., Kim, D.-K., Lambourne, L., Spirohn, K., Begg, B. E., Bian, W., Brignall, R., Cafarelli, T., Campos-Laborie, F. J., Charloteaux, B., Choi, D., Coté, A. G., Daley, M., Deimling, S., Desbuleux, A., Dricot, A., Gebbia, M., Hardy, M. F., Kishore, N., … Calderwood, M. A. (2020). A reference map of the human binary protein interactome. *Nature*, *580*(7803), 402–408. https://doi.org/10.1038/s41586-020-2188-x

McDonnell, J. M., Fushman, D., Milliman, C. L., Korsmeyer, S. J., & Cowburn, D. (1999). Solution Structure of the Proapoptotic Molecule BID A Structural Basis for Apoptotic Agonists and Antagonists. *Cell*, *96*(5), 625–634. https://doi.org/10.1016/s0092-8674(00)80573-5

Moldoveanu, T., & Czabotar, P. E. (2019). BAX, BAK, and BOK: A Coming of Age for the BCL-2 Family Effector Proteins. *Cold Spring Harbor Perspectives in Biology*, *12*(4), a036319. https://doi.org/10.1101/cshperspect.a036319

Moldoveanu, T., Grace, C. R., Llambi, F., Nourse, A., Fitzgerald, P., Gehring, K., Kriwacki, R. W., & Green, D. R. (2013). BID-induced structural changes in BAK promote apoptosis. *Nature Structural & Molecular Biology*, *20*(5), 589–597. https://doi.org/10.1038/nsmb.2563

Moldoveanu, T., Liu, Q., Tocilj, A., Watson, M., Shore, G., & Gehring, K. (2006). The X-Ray Structure of a BAK Homodimer Reveals an Inhibitory Zinc Binding Site. *Molecular Cell*, *24*(5), 677–688. https://doi.org/10.1016/j.molcel.2006.10.014

Niu, X., Brahmbhatt, H., Mergenthaler, P., Zhang, Z., Sang, J., Daude, M., Ehlert, F. G. R., Diederich, W. E., Wong, E., Zhu, W., Pogmore, J., Nandy, J. P., Satyanarayana, M., Jimmidi, R. K., Arya, P., Leber, B., Lin, J., Culmsee, C., Yi, J., & Andrews, D. W. (2017). A Small-Molecule Inhibitor of Bax and Bak Oligomerization Prevents Genotoxic Cell Death and Promotes Neuroprotection. *Cell Chemical Biology*, *24*(4), 493-506.e5. https://doi.org/10.1016/j.chembiol.2017.03.011

Placzek, W. J., Wei, J., Kitada, S., Zhai, D., Reed, J. C., & Pellecchia, M. (2010). A survey of the anti-apoptotic Bcl-2 subfamily expression in cancer types provides a platform to predict the efficacy of Bcl-2 antagonists in cancer therapy. *Cell Death & Disease*, *1*(5), e40. https://doi.org/10.1038/cddis.2010.18

Pritz, J. R., Wachter, F., Lee, S., Luccarelli, J., Wales, T. E., Cohen, D. T., Coote, P. W., Heffron, G. J., Engen, J. R., Massefski, W., & Walensky, L. D. (2017). Allosteric Sensitization of Pro-Apoptotic BAX. *Nature Chemical Biology*, *13*(9), 961–967. https://doi.org/10.1038/nchembio.2433

Reich, L. "Luther," Dutta, S., & Keating, A. E. (2016). Generating High-Accuracy Peptide-Binding Data in High Throughput with Yeast Surface Display and SORTCERY. In *Stoddard B. (eds) Computational Design of Ligand Binding Proteins* (Vol. 1414, pp. 233–247). Humana Press, New York, NY. https://doi.org/https://doi-org.libproxy.mit.edu/10.1007/978-1-4939-3569-7_14

Reyna, D. E., Garner, T. P., Lopez, A., Kopp, F., Choudhary, G. S., Sridharan, A., Narayanagari, S.-R., Mitchell, K., Dong, B., Bartholdy, B. A., Walensky, L. D., Verma, A., Steidl, U., & Gavathiotis, E. (2017). Direct Activation of BAX by BTSA1 Overcomes Apoptosis Resistance in Acute Myeloid Leukemia. *Cancer Cell*, *32*(4), 490-505.e10. https://doi.org/10.1016/j.ccell.2017.09.001

Roehrl, M. H. A., Wang, J. Y., & Wagner, G. (2004). A General Framework for Development and Data Analysis of Competitive High-Throughput Screens for Small-Molecule Inhibitors of Protein-Protein Interactions by Fluorescence Polarization. *Biochemistry*, *43*(51), 16056–16066. https://doi.org/10.1021/bi048233g

Sandow, J. J., Tan, I. K., Huang, A. S., Masaldan, S., Bernardini, J. P., Wardak, A. Z., Birkinshaw, R. W., Ninnis, R. L., Liu, Z., Dalseno, D., Lio, D., Infusini, G., Czabotar, P. E., Webb, A. I., & Dewson, G. (2021). Dynamic reconfiguration of pro-apoptotic BAK on membranes. *The EMBO Journal*, *40*(20), e107237. https://doi.org/10.15252/embj.2020107237

Sarosiek, K. A., Chi, X., Bachman, J. A., Sims, J. J., Montero, J., Patel, L., Flanagan, A., Andrews, D. W., Sorger, P., & Letai, A. (2013). BID Preferentially Activates BAK while BIM Preferentially Activates BAX, Affecting Chemotherapy Response. *Molecular Cell*, *51*(6), 751–765. https://doi.org/10.1016/j.molcel.2013.08.048

Sarosiek, K. A., Fraser, C., Muthalagu, N., Bhola, P. D., Chang, W., McBrayer, S. K., Cantlon, A., Fisch, S., Golomb-Mello, G., Ryan, J. A., Deng, J., Jian, B., Corbett, C., Goldenberg, M., Madsen, J. R., Liao, R., Walsh, D., Sedivy, J., Murphy, D. J., … Letai, A. (2017). Developmental Regulation of Mitochondrial Apoptosis by c-Myc Governs Age- and Tissue-Specific Sensitivity to Cancer Therapeutics. *Cancer Cell*, *31*(1), 142–156. https://doi.org/10.1016/j.ccell.2016.11.011

Sattler, M., Liang, H., Nettesheim, D., Meadows, R. P., Harlan, J. E., Eberstadt, M., Yoon, H. S., Shuker, S. B., Chang, B. S., Minn, A. J., Thompson, C. B., & Fesik, S. W. (1997). Structure of Bcl-XL_-Bak Peptide Complex: Recognition between Regulators of Apoptosis. *Science*, *275*(5302), 983–986.

Shepherd, N. E., Hoang, H. N., Abbenante, G., & Fairlie, D. P. (2005). Single Turn Peptide Alpha Helices with Exceptional Stability in Water. *Journal of the American Chemical Society*, *127*(9), 2974–2983. https://doi.org/10.1021/ja0456003

Singh, G., Guibao, C. D., Seetharaman, J., Aggarwal, A., Grace, C. R., McNamara, D. E., Vaithiyalingam, S., Waddell, M. B., & Moldoveanu, T. (2022). Structural basis of BAK activation in mitochondrial apoptosis initiation. *Nature Communications*, *13*(1), 250. https://doi.org/10.1038/s41467-021-27851-y

Swanson, S., Sivaraman, V., Grigoryan, G., & Keating, A. E. (2022). Tertiary motifs as building blocks for the design of protein-binding peptides. *Protein Science, Submitted*.

Tait, S. W. G., & Green, D. R. (2010). Mitochondria and cell death: outer membrane permeabilization and beyond. *Nature Reviews Molecular Cell Biology*, *11*(9), 621–632. https://doi.org/10.1038/nrm2952

Truebestein, L., & Leonard, T. A. (2016). Coiled-coils: The long and short of it. *BioEssays*, *38*(9), 903–916. https://doi.org/10.1002/bies.201600062

Tunyasuvunakool, K., Adler, J., Wu, Z., Green, T., Zielinski, M., Žídek, A., Bridgland, A., Cowie, A., Meyer, C., Laydon, A., Velankar, S., Kleywegt, G. J., Bateman, A., Evans, R., Pritzel, A., Figurnov, M., Ronneberger, O., Bates, R., Kohl, S. A. A., … Hassabis, D. (2021). Highly accurate protein structure prediction for the human proteome. *Nature*, *596*(7873), 590–596. https://doi.org/10.1038/s41586-021-03828-1

Willis, S. N., Chen, L., Dewson, G., Wei, A., Naik, E., Fletcher, J. I., Adams, J. M., & Huang, D. C. S. (2005). Proapoptotic Bak is sequestered by Mcl-1 and Bcl-xL, but not Bcl-2, until displaced by BH3-only proteins. *Genes & Development*, *19*(11), 1294–1305. https://doi.org/10.1101/gad.1304105

Willis, S. N., Fletcher, J. I., Kaufmann, T., Delft, M. F. van, Chen, L., Czabotar, P. E., Ierino, H., Lee, E. F., Fairlie, W. D., Bouillet, P., Strasser, A., Kluck, R. M., Adams, J. M., & Huang, D. C. S. (2007). Apoptosis Initiated When BH3 Ligands Engage Multiple Bcl-2 Homologs, Not Bax or Bak. *Science*, *315*(5813), 856–859. https://doi.org/10.1126/science.1133289

Youle, R. J., & Strasser, A. (2008). The BCL-2 protein family: opposing activities that mediate cell death. *Nature Reviews Molecular Cell Biology*, *9*(1), 47–59. https://doi.org/10.1038/nrm2308

Yuan, Z., Dewson, G., Czabotar, P. E., & Birkinshaw, R. W. (2021). VDAC2 and the BCL-2 family of proteins. *Biochemical Society Transactions*, *49*(6), 2787–2795. https://doi.org/10.1042/bst20210753

Zheng, J. H., Follis, A. V., Kriwacki, R. W., & Moldoveanu, T. (2016). Discoveries and controversies in BCL-2 protein-mediated apoptosis. *The FEBS Journal*, *283*(14), 2690–2700. https://doi.org/10.1111/febs.13527

Zhou, J., & Grigoryan, G. (2015). Rapid search for tertiary fragments reveals protein sequence–structure relationships. *Protein Science*, *24*(4), 508–524. https://doi.org/10.1002/pro.2610

Zhou, J., Panaitiu, A. E., & Grigoryan, G. (2020). A general-purpose protein design framework based on mining sequence–structure relationships in known protein structures. *Proceedings of the National Academy of Sciences of the United States of America*, *117*(2), 1059–1068. https://doi.org/10.1073/pnas.1908723117

CHAPTER 3

FUTURE DIRECTIONS

SECTION 1.1 BAK VS. BAX ACTIVATION SPECIFICITY

According to the literature, all known BH3-only activators (BID, BIM, PUMA, BAK, and BAX BH3 regions) can directly activate both pro-apoptotic members. Furthermore, BAK and BAX are structurally very similar with 65% sequence identity, in addition to having similar functions. However, differences in activation potency among BH3-only proteins have been reported. Specifically, it has been observed that BID preferentially activates BAK, while BIM preferentially activates BAX in permeabilized cells (Sarosiek et al., 2013). This suggests that BAK vs. BAX have underlying structural and biophysical differences that lead to differences in functional outcomes.

One of the main differences between BAK and BAX is their localization in the cell; BAK is mainly localized on the mitochondrial outer membrane while BAX is primarily in the cytosol. In order to induce MOMP, BAX requires translocation to the mitochondrial outer membrane in addition to the conformational changes required to reach the BH3-in-groove dimer. Previous groups have shown that the α9 helix of BAX must be displaced from its hydrophobic canonical binding groove as the first step in the two-step activation mechanism. Exposure of the α9 helix occurs by binding of a BH3 helix to the BAX trigger site (α1-α6 region), located on the opposite side of the canonical groove (Gavathiotis et al., 2008). The second step occurs by binding of a BH3-only protein to the canonical groove, as suggested by putative intermediate crystal structures (Czabotar et al., 2013).

Our data in **Chapter 2, Figure 17** shows that non-native dM2, dM4, and dF8 peptides induce MOMP is HeLa cells containing BAK but not BAX. This is in contrast to what is observed in BAX only cells where almost no cytochrome-c release is observed for dM2 and dF8 and only 20% release for dM4 at 10 μM peptide. This raises the question, why do dM2, dM4, and dF8 peptides activate BAK but not BAX?

To answer this question, first, activation experiments using full length BAX and liposomes must be done to corroborate this initial observation in cells. Next, assuming our non-native peptides do not activate BAX in liposome-based assays, one could hypothesize that preferential peptide-induced activation of BAK vs BAX is due to binding differences. For example, it is possible that our dM2, dF8, and dM4 peptides bind the canonical groove, but not the BAX trigger site. The opposite scenario where peptides bind the trigger site but not the canonical site is also possible. Alternatively, peptides may not be able to bind either one of the two sites.

Researchers within the apoptosis field have long been interested in creating BAK and BAX selective probes to dissect mechanism and use as therapies for cancer or neurodegenerative

diseases. High throughout small molecule screening and traditional methods to generate antibodies have led to the discovery of BAK inhibitors and activators, respectively (Delft et al., 2019) (Iyer et al., 2016). However, structure-based design combined with computational and experimental methods provide an alternative avenue for creating novel potent BAK reagents. Understanding the features of dM2, dM4, and dF8 peptides that give BAK specificity could help guide the creation of future reagents. Thus, assuming dM2, dF8, and dM4 peptides are able to bind both BAX and BAK in the canonical groove, how is BAK activation specificity achieved?

In this thesis, I have shown that point mutations of BH3-only proteins can lead to changes in BAK activation potency *in vitro*, in addition to similar effects observed for BAX (Czabotar et al., 2013). Specifically, substitution of native methionine 144 with isoleucine in PUMA gave greater BAK activation compared to WT. Similarly, substitution of native cysteine 25 with isoleucine in NOXA gave greater BAK activation. This data makes it reasonable to suggest that minor residue substitutions in our non-native peptides could lead to activation differences in both BAK and BAX.

In order to dissect specificity differences between BAK and BAX, I propose conducting a deep mutational scan of dM2, dM4, and dF8 peptides. This could be achieved using liposomes in a 96 well plate-based format in combination with either a chemically synthesized peptide library or peptide-expressing cells. Rigorous structural comparisons of BAK and BAX including sequence conservation, charge, and hydrophobicity could give additional information to guide specificity predictions.

SECTION 1.2 BAK INHIBITOR SPECIFICITY

Aside from discovering novel BAK activators, the creation of BAK inhibitors for the treatment of neurodegenerative diseases is also attractive. In this work, we discovered non-native BAK inhibitors dF2, dF3, dF4, dF7, and computationally designed BK3. Fluorescence anisotropy experiments show that dF2, dF3, and BK3 bind to anti-apoptotic members MCL-1 and BCL-X_L (data not shown) in addition to BFL-1 (Frappier et al., 2019). Because of this, it is possible that our BAK inhibitors also function as sensitizers and thus induce MOMP in cells. Although we did not test for inhibition in permeabilized cells due to technical challenges, lack of BAK selectivity sets the stage for a future protein engineering and design problem.

To circumvent cross-reaction with anti-apoptotic members, different strategies could be used to obtain such sequences including library screening and computational protein design. Directed evolution using library screening with negative selection against off-target proteins can help increase selectivity (Dutta et al., 2015). Computational optimization of stability/specificity

trade-offs and data driven models are other strategies that could be used to obtain BAK specific inhibitors (Grigoryan et al., 2009; Jenson et al., 2018).

SECTION 1.3 USING PEPTIDES TO STUDY MOMP

Recent work from Cosentino et al. involving super-resolution microscopy techniques has shed light on the importance of pore size for release of mitochondrial DNA and downstream inflammatory responses (Cosentino et al., 2022). Because of biophysical traits features that remain unknown, the availability of BAK or BAX at the mitochondrial outer membrane determines the size of the pores being formed and the timing of release of specific mitochondrial contents (Cosentino et al., 2022). The relationship between kinetics of oligomerization, apoptotic pores, and biological response will undoubtedly become an area of interest to many within the field, and tools to modulate BAK activation kinetics and pore size could become valuable tools.

In our liposome system, greater dye release is indicative of stronger activation. Similarly in cells, we assume that more cytochrome-c release is indicative of more BAK/BAX activation. Presumably, greater cytochrome-c release can be because of two reasons: bigger apoptotic pores and/or an increase in the number of apoptotic pores, both of which are dependent on protein density at the membrane.

Although the exact mechanism as to how BAK/BAX oligomerization leads to pore formation remains unclear, our data suggests that different sequences give differences in BAK activation potency and presumably kinetics of oligomerization and pore formation. Experiments in liposomes with measurable BAK concentrations show that dF8 and dM4 peptides are more potent activators compared to known activator BIM at 1.25 μM, while our dM2 peptide was less so (**Chapter 2, Figure 3**). Human BNIP5 peptide is two-fold more potent compared to BIM, while PXT1 is equally as potent (**Chapter 2, Figure 3**). Therefore, under the assumption of a constant BAK concentration, we can speculate the general idea that pore size and/or number of apoptotic pores is dependent on activator peptide sequence.

One could speculate that our novel peptide activators may serve as reagents to those interested in regulating MOMP. For example, in addition to regulating the amount of BAK or BAX present at the mitochondrial membrane, researchers could potentially regulate pore size growth dynamics through inducible expression of genetically encoded activator peptides. Though specific questions regarding MOMP dynamics that could be addressed with our peptides may not seem obvious at the moment, it is interesting to think of the broader picture of ways to regulate BAK activation potency and kinetics of oligomerization and pore formation.

SECTION 1.4 BIOLOGICAL FUNCTION OF BNIP5 AND PXT1

The discovery that BH3-only proteins BNIP5 and PXT1 induce BAK and BAX-mediated MOMP in permeabilized cells is exciting because of the unexplored biological implications this poses. Because very limited data on these proteins exist, datamining existing genetic databases searching for expression levels and patterns among tissues and looking for correlations with disease may provide some leads. Studies have shown that BNIP5 is highly expressed in the tissues that undergo constant self-renewal including colon, small intestine, pancreas, and stomach cells, making the connection between BNIP5 and apoptosis sound feasible (Luck et al., 2020). Genetic studies including tissue-specific knockout of BNIP5 may be informative of the biology associated with it. Also, proximity labeling in mammalian cells using biotin ligase TurboID could be used to identify relevant protein-protein interactions in the BNIP5 and PXT1 regulatory networks (Cho et al., 2020).

Previous studies have shown that overexpression of PXT1 leads to apoptosis in spermatocytes and as a consequence gives male infertility (Kaczmarek et al., 2011). PXT1 is expressed in later stages of spermatogenesis and contains a BH3 domain in the N-terminal region and a peroxisomal localization tag at the C-terminal end (Grzmil et al., 2007). Moreover, it has been shown that PXT1 interacts with BAT3, a member of the BCL-2-associated athanogene (BAG) family that contains a nuclear localization signal. The interaction between BAT3 and PXT1 inhibits, though not fully, PXT1 pro-apoptotic activity. This interaction, however, is not BH3-mediated, and so future studies exploring protein-protein interactions between PXT1 and other BCL-2 family members *in vivo* would be informative. From a biological perspective, the connection between PXT1-mediated apoptosis and the peroxisome remains unanswered.

Our results suggest that BNIP5 and PXT1 may have significant biological roles by functioning as both activators and sensitizers. Both BNIP5 and PXT1 are more potent activators compared to BID, BIM, and PUMA peptides both in liposome assays and cell-based assays. Furthermore, they bind all five anti-apoptotic members with affinities of <100 nM (similar to BID, BIM, and PUMA) (DeBartolo et al., 2014), and bind pro-apoptotic BAK with significantly tighter affinities compared to known activators. Why is there such a significant difference in affinity for BAK for BNIP5 and PXT1 vs known activators and what are the biological implications of this?

In order to prevent unwanted detrimental effects to the cell's integrity, BH3-only expression must be tightly regulated. Other BH3-only proteins are kept in check by transcriptional and posttranslational mechanisms (D. C. S. Huang & Strasser, 2000). For example, NOXA expression is induced by p53 upon DNA damage and BAD is phosphorylated at multiple sites as a result of

growth factor signaling. How are BNIP5 and PXT1 regulated at a transcriptional and posttranslational level and what factors external or internal factors contribute to this is a question yet to be answered.

SECTION 1.5 SEARCHING FOR ADDITIONAL HUMAN BH3-ONLY BAK BINDERS

With the goal of identifying additional signaling pathways that regulate apoptosis, numerous groups have sought to computationally and experimentally find additional BH3-only proteins in the human proteome and have generated lists of potential Bcl-2 family regulators (DeBartolo et al., 2014; Aouacheria et al., 2013; Aouacheria et al., 2015). Other projects have aimed at characterizing the protein interactome more broadly through yeast-two-hybrid screens (Luck et al., 2020). The weak affinity and transient interaction of known BH3-only binders for BAK make the novel binder search technically challenging. However, as previously done for yeast, we can pre-tetramerize BAK to achieve greater avidity and isolate weak binders through cell-surface display methods. More specifically, it would be interesting to screen a previously published 36-residue human proteome-derived peptide library for novel BAK binders using *E. coli* surface display (Hwang et al., 2022). This could potentially lead to the discovery of both canonical and non-canonical binders which would not have been detected through computational screens.

REFERENCES

Aouacheria, A., Combet, C., Tompa, P., & Hardwick, J. M. (2015). Redefining the BH3 Death Domain as a 'Short Linear Motif.' *Trends in Biochemical Sciences*, *40*(12), 736–748. https://doi.org/10.1016/j.tibs.2015.09.007

Aouacheria, A., Laval, V. R. de, Combet, C., & Hardwick, J. M. (2013). Evolution of Bcl-2 homology motifs: homology versus homoplasy. *Trends in Cell Biology*, *23*(3), 103–111. https://doi.org/10.1016/j.tcb.2012.10.010

Cho, K. F., Branon, T. C., Udeshi, N. D., Myers, S. A., Carr, S. A., & Ting, A. Y. (2020). Proximity labeling in mammalian cells with TurboID and split-TurboID. *Nature Protocols*, *15*(12), 3971–3999. https://doi.org/10.1038/s41596-020-0399-0

Cosentino, K., Hertlein, V., Jenner, A., Dellmann, T., Gojkovic, M., Peña-Blanco, A., Dadsena, S., Wajngarten, N., Danial, J. S. H., Thevathasan, J. V., Mund, M., Ries, J., & Garcia-Saez, A. J. (2022). The interplay between BAX and BAK tunes apoptotic pore growth to control mitochondrial-DNA-mediated inflammation. *Molecular Cell*. https://doi.org/10.1016/j.molcel.2022.01.008

Czabotar, P. E., Westphal, D., Dewson, G., Ma, S., Hockings, C., Fairlie, W. D., Lee, E. F., Yao, S., Robin, A. Y., Smith, B. J., Huang, D. C. S., Kluck, R. M., Adams, J. M., & Colman, P. M. (2013). Bax Crystal Structures Reveal How BH3 Domains Activate Bax and Nucleate Its Oligomerization to Induce Apoptosis. *Cell*, *152*(3), 519–531. https://doi.org/10.1016/j.cell.2012.12.031

DeBartolo, J., Taipale, M., & Keating, A. E. (2014). Genome-Wide Prediction and Validation of Peptides That Bind Human Prosurvival Bcl-2 Proteins. *PLoS Computational Biology*, *10*(6), e1003693. https://doi.org/10.1371/journal.pcbi.1003693

Delft, M. F. van, Chappaz, S., Khakham, Y., Bui, C. T., Debrincat, M. A., Lowes, K. N., Brouwer, J. M., Grohmann, C., Sharp, P. P., Dagley, L. F., Li, L., McArthur, K., Luo, M.-X., Chin, H. S., Fairlie, W. D., Lee, E. F., Segal, D., Duflocq, S., Lessene, R., … Kile, B. T. (2019). A small molecule interacts with VDAC2 to block mouse BAK-driven apoptosis. *Nature Chemical Biology*, *15*(11), 1057–1066. https://doi.org/10.1038/s41589-019-0365-8

Dutta, S., Ryan, J., Chen, T. S., Kougentakis, C., Letai, A., & Keating, A. E. (2015). Potent and Specific Peptide Inhibitors of Human Pro-Survival Protein Bcl-xL. *Journal of Molecular Biology*, *427*(6), 1241–1253. https://doi.org/10.1016/j.jmb.2014.09.030

Frappier, V., Jenson, J. M., Zhou, J., Grigoryan, G., & Keating, A. E. (2019). Tertiary Structural Motif Sequence Statistics Enable Facile Prediction and Design of Peptides that Bind Anti-apoptotic Bfl-1 and Mcl-1. *Structure*, *27*(4), 606-617.e5. https://doi.org/10.1016/j.str.2019.01.008

Gavathiotis, E., Suzuki, M., Davis, M. L., Pitter, K., Bird, G. H., Katz, S. G., Tu, H.-C., Kim, H., Cheng, E. H.-Y., Tjandra, N., & Walensky, L. D. (2008). BAX activation is initiated at a novel interaction site. *Nature*, *455*(7216), 1076–1081. https://doi.org/10.1038/nature07396

Grigoryan, G., Reinke, A. W., & Keating, A. E. (2009). Design of protein-interaction specificity affords selective bZIP-binding peptides. *Nature*, *458*(7240), 859–864. https://doi.org/10.1038/nature07885

Grzmil, P., Burfeind, C., Preuss, T., Dixkens, C., Wolf, S., Engel, W., & Burfeind, P. (2007). The putative peroxisomal gene Pxt1 is exclusively expressed in the testis. *Cytogenetic and Genome Research*, *119*(1–2), 74–82. https://doi.org/10.1159/000109622

Huang, D. C. S., & Strasser, A. (2000). BH3-Only Proteins—Essential Initiators of Apoptotic Cell Death. *Cell*, *103*(6), 839–842. https://doi.org/10.1016/s0092-8674(00)00187-2

Hwang, T., Parker, S. S., Hill, S. M., Grant, R. A., Ilunga, M. W., Sivaraman, V., Mouneimne, G., & Keating, A. E. (2022). Native proline-rich motifs exploit sequence context to target actin-remodeling Ena/VASP protein ENAH. *ELife*, *11*, e70680. https://doi.org/10.7554/elife.70680

Iyer, S., Anwari, K., Alsop, A. E., Yuen, W. S., Huang, D. C. S., Carroll, J., Smith, N. A., Smith, B. J., Dewson, G., & Kluck, R. M. (2016). Identification of an activation site in Bak and mitochondrial Bax triggered by antibodies. *Nature Communications*, *7*(1), 11734. https://doi.org/10.1038/ncomms11734

Jenson, J. M., Xue, V., Stretz, L., Mandal, T., Reich, L. "Luther," & Keating, A. E. (2018). Peptide design by optimization on a data-parameterized protein interaction landscape. *Proceedings of the National Academy of Sciences*, *115*(44), 201812939. https://doi.org/10.1073/pnas.1812939115

Kaczmarek, K., Studencka, M., Meinhardt, A., Wieczerzak, K., Thoms, S., Engel, W., & Grzmil, P. (2011). Overexpression of peroxisomal testis-specific 1 protein induces germ cell apoptosis and leads to infertility in male mice. *Molecular Biology of the Cell*, *22*(10), 1766–1779. https://doi.org/10.1091/mbc.e09-12-0993

Luck, K., Kim, D.-K., Lambourne, L., Spirohn, K., Begg, B. E., Bian, W., Brignall, R., Cafarelli, T., Campos-Laborie, F. J., Charloteaux, B., Choi, D., Coté, A. G., Daley, M., Deimling, S., Desbuleux, A., Dricot, A., Gebbia, M., Hardy, M. F., Kishore, N., … Calderwood, M. A. (2020). A reference map of the human binary protein interactome. *Nature*, *580*(7803), 402–408. https://doi.org/10.1038/s41586-020-2188-x

Sarosiek, K. A., Chi, X., Bachman, J. A., Sims, J. J., Montero, J., Patel, L., Flanagan, A., Andrews, D. W., Sorger, P., & Letai, A. (2013). BID Preferentially Activates BAK while BIM Preferentially Activates BAX, Affecting Chemotherapy Response. *Molecular Cell*, *51*(6), 751–765. https://doi.org/10.1016/j.molcel.2013.08.048